# Characterising novel mitotic microtubule associated proteins in the early *Drosophila* embryo

Submitted by Stacey Jane Scott to the University of Exeter

As a thesis for the degree of

Masters by Research in Biosciences

In September 2015



I certify that all material in this thesis which is not my own work has been identified and that

no material has been previously submitted and approved for the award of a degree by this

or any other University.

(Signature)……

Acknowledgements

There are many people I need to say thank you to. Without every one of you I don't think finishing this project would have been a possibility.

First, my supervisor James Wakefield for giving me this opportunity, and for helping and supporting me throughout. To the rest of the Wakefield lab past and present; Jack Chen you have been an absolute star and without your patience for my constant questions who knows how things may have turned out. To Lucy Green for showing me the ropes and to Lizzy Anderson and James Marks, my fellow minions; thank you both for being such wonderful lab mates.

The Council of Ladies – Charli Mardon, Kate McIntosh and Sam Mitchell. Thank you for being a shoulder to cry on, for providing your words of wisdom and for being incredible friends to me over the past two years. I owe you a lot. The rest of the front office; Kat Curry, Andy Early, Ben Meadows, and the rest of Lab 211 for creating such an enjoyable working environment, something I am really going to miss!

My biggest thanks needs to go to my family. Mum, Dad and Emma I cannot thank you guys enough for everything you have done, not just in my quest to get those all-important letters after my name but in everything I have set out to achieve.

To my best friends Charmaine and Becky; thank you for the coffee breaks, the words of advice and the unwavering friendship. I am so grateful to you both.

Finally, to Ian. Thank you for just being you.

Abstract

Cell division is a fundamental biological process driven by the formation of a microtubule (MT) based mitotic spindle, ensuring the accurate segregation of chromosomes. MT length, nucleation and dynamics are all determined by microtubule associated proteins (MAPs). Following on from previous work carried out by the Hughes *et al*., (2008) this investigation has applied quantitative comparative proteomics to cycling and mitotic *Drosophila* embryo extracts prepared via MT co-sedimentation assay, in order to compare their MAP complements as they progress though the cell cycle or whilst fixed at the metaphase-anaphase transition. We have demonstrated that many MAPs known for their roles in cell division increase their association with MTs during mitosis, and in addition our approach has identified a number of protein classes not previously characterised as a MAP, binding to MTs during mitosis. One of these protein classes was the Replication Factor C complex (RFC). The RFC complex is most well-known for its role as the sliding clamp loader in DNA replication, however it is now presenting as MAPs with a potential mitotic function. By combining techniques from biochemistry, fluorescence microscopy and further proteomic analysis we have been able to begin to investigate the localisation and functions of this complex during mitosis. Thus far we have been able to biochemically show that the RFC complex is a true MT binding protein and that all three alternative RFC complexes, as well as the archetypal complex, are present in mitotic embryo extracts following immunoprecipitation of RFC3. We have also shown via fluorescence imaging that the RFC complex presents a weak localisation to the mitotic spindle. Application of these techniques has also led to further investigation into the known MAPs, Asp and DTACC, for which we have identified novel protein interactors and investigated localisation during the process of *Drosophila* embryonic spindle self-assembly.

Table of contents

List of figures

List of tables

List of supplementary figures

List of supplementary tables

List of abbreviations

Asp – Abnormal spindle protein

DTACC – *Drosophila* transforming acid coiled coil

GFP – Green fluorescent protein

MAP – Microtubule associated protein

MS – Mass spectrometry

MT – Microtubule

MTOC – Microtubule organising centre

NEB – Nuclear envelope breakdown

PAGE – Polyacrylamide gel electrophoresis

PCM – Pericentriolar material

QC – Quantitative comparative

RFC – Replication factor C

RFP – Red fluorescent protein

RISC – RNAi induced silencing complex

SAF – Spindle assembly factor

γTURC - gamma tubulin ring complex

## 1. Introduction

Cell division is a fundamental biological process, that in eukaryotes is driven by the formation of a microtubule (MT) based mitotic spindle, ensuring the accurate segregation of duplicated chromosomes. MT length, nucleation and dynamics are determined by the actions of MT associated proteins (MAPs). By understanding the function of MAPs we can further develop our knowledge of how the MT network acts to ensure faithful chromosome segregation, avoiding genome instability. If chromosomes are not able to separate correctly DNA can become damaged; this ultimately leads to the development of a number of disorders, with cancer being at the forefront.

### 1.1 Cell division and MTs

Cell division occurs in five main stages; prophase, prometaphase, metaphase, anaphase and telophase (Figure 1-1). Prior to prophase cells go through a period known as interphase, where DNA replication occurs (S phase of the cell cycle). These stages occur once in mitosis and twice in meiosis; however in the second interphase of meiosis there is no further DNA replication, resulting in two haploid daughter cells. Two subcellular structures, the bipolar spindle and the central spindle, are required for accurate cell division. The bipolar spindle ensures that the chromosomes are segregated correctly and the central spindle is required for successful cytokinesis of the two daughter cells (Bonaccorsi *et al.,* 1998). The bipolar spindle begins assembly in prophase, and is fully formed by the onset of metaphase to align the replicated sister chromatids.

A basic outline of cell division has been described by Scholey *et al* (2003). The main goal of mitosis is to distribute identical copies of replicated chromosomes to newly formed daughter cells, through the combined efforts of spindle MTs and microtubule associated proteins (MAPs). In prophase, at the onset of mitosis, duplicated centrosomes migrate around the nuclear envelope, which in Metazoa then breaks down in prometaphase. It is during this stage that spindle MTs are able to capture the chromosomes and direct them to the cell equator. In metaphase the pairs of sister chromatids are lined up along the equator, facing opposing poles. Once this has occurred the cell progresses into anaphase, where the cohesion between the sisters is lost and so allowing them to be moved toward opposing poles (Anaphase

A), which have now moved further apart (Anaphase B). During this stage the spindle also signals to the cell cortex, defining the position of the contractile ring which will drive cytokinesis. Formation of a contractile ring produces a cleavage furrow indicating where the two new daughter cells will divide. Once at the poles, the nuclear envelope reforms around the segregated sister chromatids as they begin to de-condense. Finally the cleavage furrow seals itself resulting in the formation of two identical daughter cells (Scholey *et al.,* 2003).

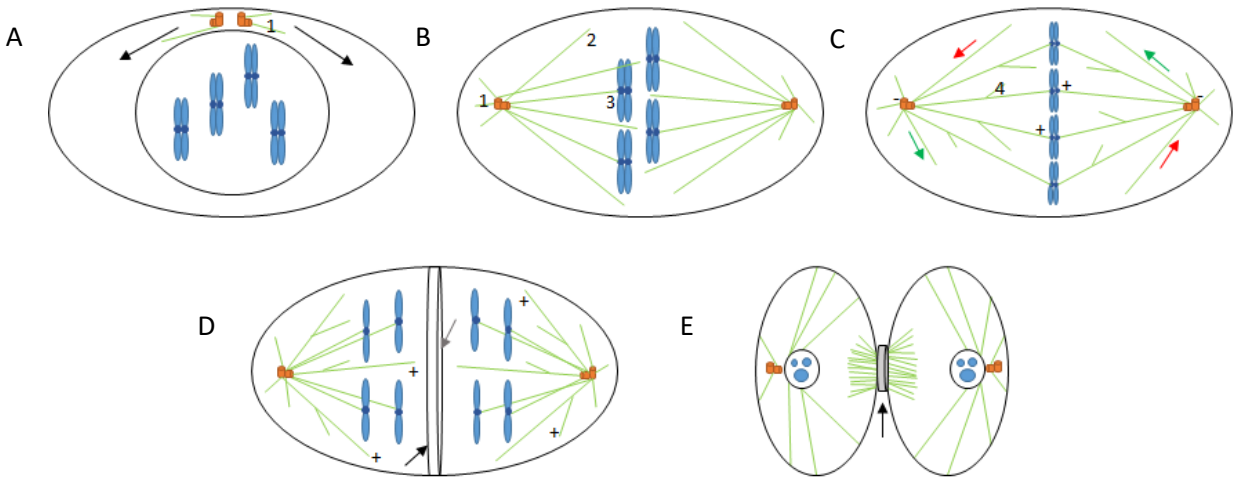


Figure 1-1 Microtubule populations during the different mitotic stages.

A] In prophase the centrosomes duplicate and move to the opposing poles (indicated by the arrows). The nuclear envelope is still intact at this stage, and the chromatin is condensing into chromosomes. Astral MTs [1] are forming from the centrosomes. B] In prometaphase the centrosomes are at the opposite poles and the nuclear envelope has broken down, allowing the kinetochore MTs [3] to attach to the kinetochores. C] By metaphase the bipolar spindle has formed and the chromosomes are aligned at the cell centre. There are now four subpopulations of MTs – 1] astral MTs, 2] interpolar MTs 3] kinetochore MTs and 4] Augmin generated MTs. Dynamic instability is also occurring within the spindle; MTs are able to grow [green arrow] and shrink [red arrow]. D] In anaphase the chromosomes move towards the poles and the spindle midzone consisting of the central spindle and the contractile ring. E] In telophase the midbody, a dense structure of central spindles is formed. This is created when the contractile ring causes a cleavage furrow.

Figure has been adapted from Wittmann *et al.,* 2001, Glotzer 2009 and Sarah Campbell MbyRes thesis 2014.

As described by Karsenti in 1993, MTs are an essential component of eukaryotic cells. During interphase, MTs are responsible for a number of processes including intracellular transport and maintaining the architecture of the cell (Hughes et al., 2008). As the cell progresses into mitosis the MTs are then primarily responsible for ensuring accurate chromosome segregation (Karsenti 1993). Within the mitotic spindle there are at least three different sub populations of MTs: astral MTs, interpolar MTs and kinetochore MTs (Figure 1-1). At the spindle poles astral MTs are nucleated and directed away from the centrosome in order to orient and position the mitotic spindle. Extending into the centre of the spindle are the interpolar MTs. Originating from opposing poles interpolar MTs interact with one another in an antiparallel fashion to stabilise the spindle's bipolarity. Kinetochore MTs connect the chromosomes to the spindle poles, and terminate at the outer region of the kinetochore (reviewed in Wittmann *et al.,* 2001).

MTs are dynamic polymers of α and β tubulin (Li *et al.,* 2012) in the form of a heterodimer, the head to tail association of which results in the formation of a MT protofilament, 13 of which associate to form the cylindrical MT structure (Amos and Klug 1974). During mitosis a number of changes in MT organisation occur. As the centrosome duplicates in prophase and the mother and daughter migrate around the nucleus, new MTs are nucleated and the MT network formed in interphase begins to fragment. In metaphase the MTs shorten dramatically and astral MTs are nucleated from the centrosome. At this stage MTs become highly dynamic, brought about because of changes of frequency between MT growth and shrinkage, any new MT growth now directed preferentially towards the centrosome (Karsenti 1991, Karsenti 1993).

### 1.1.1 Dynamic instability

MTs undergo dynamic instability; cycles of rapid polymerisation and depolymerisation that are transitionally repeated through events known as rescue and catastrophe (Figure 1-2). In terms of energy, dynamic instability is a costly process, however the fact that it is an evolutionarily conserved process would indicate it is of biological importance (Desai and Mitchison, 1997). The first evidence of the mitotic spindle being made up of dynamic linear components came from the arrival of polarisation microscopy; this allows MTs inside living cells to be observed

(Desai and Mitchison 1997; Inoué and Salmon 1995). MTs within the spindle are dynamic and display a half-life of around 60-90 seconds (Saxton *et al.,* 1984; Salmon *et al*., 1984). This rapid MT turnover is highly conserved and has been witnessed in a number of different cell types including fungal, invertebrate, vertebrate and plant cells (Hush, 1994; Zhai *et al*., 1996).

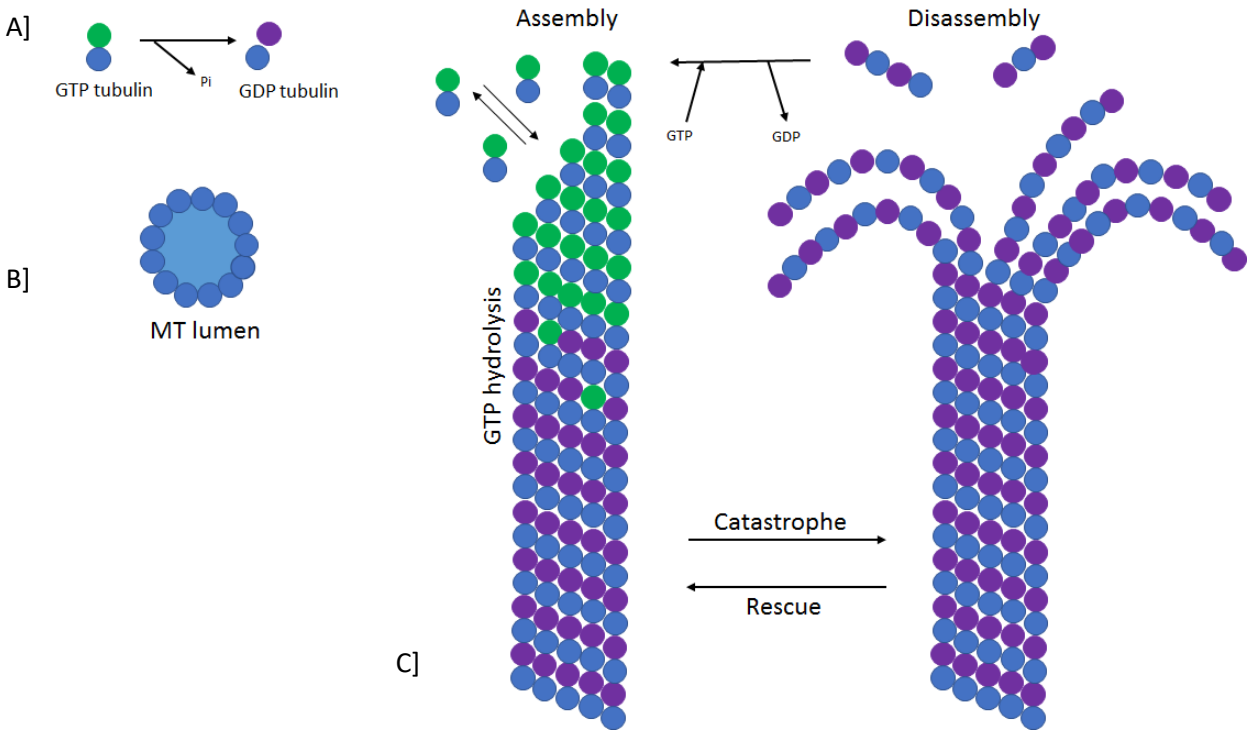


Figure 1-2 MT structure and dynamic instability.

A] MTs are composed of polymers of α (blue) and β (green/purple) tubulin.

B] Cross section of a MT. MTs are composed of 13 protofilaments forming a hollow tube.

C] Dynamic instability; cycles of rapid polymerisation and depolymerisation cause MTs to grow and shrink. Loss of the GTP cap from tubulin polymers causes the MT to become unstable and so catastrophe occurs.

Figure adapted from Al-Bassam and Chang 2011.

## 1.2 Pathways to mitotic spindle formation

The antiparallel array of MTs, minus ends at the spindle poles and plus ends growing towards the chromosomes, makes up the primary structural component of the mitotic spindle (Wittmann *et al.,* 2001). Building the mitotic spindle requires firstly that the MTs undergo structural changes, going from a state of polymerisation to depolymerisation via dynamic instability (Desai and Mitchison 1997). The length of the mitotic spindle is a key factor in the positioning of the chromosomes, particularly the spindle length in metaphase and anaphase B (Goshima and Scholey 2010). In the *Drosophila* embryo, at cycle 11 the metaphase spindle is on average 11.8 µm, it then extends to 16 µm post Anaphase B (Brust-Mascher et al., 2009). This change in length facilitates the separation of the chromosomes to the spindle poles.

At the onset of mitosis the cytoplasmic MTs disassemble and a bipolar spindle forms in their place (Cullen *et al*., 1999), this bipolarity ensuring that chromosomes are equally segregated into the two resulting daughter cells. Both the centrosome and the kinetochore can act as MT organising centres for MT nucleation and capture to regulate MT dynamics (Mitchison and Kirschner 1984; Hyman and Mitchison 1990). As well as at the centrosome and kinetochore, MTs can also be nucleated via chromatin and the protein complex Augmin (Figure 1-3); details of all of these mechanisms have been outlined below.

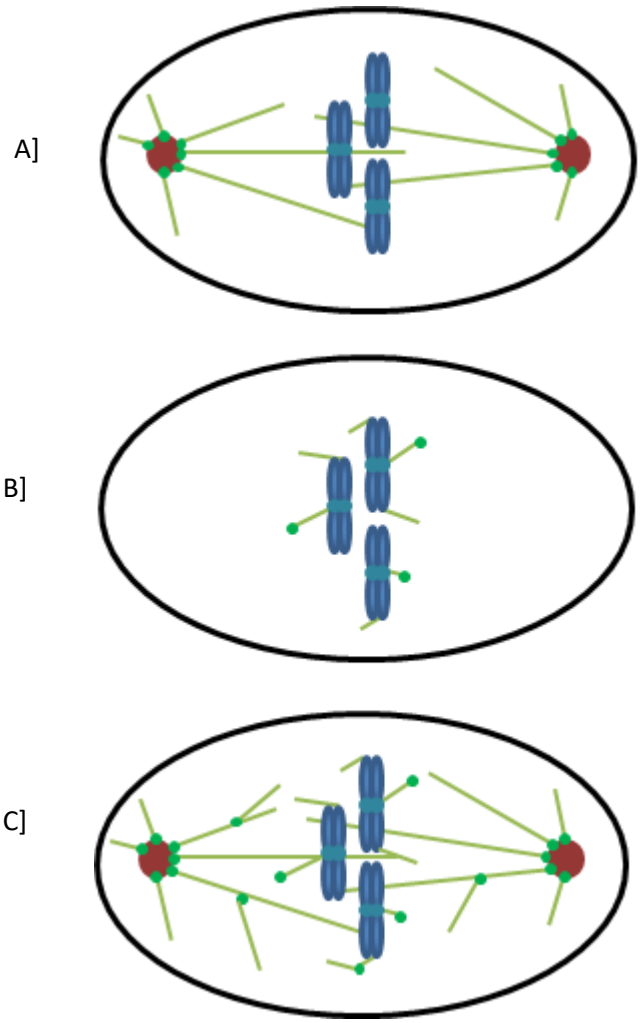


Figure 1-3 Mechanisms of mitotic spindle formation.

A] Centrosome mediated; MTs are nucleated from the spindle poles.

B] Kinetochore and chromatin mediated. This process typically occurs in the absence of centrosomes.

C] Augmin generated. The Augmin complex nucleates new MTs by recruiting γ tubulin to the pre-existing spindle.

Figure adapted from Duncan and Wakefield 2010.

### 1.2.1 Centrosomal nucleation of MTs

As stated, a number of early experiments have established that in animal cells the primary centre of MT organisation is the centrosome (Varmark 2004). The centrosome consists of a pair of centrioles that sit perpendicular to one another; these centrioles organise the surrounding pericentriolar material (PCM) (Bobinnec *et al.,* 1998). The increase in MT nucleation from the centrosome required to generate a spindle at the onset of both mitosis and meiosis, is dependent upon the actions of the centrioles and the PCM to recruit increased levels of the MT nucleating template gamma tubulin ring complex (γ-TuRC) at the spindle pole. This increase in MT nucleation at the centrosome results in the formation of astral MT arrays. These MT arrays initially grow radially, then grow directionally towards the chromosomes to ensure that the MT density between centrosome and chromosome is greater than that between the centrosome and cell cortex (Duncan and Wakefield 2010). This directionality leads to the capture of chromosomes at the kinetochore and the formation of the bipolar spindle structure.

### 1.2.2 Chromatin mediated MT nucleation

It is clear that not all cells utilise the centrosome mediated pathway of MT generation (Shimamura *et al*., 2004). The first genetic evidence that cells usually containing centrosomes could form a functional spindle without these structures, came from experiments carried out in *Drosophila melanogaster.* Centrosome maturation in humans is facilitated by the protein Pericentrin (Zimmerman *et al.,* 2004). In *Drosophila* the Pericentrin homologue Pericentrin-like Protein (D-PLP) carries out this function in conjunction with Centrosomin (Cnn) (Martinez-Campos *et al.,* 2004). In Cnn null mutants, the PCM fails to recruit to the centrosome; rendering them inactive, these mutants are however still able to form a spindle. These spindles are lacking in astral MTs yet are otherwise fully functional, adult flies being capable of developing into adulthood with very few observable defects (Megraw *et al.,* 2001). Given that these cells were still able to produce a mitotic spindle in the absence of centrosomes, it would indicate that other mechanisms of spindle formation are in place. Perhaps the most well characterised pathway of alternative spindle formation is that of chromatin mediated MT formation.

Formation of MTs around chromatin is dependent upon the small GTPase Ran (Carazo-Salas *et al*., 1999; Kaleb *et al.,* 1999), via the localisation of its guanine nucleotide exchange factor RCC1 (Moore *et al*., 2002; Li *et al.,* 2003). When nuclear envelope breakdown (NEB) occurs, RCC1 binds to the chromatin, generating a RanGTP gradient at the chromosomes resulting in MT assembly and hence formation of a spindle (Duncan and Wakefield 2010). Chromatin mediated spindle formation has been most clearly described in *Xenopus* egg extracts. The addition of chromatin coated beads to *Xenopus* egg extracts lacking in centrosomes initiates spindle formation. The spindles formed in this fashion were demonstrated to initiate at the chromatin, polarise into antiparallel arrays and ultimately focus at the poles, leading to morphologically normal, but anastral, spindles of a comparable length to those observed in the classical mitotic spindle (Heald *et al.,* 1996).

More recent work by Hayward *et al*., (2014) using *Drosophila* embryos, which are traditionally thought of forming exclusively using centrosomally-derived MTs, demonstrated that depolymerising the metaphase spindle via cold treatment and returning the embryos to room temperature caused spindles to regenerate predominantly from the chromatin. This chromatin based MT nucleation is meditated by the *Drosophila* homologue of the spindle assembly factor (SAF) HURP, and is dependent upon the MT amplification factor Augmin (detailed in section 1.2.4). A further, related, study also demonstrated again that chromatin mediated MT nucleation is dependent upon the generation of a RanGTP gradient (Hayward and Wakefield 2014).

### 1.2.3 Kinetochore driven MT nucleation

The third mechanism by which MTs can be generated is via the kinetochores. It was discovered a number of years ago that in mammalian tissue cells kinetochores can initiate MT polymerisation (McGill and Brinkley 1975; Snyder and McIntosh 1975). Since then it has been shown that in a normal mitotic cell the kinetochore MTs are incorporated into the growing spindle via capture by astral MTs (Khodjakov *et al*., 2003; Maiato *et al.,* 2004). Astral MTs seek out kinetochores in the classical search and capture model for chromosome alignment (Kirchner and Mitchison 1986). In this model, astral MTs from opposing poles attach to the kinetochore, however if MTs from the same centrosome attach to the kinetochore, the MT interaction will be

destabilised until the correct relationship is established (Duncan and Wakefield 2010). The mechanism by which kinetochores nucleate MTs appears to be dependent on RanGTP; depletion of SAFs HURP and TPX2 reduce MT formation at the kinetochores following catastrophe (Tulu *et al.,* 2006; Yang and Fan 2008).

### 1.2.4 Augmin generated MTs

The fourth mechanism of nucleating MTs is via the protein complex Augmin. Originally identified in *Drosophila,* (Hughes *et al.,* 2008 Goshima *et al.,* 2008), this Augmin complex localises together with a sub population of γ tubulin on existing spindle MTs; cells without Augmin form spindles with a lower MT density and an increased population of astral MTs (Goshima *et al*., 2008; Hughes *et al.,* 2008). The 8 subunit Augmin complex has been proposed to increase overall MT density by targeting the MT nucleating γ Tubulin ring complex (γTURC) to the pre-existing spindle MTs (Goshima *et al*., 2008; Uehara *et al.,* 2009).

## 1.3 Microtubule Associated Proteins

The normal function of the mitotic spindle is dependent upon the presence and actions of its associated structural components, including microtubule associated proteins (MAPs) (Ripoll *et al.,* 1985). Originally identified in mammalian brain tissues (Borisy *et al*., 1975) a MAP can be defined as a protein that forms an association with MTs, including MT motors and their cargoes (Collins and Vallee 1989). Proteins that bind MT ends (Vasquez *et al*., 1994) and those that associate with MTs in a manner dependent on the cell cycle (Maiato *et al.,* 2004) can also be described as MAPs. MAPs control the specific structure of MT networks (Cassimeris and Spittle 2001) and so demonstrate how protein-protein interactions can regulate function (Hughes *et al.,* 2008). With regards to the wider application of the study of MAPs, an understanding of MAP function and regulation is key to understanding the basic mechanisms of tumorigenesis and so can be a valuable tool in the design of novel cancer therapies (Tan *et al.,* 2008).

## 1.4 Using Drosophila as a model system

The *Drosophila* embryo exists as a 500 µm long syncytial cell. This syncytium contains a monolayer of between 1 and 1000 mitotic spindles of around 10 µm in length, depending upon developmental stage (Kellogg, Field and Alberts 1989). The lengths of these spindles are controlled by both intrinsic spindle mechanisms and by incomplete actin based metaphase furrows that form boundaries around the spindle (Sullivan and Theurkauf 1995). The study of MAPs in the *Drosophila* early embryo is particularly advantageous as embryos are readily available in a large quantity for biochemical analysis, and are amenable to techniques such as immunofluorescence and microinjection (Kellogg *et al*., 1989). Following fertilisation the somatic nuclei of the *Drosophila* embryo undergo 13 rounds of consecutive divisions (Foe and Alberts 1983). Up until round 7 of division the nuclei are all located within the interior of the embryo. During cycles 8 and 9 the nuclei migrate to the periphery where they form a monolayer beneath the plasma membrane early in the interphase of cycle 10. This is followed by four more rounds of division before cellularisation occurs at cycle 14 (Karr and Alberts 1986). When the migrating nuclei reach the periphery of the embryo, the nuclei are initially identical, however as they approach cycle 13 the nuclei appear to be different in their transcriptional patterns (Hafen *et al*., 1984).

*Drosophila melanogaster* is ideally suited as a model organism for the study of MAPs as its mitotic apparatus; the centrosome, kinetochores and spindle are similar to those found in mammalian cells (Moritz *et al.,* 1995). Furthermore, sequencing of the *Drosophila* genome revealed that 60% of human disease genes have *Drosophila* homologues (Schneider 2000) making flies an ideal disease model. Using *Drosophila* as a model system also allows MAPs to be studied within the context of a living organism (Cullen *et al.,* 1999).

## 1.5 Aims of this Masters by Research

The main aim of this Masters by Research was to focus on understanding the role of MT associated proteins in the formation of the mitotic spindle. By combining the techniques of biochemistry, proteomics and fluorescence imaging, I set out to identify and characterise the role of a subset of novel mitotic MAPs in order to understand how their cellular function and localisation may impact on the formation of the mitotic spindle. Secondly this project aimed to re-evaluate two known mitotic

MAPs – Abnormal Spindle Protein (Asp) and Drosophila Transforming Acid Coiled Coil (DTACC), to further understand and gain new insight into their roles in mitosis and bipolar spindle formation.

## 2. Materials and Methods

### 2.1 Resources used in this thesis

#### 2.1.1 *Drosophila* stocks

| **Stock name** | **Reference** | **Comment** |
|---|---|---|
| AspGFP | Renata Basto | GFP |
| D-TACCGFP | Jordan Raff | GFP |
| Histone 2B-RFP.pUASp-EB1GFP | Wakefield lab (D.Hayward) | GFP,RFP |
| Histone 2B-RFP.pUASp-EB1GFP/CyO; maternalαtubulin Gal4/MKRS | Wakefield lab (J.Chen) | GFP,RFP, driver |
| TRiP CG8142 RNAi(20) stock number 42489 | Bloomington | RNAi Valium 20 |
| TRiP CG8142 RNAi(22) stock number 36609 | Bloomington | RNAi Valium 22 |
| pUBQ RFC2GFP | This thesis | GFP |
| pUBQ RFC3GFP | This thesis | GFP |
| pUBQ RFC4GFP | This thesis | GFP |
| TRiP CG11788 RNAi (20) stock number 54043 | Bloomington | RNAi Valium 20 |

Table 1 – *Drosophila* stocks used throughout the duration of this MbyRes

2.1.2: Antibodies

| Antibody name | Type | Concentration | Reference |
|---|---|---|---|
| Mouse anti-GFP | Mouse polyclonal | 1:1000 | Roche - 11814460001 |
| Rabbit anti-mouse IgG-HRP | Rabbit polyclonal | 1:10000 | Sigma – A9044 |
| α Tubulin DM1A | Mouse monoclonal | 1:1000 | Sigma – T6199 |

Table 2 – Antibodies used in this MbyRes

2.2 *Drosophila* work

2.2.1 Maintaining stocks

Flies were kept on basic culture medium in either plastic vials or bottles sealed with flugs - bonded, dense weave cellulose acetate plugs (all from Dutscher Scientific). All fly work was carried out at room temperature and stocks kept at 25°C. To alter expression of RNAi, or to slow development stocks were moved to 18°C or 28°C to accelerate said processes. Adult fly stocks were knocked into new vials/bottles once every two days; distilled water and dried yeast was added when necessary for further maintenance of media. Lab stocks were knocked into new food once every two weeks. Fly pushing techniques were carried out as described by Greenspan (2004).

2.2.2 Collecting flies for crosses

Flies were collected twice a day, and maintained at 25°C (TRiPCG8142 RNAi Valium 22 was kept at 18°C to reduce expression of RNAi). Virgin females are recognisable by the presence of meconium in the abdomen; this indicates recent emergence from the pupae and hence an inability to mate.

2.2.3 Collecting embryos

Flies were knocked into a collection chamber sealed with an apple juice agar plate (30% apple juice, 2.5% agar – Agar No 2 Bacteriological Lab M Limited). Flies were left to lay at 25°C, with a small amount of yeast paste (dried baker's yeast and distilled water) on the agar plate for sustenance. Embryos collected for biochemistry

were 0-3 hours old, those for imaging 0-2 hours old. Embryos were bleach dechorionated and then flash frozen with liquid nitrogen, and stored at -80° if not being immediately used.

### 2.2.4 Treating embryos with MG132

Embryos were collected as outlined above, and then added to a solution containing 2 mL PBS (Melford), 10 µL 10mM MG132 (Sigma) and 1 mL heptane (Fisher Scientific). The embryos were incubated at room temperature, with shaking, for 20 minutes. Post incubation embryos are removed from solution using a cut pipette tip, and washed in collection apparatus with “embryo wash” (distilled water containing 0.05% Triton X-100 (Sigma) Embryos were then flash frozen and stored as detailed above.

### 2.2.5 Hatch rates

Flies were knocked into a collection chamber (see 2.1.4) and allowed to lay overnight (4pm – 9am). From the overnight plate 100 embryos were placed in groups of 10 around the edge of a fresh apple juice agar plate. These embryos were then incubated at 25°C (18°C for TRiPCG8142 RNAi (22)) for 24 hours, and then the number of hatched embryos recorded. Plates were then incubated for a further 12 and 24 hours, with hatch rates being recorded at each time point.

### 2.2.6 Fixing MG132 treated embryos

MG132 treated embryos were added to a tube containing 0.5 mL heptane (Fisher Scientific) and 0.5 mL methanol, then shaken for 30 seconds. The embryos were allowed to settle, and then all liquid was removed and replaced with 1mL methanol. The tube was inverted, and once the embryos had settled, all liquid removed and replaced. This was carried out a total of 3 times. Fixed embryos were then stored at 4°C.

### 2.2.7 Staining embryos

The methanol was removed from fixed embryos, and 1mL of PBST (PBS 0.1% Tween 20 (Sigma)). was added. Embryos were left to rotate in the PBST for 10 minutes. The PBST was then removed and this step repeated twice more. Embryos were then blocked in PBST 3% BSA (Sigma) for 30 minutes, rotating at room

temperature. Block was then removed and an appropriate primary antibody was added in PBST, embryos were then incubated at 4°C overnight. Embryos were transferred to a fresh tube and washed 3x with PSBT for 10 minutes. An appropriate 2° antibody was then added in PSBT and the embryos incubated for 2 hours at room temperature. The secondary antibody was removed and the 3x PBST washes repeated. Embryos were then washed with 1/1000 5 mg/mL Hoechst (Sigma) in PBST for 10 minutes. Hoechst wash was removed and a final PBST wash carried out. Embryos were pipetted up and allowed to settle, then dropped onto a 76 mm x 22 mm microscope slide (Fisher brand). 2 drops of mounting media (0.25 g N-N-Propylgallate, 1.5 mL $dH_20$ and 10 mL glycerol) was added and a 22 x 22mm coverslip placed on top of the embryos, the edges sealed with clear nail polish. Slides were stored at -20°C.

## 2.3 Genetic crosses

### 2.3.1 Cross set up to generate non MKRS males

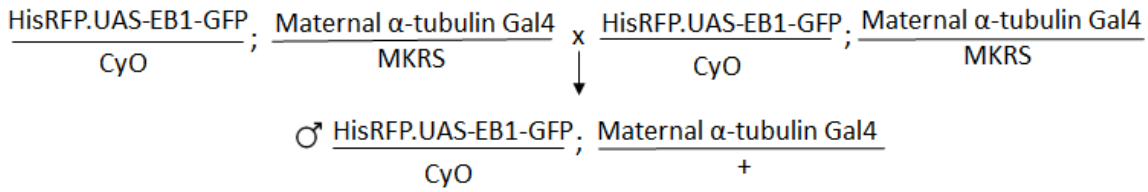


Figure 2-1 Genetic cross set up to generate non MKRS males, for crossing to virgin females of each RNAi line

Maternal α-tubulin is a driver for the RNAi. Using non-MKRS flies ensures homozygosity on the 3rd chromosome carrying the driver. HisRFPUasEB1GFP/CyO refers to flies carrying RFP tagged histone and GFP tagged EB1 over the CyO balancer.

## 2.3.2 Crosses set up to drive the RNAi, and express HisRFP and EB1GFP

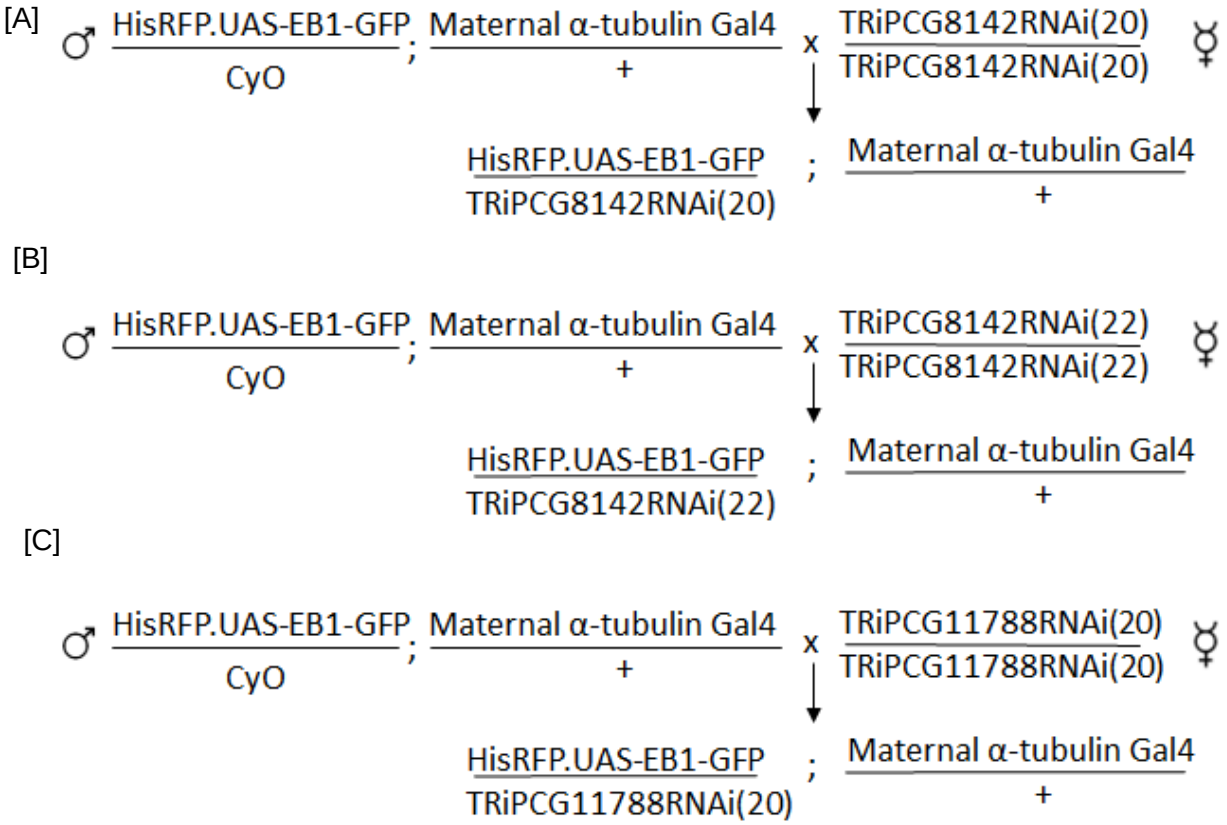


Figure 2-2 Crosses set up to drive the RNAi, and express HisRFP and EB1GFP for RNAi lines TRiPCG8142RNAi (20) [A], TRiPCG8142RNAi (22) [B] and TRiPCG11788RNAi (20) [C]

Embryos laid by the crosses below were collected and used for imaging.

Note – TRiPCG8142RNAi (20) is on the 2nd chromosome, TRiPCG8142 (22) and TRiPCG11788RNAi is on the 3rd chromosome.

## 2.4 Cloning

### 2.4.1 Cloning the RFC subunits (RFC2, RFC3 and RFC4)

Entry clones were produced by GeneArt® (Life Technologies, USA). CDS regions of the desired RFC subunits were cloned into pENTR vectors generating pDONR RFC entry clones (for vector maps and all sequences see Supplementary Information). To generate RFCGFP flies, LR Clonase II™ (Invitrogen, USA) was used to transfer the pDONR RFC into the 69-pUBQ-mGFP-CT-Dest destination vector (gifted by Jordan Raff, University of Oxford), tagging the RFC subunit with mGFP at the C terminus (for full cloning procedure see the Gateway™ technology manual – Life Technologies, USA). Vectors were then transformed into One Shot® Top 10 Competent *E.coli* (Life Technologies, USA). 69-pUBQ-mGFP-CT-dest RFC plasmids were harvested from 2mL bacterial cultures formed from single colonies grown on LB kanamycin agar plates, using a QIAprep Spin Miniprep Kit (Qiagen, Netherlands). Restriction digests using either *Bam*HI or *Bgl*II and *Eco*RV enzymes (New England Biolabs, USA), and DNA gel electrophoresis on a 1% gel was performed to select plasmids containing the RFC subunits. Selected colonies were sequenced using self-designed primers to check for mutations (Eurofins MWG, Germany). Plasmids were then sent to BestGene, Inc, USA, where they were injected into $w^{1118}$ *Drosophila* embryos. 69-pUBQ-mGFP-CT-dest RFC flies were then selected based on the presence of the mini white gene in the destination vector, producing an orange/red eye colour.

For full gene sequences and vector maps see Supplementary Figures S2-S5

### 2.4.2 Sequence analysis

All sequence analysis and alignments were carried out using BLAST – Basic Local Alignment Search Tool (NCBI). ApE (Wayne Davis, University of Utah) was used to generate plasmid maps. FASTA and CDS sequences for the RFC subunits were obtained from Flybase.

## 2.5 Biochemistry

### 2.5.1 Making embryo extracts

Frozen 0-3 hour embryos were homogenised with equal volumes of C-Buffer (50mM HEPES pH 7.3, 50mM KCl, 1mM $MgCl_2$, 1mM EGTA, 1mM PMSF, 0.1% NP40, protease inhibitor [Roche], phosphatase inhibitor [Roche]), using a dounce homogeniser attached to an electric drill.

Note: for the MT spin down assay carried out using Benzonase nuclease (Sigma), 25µL of nuclease was added to the homogenised embryos which were left to incubate at 4°C for 40 minutes. The protocol then continues as described in section 2.5.3.

### 2.5.2 Sample preparation for biochemistry

To samples required for biochemistry, 2x protein sample buffer (PSB) (88% PSB [62.5 mM Tris-HCL, 2.5% SDS, 0.002% bromophenol blue, 0.7135 M (5%) β –mercaptoethanol, 10% glycerol] 12% 1M dithiothreitol [DTT]) was added, and then samples incubated at 95°C for 10 minutes.

### 2.5.3 Clarifying embryo extracts

Embryo extracts were centrifuged at 15,000g at 4°C for 10 minutes (Sigma 1-14 table top centrifuge). Supernatant was transferred to a micro ultracentrifuge tube (Beckman Coulter) and centrifuged at 100,000g at 4°C for 45 minutes (Beckman Coulter Optima Max ultracentrifuge). Supernatant was then transferred in a clean tube, using a needle and syringe, then centrifuged at 100,000rpm for a further 15 minutes. Final supernatant was transferred to a clean tube with a needle and syringe.

### 2.5.4 Microtubule spin down assay

To clarified embryo extract generated from ~200 mg embryos, GTP (Sigma) and DTT (Sigma) was added to a final concentration of 1mM. Extract was then quickly vortexed and split into two equal fractions. Both fractions were incubated at 25°C for 10 minutes, then one fraction put on ice. To the other sample, Taxol (Sigma) was added to a final concentration of 10µM, this was then incubated at 25°C for 10 minutes. Post incubation samples were layered over two volumes of C-Buffer with a

40% sucrose (Sigma) cushion, and centrifuged at 100,000g at 4°C for 30 minutes. 50µL of resulting supernatant was removed and added to 50µL of 2x sample buffer, the remaining supernatant discarded. 100µL of C-Buffer was pipetted onto the surface of the sucrose cushion, then immediately removed, to wash the interface. All remaining buffer was removed and to the resulting pellet 50µL of 1x sample buffer was added. Once the pellets were solubilised the samples were heated at 95°C for 10 minutes.

### 2.5.5 Immunoprecipitation assay

Embryo extract generated from ~400mg of embryos was centrifuged at 11,000g for 10 minutes at 4°C (Sigma 1-14 table top centrifuge). Using a needle and syringe the supernatant was transferred to a clean micro ultracentrifuge tube then centrifuged at 100,000g for 10 minutes at 4°C. The supernatant was transferred to a new tube and centrifuged at 100,000g for 60 minutes at 4°C. 30 µL GFP-TRAP-A beads were added to 1mL of C-Buffer then spun at 2000rpm for 30 seconds, rotated 180° and spun for a further 30 seconds. The C-Buffer was removed and replaced with a further 1mL. This was repeated twice more. 20µL of high speed supernatant was added to 20µL 2x sample buffer for western blotting. The beads were then added to the remaining high speed supernatant, and left to incubate for 2 hours at 4°C. A sample of the supernatant was taken and added to 2 times sample buffer as before, then all other supernatant discarded. The beads were then washed three times (as above). 100µL of beads were taken and added to a new tube, the 2 samples (100µL and 900µL) were centrifuged for 30 seconds, with rotation. From the 900µL sample, all supernatant was removed and the beads flash frozen to be sent for mass spectrometry (Bristol proteomics facility). From the 100µL sample, 80µL was removed and replaced with 20µL 2x sample buffer. Samples containing sample buffer were heated at 95°C for 10 minutes and analysed via western blot.

### 2.5.6 GFP loading control

1µL of 17µg/µl GFP was added to 1ml 1x PSB, then 200µl of this was added to 1mL $dH_2O$ resulting in a final dilution of 1/5000.

### 2.5.7 Gel electrophoresis

SDS polyacrylamide gel electrophoresis (SDS-PAGE) was used to analyse protein samples obtained from the microtubule spin downs and immunoprecipitations. The protein samples were loaded on 10% gels and run at 150V (constant) for 90 minutes at room temperature. Gels were then prepared for western blotting.

### 2.5.8 Western blotting

Following gel electrophoresis, protein samples were transferred onto nitrocellulose membrane (Fisher Scientific) for 60 minutes at 250 mA (constant). The membrane was then blocked in a solution of 5% milk powder in TTBS (0.1% Tween-20 and 1 X TRIS buffered saline) for 30 minutes. An appropriate 1° antibody in block was added and the membrane probed, rotating at 4°C overnight. Following 3x 5 minute washes in TTBS an appropriate 2° antibody was added in block and the membrane incubated, with rotating for 2 hours at room temperature. Membrane was then subjected to a further 3x 5 minute washes in TTBS before being transferred to MilliQ water. The antibody was then detected using X-ray film, using ECL Western Blotting substrate (Pierce), as according to manufacturer's instructions.

## 2.6 Imaging

### 2.6.1 Imaging live embryos

To visualise the sub-cellular distribution of GFP fusion proteins, time-lapse fluorescence microscopy was carried out on 0-2 hour old transgenic embryos expressing the relevant construct. Embryos were removed from the collection plate using a fine paintbrush, and gently placed on a piece of double sided tape. Embryos were then dechorionated under a dissecting microscope, using tweezers. Dechorionated embryos were then placed on a 22x22 coverslip coated with a thin line of heptane glue, and covered with halocarbon oil (Sigma) to prevent desiccation. The embryos were imaged on a Yokogawa CSU-X1 spinning disc confocal microscope. A time lapse series typically consisting of a 5-image Z stack (1µm between images) every 2 seconds was carried out for a round of mitosis in cycle 9-13 embryos at 60x magnification. Movies and images were then analysed using Image J software.

### 2.6.2 Cold treating embryos

For the cold treatment assays, embryos were prepared and imaged as above, until metaphase was reached. At this point the coverslip was removed and placed into a 50mm ice cold Petri dish, the covered in 4°C halocarbon oil. Following a 90 minute incubation on ice the embryos were imaged further, with typically 30 seconds between removal from the ice and return to imaging.

## 3. Application of proteomics to identify novel mitotic MAPs

### 3.1. Introduction

Whilst the genome of an organism will not vary from cell to cell, the proteome will differ (Han *et al*., 2008). The proteome refers to the full complement of proteins expressed in an organism; proteomics can therefore be described as the study of the structure and function of proteins (National Cancer Institute). Using proteomics allows for information such as protein abundance, variations and modifications to be assessed on a large scale and hence can lead to a greater, more comprehensive understanding of specific cellular processes.

The use of proteomics should ultimately aim to address one of the following questions: will it enable the generation of protein linkage maps, allow for protein identification that could potentially alter or correct genomic sequences, or can the results be used to analyse protein expression profiles to infer cellular function or state? (Aebersold and Mann 2003).

The field of proteomics is made up of a number of different techniques, with mass spectrometry (MS) being at the forefront for analysis of complex protein samples. Advances in MS have led to the expansion of the proteomics field in recent years. The use of MS based protein identification has allowed for high-throughput analysis of proteomes being a reality (Gstaiger and Aebersold, 2009). MS is a tool that allows the mass of a molecule, or more specifically the mass to charge (m/z) ratio to be accurately measured. Mass analysis uses an electromagnetic field within a vacuum, meaning that before they can be analysed molecules need to carry an electric charge and be in the gaseous phase. Once in this state the m/z ratio of the molecules can be determined based upon their trajectory within the electromagnetic field (Figure 3-1). In most cases it is the mass of a protein's constituent peptides that is measured, rather than the mass of the protein itself; this yields a mass spectrum of m/z ratios plotted against an ion current. Peptides can also be fragmented via collision with an inert gas. This then produces a tandem mass spectrum (MS/MS): a list of m/z ratios for the different fragments rather than the whole peptide mass (Walther and Mann 2010).

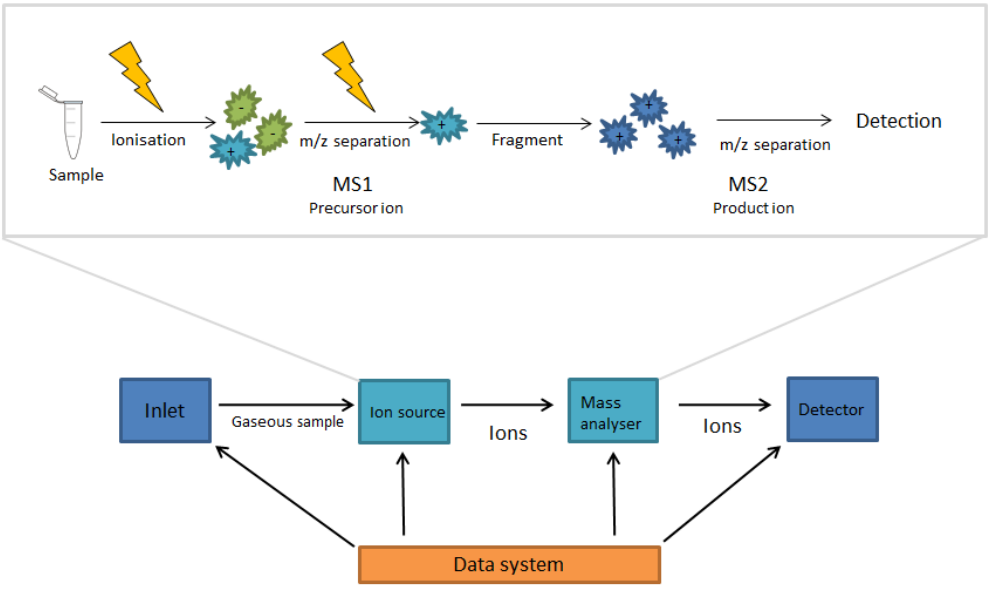


Figure 3-1 Schematic of a mass spectrometer (Adapted from Kang 2012).

Gaseous molecules are ionised in the ion source forming molecular ions, some of which will fragment. The ionised sample is sorted according to its mass to charge ratio. Ions of differing mass to charge ratio will pass through the analyser, towards the detector, one at a time. When an ion hits the detector it is converted into an electrical signal (Sparkman, 2000). These signals produce an output, giving information about the relative abundance of each ion in the original sample.

In many cases it is important to define how the levels of a protein change from one condition to the next. Protein abundance is a crucial variable, the goal of many biological purifications being to determine if a particular protein is enriched in a specific fraction, rather than simply identifying if it is present (Walther and Mann 2010). MS is not an inherently quantitative process therefore specialist techniques are required to obtain information regarding protein abundance. Historically this has been overcome by using MS in combination with gel electrophoresis, however more recently a number of labelling techniques have been developed that allow for the comparison of protein samples (Veraska 2010).

Quantitative proteomics has been successfully applied in *Drosophila* in recent years (Veraska 2010). *Drosophila* has always been a favoured model system when studying fundamental genetic principles, however it has now emerged as an important organism in the experimental analysis of higher eukaryotes and human disease (Beller and Oliver 2006; Bier 2005). There are a number of advantages to using *Drosophila* as a proteomic model system. *Drosophila* allow for the rapid progression from high throughput screen to functional assay. Mutant alleles, transgenic construct and inducible RNAi reagents are available for many *Drosophila* genes, making transitioning from screen to assay a quick process (Veraska 2010). Many of the regulatory mechanisms and signalling pathways of the cell are conserved between flies and mammals, making them an ideal model for studying human disease (Bier 2005; Veraska, Del Campo and McGinnis 2000). *Drosophila* is also ideal for large scale biochemical assays because of their developmental process. The *Drosophila* life cycle has four distinct stages: embryo (0-24 hours), 3 larval stages (4 days), a pupal stage (4-4.5 days) and finally the adult stage which can last up to one month (Ashburner, Howley and Golic 2005); at each stage of the life cycle *Drosophila* can be separated and collected in large quantities of either cycling or synchronised populations (Veraska 2010).

Tandem tags, now typically known as isobaric tags, were so named to indicate their use in tandem MS (MS/MS) (Thompson et al., 2003). Isobaric tags are a useful tool as they facilitate the analysis of multiple samples at one time: commercially available tags allowing up to 8 samples to be analysed in one MS run. Tags will differ between manufacturers but the basic components will remain the same, consisting of a mass reporter with a unique number of $^{13}C$ substitutions and a mass normaliser to balance

the mass of the tag making all tags equal in mass. By having equal masses the tags allow both heavy and light isotopologues to co-elute. Isobaric tags are designed so that upon high energy collision induced dissociation they will cleave at a specific linker region; this cleavage yields different sized tags that can be quantified by liquid chromatography (LC) MS/MS. Before samples can be tagged they must first be digested using an enzyme such as trypsin. Digested proteins are then mixed with the tags, combined to make one sample and then analysed using MS/MS.

In this thesis quantitative proteomic analysis has been applied to distinguish between protein classes that differentially associate with microtubules (MTs) depending upon cell cycle stage, and thus aiding the identification of microtubule associated proteins (MAPs) in the *Drosophila* early embryo. Prior to the start of this study, MT co-sedimentation assays were carried out in triplicate on both cycling and MG132 treated mitotic populations of 0-3 hour *Drosophila* embryos (see Materials and Methods). MG132 is a drug that inhibits the 26S proteasome and therefore arrests cell cycle progression at the metaphase/anaphase transition. Unlike other drugs that arrest the cell cycle in mitosis, such as colchicine, nocodazole or taxol, this occurs without changes to MT dynamics. The samples obtained from the co-sedimentation were analysed using tandem mass tagging MS (Figure 3-2).

Application of quantitative comparative (QC) MAP proteomics has shown that as predicted, a number of MAPs that function during cell division increase their association with MTs in mitosis. As detailed below, analysis of this data set has allowed me to identify identified a number of other protein classes, not previously recognised as MAPs, which bind to MTs in both cycling and mitotic populations, but that show a statistically significant increase in their affinity for MTs during mitosis.

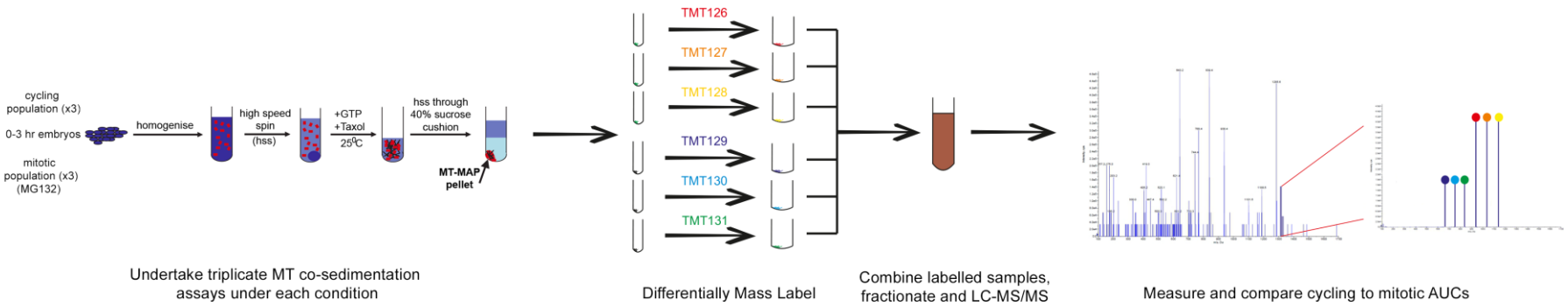


Figure 3-2 Preparation of samples for tandem mass tagging liquid chromatography (TMT LC) MS/MS.

Samples were generated from triplicate repeats of MT co-sedimentation assays of cycling and mitotic 0-3 hour Drosophila embryos. Samples were then digested with trypsin then tagged using isobaric mass tags. Tagged samples were then combined and analysed using LC MS/MS, creating an ion spectrum. This spectrum can then be assigned to specific peptide sequences and organised into a predicted protein sequence (Life technologies).

Figure courtesy of J.G.Wakefield

## 3.2 Results and Discussion

### 3.2.1 QC proteomics reveals a number of novel mitotic MAPs

The project began by filtering and analysing the raw mass spectrometry data obtained from the 6-plex, cycling versus mitotic, comparative proteomics. Three linked filters were applied (i) a 95% confidence rate, (ii) a score of >30 and (iii) >3 peptide hits. A 95% confidence interval indicates if the same sampling method is used, we would expect the true population parameters to fall within our interval estimates 95% of the time (Stattrek.com). MS score is a composite, comparative value that encompasses factors such as area under the curve, number of peptides and percentage coverage. The score and peptide filters were applied as proteins with an MS score of <30 or <3 peptide hits are likely to be mis-reads and not actually present in the sample (for full data set see Supplementary Table 1).

This filtering resulted in the inclusion of 735 individual proteins that co-sedimented with MTs in all 6 samples. These results are comparable to a previous screen carried out by Hughes *et al*., (2008) which identified 270 proteins; 70% of the proteins identified in the Hughes screen were present in our data set (60% included, 10% excluded by data filter). The large difference in number between the two screens is reflective of the methods carried out. Hughes undertook 1D and 2D gel electrophoresis prior to MS and did not process all of the 2D spots identified as MAPs. Moreover, the sensitivity of MS has increased since the Hughes study was published (2008). As an initial validation step the Gene Ontologies (GO) of the MAPs were manually identified using the functional GO annotations on Flybase. To determine whether functional classes of verified MAPs behaved consistently in terms of their association with MTs under the two experimental conditions, I initially focused on ribosomal proteins. 87 MAPs had a functional GO of ribosome, of these 85 showed a decrease in mitosis, indicating that ribosomes decrease their association with MTs during cell division. Next, I identified all MAPs with known mitotic functional GOs. 123 proteins in the data set have previously recorded mitotic GOs, of which 89 proteins increased their MT affinity during mitosis when compared to cycling levels (Figure 3-3). Together this preliminary analysis provides strong evidence that functionally related proteins behave consistently between conditions.

A]

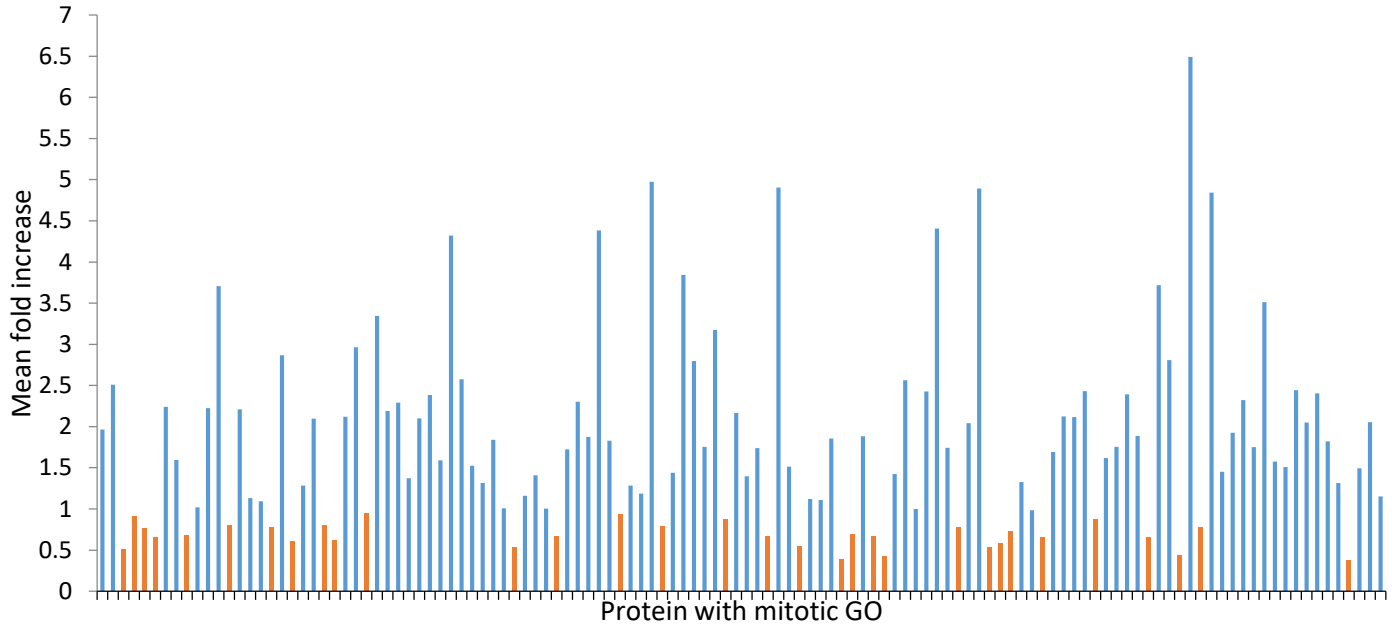


B]

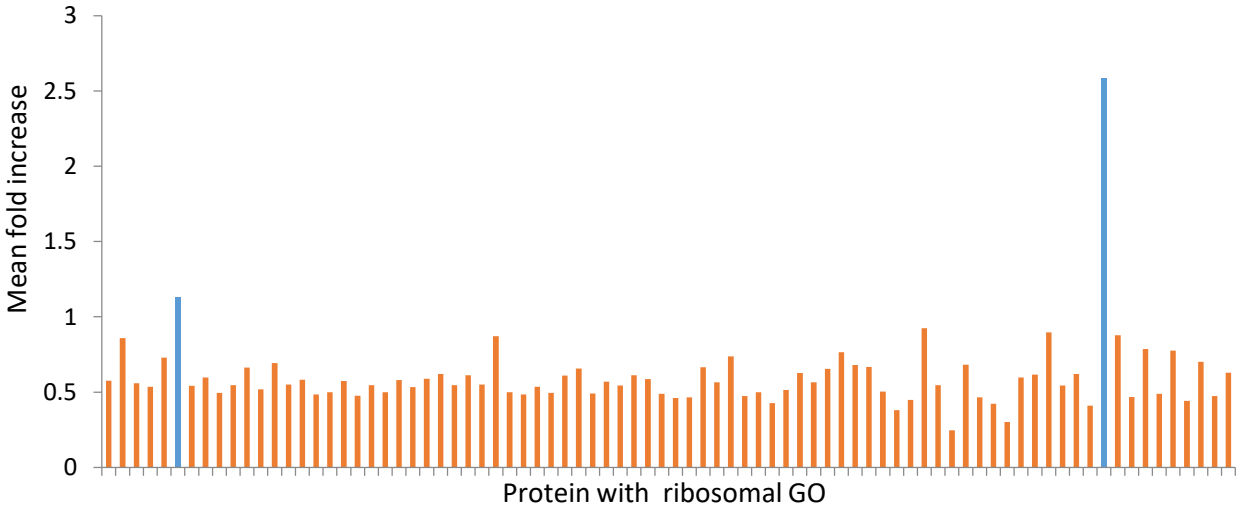


Figure 3-3: Screen identifies 123 MAPs with known mitotic function GOs, 89 of which show increased mitotic MT association.

A] Mean fold increase of MAPs with known mitotic function GOs in mitotic samples when compared with the cycling populations.

B] Mean fold increase of known ribosomal proteins in mitotic samples, compared with the cycling populations.

Bars in red indicate a decrease in association. For full data set see Supplementary Table 2 and 3.

### 3.2.2 Stringent statistical analysis reveals 16 proteins with a significantly increased MT association in mitosis

The whole data set was next analysed statistically via independent t-test, in order to identify proteins that are significantly over or under represented in mitosis. Out of 735 proteins tested only 16 showed a statistically significant increased association with MTs in mitosis (Table 3), including members of the Augmin complex: Dgt2-6 and Wac. Formation of a functional mitotic spindle requires MTs to be nucleated from within the spindle; this process is dependent upon Augmin (Kamasaki *et al*., 2013).In both humans and *Drosophila* the Augmin complex is made up of 8 proteins (Uehara *et al*., 2009). This result correlates with the Hughes study, which identified all 8 Augmin subunits, showing they were required for spindle formation.

The assay also identified the spindle assembly factor Mars/dHurp (*Drosophila* homologue of HURP) as having a significantly increased association with MTs in mitosis. Mars localises to the nuclei in interphase, this localisation then shifts to the mitotic spindle, specifically the poles; Mars being required for the organisation and stability of the mitotic spindle (Zhang *et al*., 2009); Mars is also required in chromatin mediated MT nucleation (Hayward 2014).

Finally of known mitotic function, with a significant increase in MT association in mitosis were the proteins Patronin and Klp10A. In a study by Goodwin and Vale (2010) it was stated that in *Drosophila* S2 cells, Patronin was required to stabilise the MT minus ends; a loss of Patronin causing the minus ends to lose subunits, resulting in sparse arrays of MTs in interphase and short disorganised spindles during mitosis. This study also reported that Patronin may act as a cap to stabilise the MT minus ends, thus giving it a critical role in MT organisation and spindle formation (Goodwin and Vale, 2010). Like Patronin, Klp10A also has a number of different mitotic functions. It has been reported that during interphase and prophase Klp10A concentrates at the MT plus ends, then re-localises to the centromeres and spindle poles upon NEB where it remains for the remainder of mitosis (Goshima and Vale 2005). It was presented in a study by Goshima and Vale (2005) that RNAi of Klp10A in S2 cells, results in the formation of monopolar and monastral bipolar spindles with long astral MTs. Rogers *et al* (2004) suggested that Klp10A also plays a role in anaphase A chromosome motility, and is able to drive MT depolymerisation at the centrosome.

Based on the information presented above, it is unsurprising that this particular subset of proteins showed a significant increase in MT association during mitosis. The assay also identified three proteins, CG14309, Row and Hop which have not been previously recognised as MAPs, or as having any mitotic function. There is very little information regarding the localisation and function of CG14309; however it was recorded by Cermelli *et al* (2006) to be a lipid droplet protein. It has also been regarded as a potential regulator of early embryogenesis in *Drosophila*, as inferred by 2D gel electrophoresis (Krauchunas, Horner and Wolfner, 2012). However there is no evidence to suggest CG14309 associates to the MTs or has a mitotic function. The *Drosophila* protein Relative of Without Children (Row) is a zinc finger protein that alongside Without Children (Woc) acts as a putative transcription factor. Row and Woc also act together to facilitate the binding of the *Drosophila* homologue of heterochromatin protein 1 (Hp1c) to chromatin; these proteins together have been reported to regulate a gene expression programme that is partially executed in the nervous system (Font- Burgada *et al*., 2008). Like CG14309, there is currently no evidence to suggest this protein is a MAP. The final protein shown to be significant following our stringent data analysis, yet not reported as a MAP was Hsp70/Hsp90 organising protein homologue (Hop). The primary role of Hop was first inferred based on a structural similarity to the *S. cerevisiae* protein STI1; this protein playing a role in unfolded protein binding and protein folding (Flybase, 1992). Hop was reported to act as a co chaperone that directly associates with heat shock proteins Hsp70 and Hsp90, and is proposed to act as an adaptor directing Hsp90 to Hsp70 protein complexes in the cytoplasm (Odunuga, Longshaw and Blatch 2004). Hop is primarily a nuclear protein therefore it was surprising that it appears not only as a MAP, but as a MAP showing a 2 fold increased MT association in mitosis, despite there being no evidence for a mitotic role or MT interaction.

Following the first round of analysis we found that only 13%of known mitotic MAPs fell above the alpha value for significance ($p \leq 0.05$). To test whether this low proportion was a result of variability between individual datasets, further statistical testing using a Levenes test for homogeneity of variance was carried out (Supplementary Figure S6). As suspected, the analysis revealed that there was a significant difference between the data points about the mean for the mitotic data set. Looking more specifically, the 3$^{rd}$ mitotic repeat appeared to be much lower

scoring than the previous 2 rounds. Based upon this observation it was decided to remove this data set and repeat the original independent samples t-test. This resulted in many more known mitotic MAPs becoming significantly enriched in the mitotic co-sedimentation analysis. For example, the protein Abnormal Spindle (Asp), a protein required for mitotic spindle organisation and aster formation (do Carmo Avides and Glover 2001) fell outside of the original highly stringent significance cut-off, but was significant once the 3rd mitotic data set was excluded.

By applying this practice to the entire data set, 209 proteins now presented as being significantly increased in their biochemical association with MTs during mitosis; 64 of these had an existing mitotic GO, as described in Flybase. When looking only at the known mitotic MAPs, 64% now show a significant increase in MT association in mitosis having applied data filter described above, compared to the 13% when looking at the data set as a whole. Those that remain non-significant maintained, or presented a slight decrease in their level of MT association between the cycling and mitotic populations. One of the highest scoring non-significant mitotic MAPs is Map205, with a cycling mean of 1.3 and a mean score of 1.2. Map205 is the *Drosophila* homologue of MAP4, a general MAP that appears to bind all MTs non-specifically in human cells. Map205's role in mitosis was identified through its association with Polo (Archambault *et al*., 2008) where it localises to centrosomes and the mitotic spindle in order to facilitate the MT binding of the mitotic kinase, Polo (Pereira *et al*., 1992). Given that it scored so highly MS (score 802.2) it is likely this MAP does not need to increase its MT association in order to carry out its mitotic role.

| Name | Score | Mean (cycling) | SD | Mean (mitotic) | SD | P value | MFI |
|---|---|---|---|---|---|---|---|
| CG14309 | 40.25 | 1.458 | 0.451 | 2.9 | 1.49 | 0.004 | 1.98 |
| Row | 40.25 | 1.458 | 0.451 | 2.9 | 1.49 | 0.004 | 1.98 |
| Patronin | 33.28 | 1.398 | 0.352 | 2.9 | 0.60 | 0.022 | 2.07 |
| Mars | 199.80 | 1.431 | 0.379 | 3.0 | 0.37 | 0.006 | 2.09 |
| Hop | 246.68 | 1.248 | 0.246 | 2.7 | 0.83 | 0.047 | 2.16 |
| Grip84 | 58.13 | 1.495 | 0.457 | 3.6 | 1.17 | 0.042 | 2.46 |
| CaM | 187.29 | 1.163 | 0.147 | 3.9 | 1.95 | 0.037 | 3.35 |
| Nup358 | 349.21 | 1.598 | 0.563 | 5.6 | 1.76 | 0.02 | 3.50 |
| Klp10A | 320.10 | 1.512 | 0.553 | 5.6 | 1.31 | 0.007 | 3.70 |
| Cep135 | 67.14 | 1.368 | 0.320 | 5.7 | 1.70 | 0.013 | 4.16 |
| Dgt5 | 170.42 | 1.595 | 0.635 | 6.9 | 1.014 | 0.002 | 4.32 |
| Dgt2 | 71.82 | 1.582 | 0.649 | 7.0 | 0.796 | 0.001 | 4.42 |
| Dgt3 | 49.41 | 1.674 | 0.679 | 8.1 | 2.32 | 0.01 | 4.83 |
| Wac | 66.99 | 1.641 | 0.621 | 8.0 | 1.94 | 0.006 | 4.87 |
| Dgt6 | 110.34 | 1.604 | 0.700 | 8.0 | 1.249 | 0.002 | 4.98 |
| Dgt4 | 50.07 | 1.592 | 0.657 | 10.3 | 1.706 | 0.001 | 6.46 |

Table 3: Only 16 proteins showed a significant increase in association with MTs in mitosis.

Following stringent statistical testing, only 16 proteins showed a significant increase in their MT association in mitosis. Of the 16 proteins, 3 (highlighted) had previously not been recorded as a mitotic MAP.

Proteins have been sorted according to mean fold increase.

### 3.3 Less stringent statistical analysis reveals a number of protein complexes

Having now identified a larger subset of proteins showing a significant increase in MT association in mitosis, the next step was to assess them qualitatively. Using information from Flybase, the proteins were annotated according to their primary GO; taken from the biological processes and cellular component information given about each individual protein. This annotation led to the identification of a number of protein complexes of various attributed cellular functions (Table 4).

#### 3.3.1 The cohesin and condensin complexes

The human cohesin complex is composed of 4 core subunits; two structural maintenance of chromosome proteins Smc1 and Smc3, a kleisin family protein Scc1 and an accessory factor Scc3 (Ishiguro and Watanabe, 2007). In *Drosophila* the cohesin complex is made up of 3 proteins: the core structural maintenance of chromosomes (SMC) proteins SMC1 and SMC3 (Cap-D2), and Stromalin (SCC3) (Rollins *et al*., 2004), all three of which were significantly increased in our screen. The cohesin complex subunits showed around a 1.8-3.3 fold increase in association with MTs during mitosis, when compared to the cycling population.

The main role of the cohesin complex is to hold together the sister chromatids. Correct cohesion of the sisters is important in ensuring the correct alignment along the metaphase plate. Cohesion is also responsible for creating the tension across the centromeres that counteracts the force of spindle MTs; this force balance ensures the correct bipolar attachment of chromosomes (Ishiguro and Watanabe 2007).

Also significantly increased was the chromatin binding protein Nipped-B (SCC2) and Pds5, known for its role in linking the chromatin with the cohesin complex (Ishiguro and Watanabe 2007). Nipped-B has multiple cellular roles and is highly conserved throughout eukaryotes (Gause et al., 2008). Nipped-B is a functional homologue of the yeast adherins, and is required for the cohesin complex to associate with chromosomes (Rollins *et al*., 2004).

The *Drosophila* cohesin complex has not been previously identified as MT associated; however in 2001 Gregson *et al.,* reported that in humans there may be a potential role for cohesin in the assembly of mitotic MT asters. The study showed that cohesin localised to the mitotic spindle poles where it interacted with NuMA, a

protein required for mitotic spindle organisation. In the absence of cohesin *in vitro* the mitotic asters failed to form, which could suggest a role for cohesin in mitotic spindle assembly (Gregson *et al*., 2001). The localisation of cohesins to the spindle pole has also been observed by Valdeolmillos *et al.* (2004) who reported the presence of Stromalin at the spindle pole during anaphase in S2 cells. This potential cohesin function could therefore indicate why the cohesin complex is showing increased MT association in mitosis.

Like the cohesin complex, the condensin complex subunits Gluon (Glu)/SMC4, CAP-D2 and SMC2 also showed a 2-3 fold increase in MT association during mitosis (Table 4). The condensin complex is an essential 5 subunit protein complex necessary for chromosome compacting and segregation (Hirano 2012). Higher eukaryotes contain 2 condensins: condensin I and condensin II; these complexes typically consisting of a pair of SMC subunits and 3 chromosome associated polypeptide (CAP) proteins (Lau and Csankovski 2015). Although functionally similar, condensin I and II present different localisations. Condensin I is cytoplasmic until prometaphase (post NEB), when it localises to the chromosomes. Condensin II however is nuclear in interphase, then binds to chromosomes at the onset of condensation in prophase (Ono *et al.,* 2004).

*Drosophila* studies show that only condensin I subunits Glu, CAP-H, CAP-G and CAP-D2 are needed for the correct assembly and segregation of the mitotic chromosomes (Hirano 2012). In our screen both Glu and CAP-D2 were identified as mitotic MAPs. Although not previously identified as MAPs, a screen by Goshima *et al* .(2007) inferred through mutant phenotype a potential role for both proteins in mitotic spindle assembly. It could therefore be postulated that it is this secondary role at the mitotic spindle causing these particular condensin subunits to present an increased MT association during mitosis.

### 3.3.2 The RISC complex, ATP dependent RNA helicase activity (DEAD-box) and Polar granules

The next set of complexes identified share some of their protein constituents, all of which have an RNA related function. In our biochemical assay, subunits of the RNA induced silencing complex (RISC), P granules and DEAD-box proteins were found to

show a 1.7 fold up to 4.8 fold increase in MT association in mitosis, when compared to controls (Table 4).

P granules are cytoplasmic non membranous RNA/protein complex aggregates found in the germ cells of many higher eukaryotes (Schisa *et al*., 2001). Spn-E (Spindle-E), a P granule protein with ATP dependent RNA helicase activity, showed the greatest fold increase in MT association in mitotic samples but it has not been previously recognised as a MAP. Spn-E has a number of different cellular roles involving mRNA and cell polarity, however a study by Pek and Kai (2001) indicated a role for this protein in chromosome condensation. It was reported that Spn-E co-immunoprecipitated with the P granule protein, Vas (present in our screen but non-significantly enriched on MTs in mitosis) and the condensin I protein Barr (CAP-H). Spn-E has also been shown to co-localise with Vas to the chromosomes; Vas localisation to the chromosome being dependent on Spn-E and the P granule protein, Aubergine (Aub). Whilst Vas and Spn-E have no recorded interaction with MTs, the biochemical screen by Hughes *et al* (2008) found Aub to be a MAP.

The protein Belle (Bel) falls into all three of the RNA based complexes detailed in this section. In our screen Bel was 3 fold enriched in mitotic samples, and was present in the Hughes *et al* (2008) screen for mitotic MAPs. This would therefore suggest that Bel is a MAP, however nothing is known about its role at the MT level. Another DEAD-box/P granule protein showing 3- fold levels of enrichment is Me31B. Like Bel, Me31B was identified as a MAP by the Hughes screen and there has been evidence that Me31B may have a role in the mitotic G2 DNA damage checkpoint (Kondo and Perrimon, 2011).

The only other protein present in the RISC/DEAD-box/P granule complexes that had been previously linked to MTs is Trailer-hitch (Tral). Snee and Macdonald (2009) reported that Tral has a role alongside Bicaudal C in the organisation of the MT cytoskeleton. There is however no evidence for a mitotic function.

For many of the proteins we have identified and classified as RISC/DEAD-box/P granule proteins there is little evidence to suggest they would have a role as a mitotic MAP despite the significant increase in association with MTs during mitosis. This would therefore suggest that these proteins could form subset of novel mitotic MAPs. One explanation for the increased association of these complexes could be to

ensure the accurate redistribution of P granules during cell division. By binding to the spindle MTs, when the cell divides the proteins would also accurately segregate into the new daughter cells. There is however currently no evidence for this being the case.

### 3.3.3 The Replication factor C complex

The final protein complex identified in the screen was the Replication factor C (RFC) complex. In eukaryotes the classical RFC complex is a heteromeric protein made up of one large subunit: RFC1/Gnf1, and 4 small subunits: RFC2/CG8142, RFC3, RFC4 and in *Drosophila* RFC38 (Tsuchiya *et al.,* 2007). Our screen revealed that the four small subunits of the RFC complex showed around a 2.2-2.5 fold increase in MT association in mitosis. RFC1 also presented an increased association however its significance level fell just above the alpha value ($p \leq 0.05$).

There is evidence to suggest a mitotic role for both RFC2 (Hughes *et al*., 2008) and RFC4 (Krause *et al.,* 2001) but no evidence, as yet, for RFC3 and RFC38. Based upon what is already known about this complex and its role in the cell it was decided to investigate the RFC complex further. The next chapter of this thesis details how, through the creation of GFP fusions of the small subunits RFC2, RFC3 and RFC4 the localisation and function of the RFC complex has been investigated, in order to identify a novel mitotic role for this particular set of proteins.

## 3.4 Summary

In summary, by combining biochemical assays with proteomic analysis, we have been able to identify a number of novel mitotic MAPs. Stringent analysis of the MS data revealed a small subset of proteins showing significantly increase MT associations in mitosis; this analysis also indicated the need for further statistical testing and so yielded a more extensive list of novel MAPs with potential mitotic function. Further analysis indicated that our significant proteins fell into a number of different protein complexes, some with no previous mitotic function yet showing an increased MT association during this process. The following chapters in this thesis will go on to describe in more detail one of these protein complexes, and aim to investigate further the roles of two known mitotic MAPs: Abnormal spindle (Asp) and *Drosophila* transforming acid coiled coil (DTACC).

| Complex name | Subunit name | MFI | P value |
|---|---|---|---|
| Cohesin complex | Nipped –B | 2.21 | 0.037 |
| | Pds5 | 1.85 | 0.091 |
| | Stromalin | 3.04 | 0.030 |
| | Smc1 | 3.30 | 0.006 |
| Condesin complex | Smc2 | 3.14 | 0.044 |
| | Cap-D2 | 2.04 | 0.179 |
| | Glu | 2.95 | 0.035 |
| ATP dependent RNA helicase activity | Bel | 2.98 | 0.018 |
| | Me31B | 2.92 | 0.015 |
| | Rm62 | 2.20 | 0.007 |
| | Spn-E | 4.83 | 0.016 |
| RNA induced silencing complex | Bel | 2.98 | 0.018 |
| | Fmr1 | 1.79 | 0.019 |
| | Tudor-SN | 1.33 | 0.021 |
| Replication factor C complex | CG8142 | 2.49 | 0.010 |
| | RFC3 | 2.31 | 0.017 |
| | RFC4 | 2.34 | 0.019 |
| | RFC38 | 2.23 | 0.016 |
| P granules | Aub | 2.76 | 0.017 |
| | Bel | 2.98 | 0.018 |
| | Me31B | 2.92 | 0.015 |
| | Spn-E | 4.83 | 0.016 |
| | Tral | 2.92 | 0.025 |
| | Tud | 3.55 | 0.027 |

Table 4: Less stringent data analysis reveals a number of different protein complexes**.**

Following GO annotation of the data set post analysis via Levenes test and independent samples t-test, a number of protein complexes have been identified with varying cellular function. Complexes of particular interest/most complete include the cohesin and condensin complex, proteins involved in ATP dependent RNA helicase activity, the RISC complex, the RFC complex and the P granules. The most complete complex present is the RFC complex, as all five subunits showed an increase in MT association during mitosis.

## 4. Investigating novel mitotic functions of the Replication Factor C (RFC) complex

### 4.1 Introduction

Replication and repair of DNA requires a series of coordinated actions carried out by a number of different proteins. In some cases a protein or protein complex will have a role in both processes. One such example is the multi-functional sliding clamp, clamp loader and accessory protein complex, composed of Proliferating Cell Nuclear Antigen (PCNA), Replication Factor C (RFC) and Replication protein A (RPA) respectively (Tomida *et al*., 2008).

The role of sliding clamp loader is the primary function of the RFC complex. The eukaryotic sliding clamp loader was first discovered as a protein complex necessary for *in vitro* replication of SV40 (Fairman *et al.,* 1988), yet at the time of discovery its function remained unknown (Waga and Stillman 1994).

The RFC complex forms a stable ATP dependent complex with PCNA, which then binds specifically to primed sequences of DNA. Recognition of this primed sequence stimulates ATP hydrolysis, resulting in the dissociation of RFC from PCNA ready for the next round of DNA synthesis (Bowman *et al*., 2004). The RFC subunits contain a region of homology to the AAA+ protein family. The AAA+ domains form a right hand helix when bound to ATP, generating a binding site for DNA in the middle of the RFC complex. DNA is able to enter the RFC complex through a gap between the AAA+ domains of two of the subunits. Entry of DNA also requires there to be a gap in the PCNA clamp. The PCNA clamp is opened when the AAA+ domains of the clamp loader binds to it, ATP hydrolysis then allows the clamp to close, causing the RFC complex to be ejected (Yao and O'Donnell 2012). The clamp loader binds to the same surface of the clamp as DNA polymerase, meaning that once PCNA has been loaded onto the DNA, the RFC complex must be removed generating access for the polymerase (Yao and O'Donnell 2012).

The RFC complex is a heteromeric protein complex made up of 5 subunits; the large RFC1 subunit and the four small RFC2, RFC3, RFC4 and RFC5 subunits (Tsuchiya *et al*., 2007). The calculated mass of each of the RFC subunits was originally inferred from their amino acid sequences: 128.3, 39, 40.5, 39.6 and 38.5 kDa (RFC1-5 respectively). The subunits are however commonly annotated with regard to their migratory position on SDS PAGE: 140, 40, 38, 37 and 36 kDa respectively

(Mossi *et al.,* 1997). The nomenclature of the *Drosophila* RFC homologues differs to that of the human subunits: further chapters will refer to *Drosophila* nomenclature only (Table 5). RFC1 is commonly known as the large subunit as in *S.cerevisiae* its N-terminal and C-terminal regions span past its region of homology with the other RFC subunits (Tomida *et al*., 2007). All of the RFC subunits contain seven conserved domains known as RFC boxes II to IIIV. *In S.cerevisiae*, alignment of the amino acid sequences of all five subunits revealed a common conserved ATP/GTP binding region. The regions consists of several motifs in the N-terminal half of the small RFC subunits and the equivalent region of the large RFC1 subunit (Cullmann *et al.,* 1995).

A number of different organisms present protein complexes with functional equivalence to the RFC complex. In *Drosophila* the large RFC1 subunit shows a great degree of similarity to that of the human RFC complex, and all other RFC subunits have *Drosophila* orthologues.

As explained in the previous chapter, our QC-MAP proteomics data analysis highlighted the RFC complex as a MAP complex showing a significantly increased MT association during mitosis. The large RFC subunit RFC1 can be replaced by a number of additional paralogues, which results in a modified RFC complex function; for more details see section 4.2. The aim of the next set of experiments was to therefore investigate the role of this complex in mitosis by investigating its cell cycle dependent localisation and identifying its protein interactors, from which we can begin to develop an understanding of why the RFC complex associates biochemically with mitotic MTs.

| Human nomenclature | Drosophila nomenclature | Size (kDa) |
|---|---|---|
| RFC1 | RFC1 (GNF1) | 140 |
| RFC2 | RFC4 | 40 |
| RFC3 | RFC38 | 38 |
| RFC4 | RFC2 (CG8142) | 37 |
| RFC5 | RFC3 | 36 |

Table 5: Human and *Drosophila* nomenclature and sizes of the archetypal RFC subunits.

## 4.2 Results and Discussion

In order to investigate the role of the RFC complex in the early *Drosophila* embryo, GFP fusions of the three small subunits RFC2, RFC3 and RFC4 were generated. GeneArt projects were generated using the sequences of each gene, expressed in the early *Drosophila* embryo as annotated by Flybase, and Entry vectors produced by Life Science Technologies (Materials and Methods). Standard LR cloning was then undertaken, to transfer the coding sequences into the *Drosophila* P element-derived expression vector 69pUBQmGFPCTDest. Successful clones were sequenced to confirm correct incorporation of the transgene, and sent for germline transformation using BestGene Inc. Individual transformed lines were balanced, and heterozygote or homozygote populations used for the following experiments.

To firstly establish if the RFC-GFP transgenes were being expressed, 0-3 hour embryos were collected and extracts analysed via SDS-PAGE and Western blot (Figure 4-1). The expected band sizes for RFC2-GFP, RFC3-GFP and RFC4-GFP are 64kDa, 63.5kDa and 67kDa respectively. In each case, western blotting of extracts probed using an antibody to GFP showed bands of the predicted size, indicating that the cloning was a success and that GFP tagged RFC subunits are being expressed in the early embryo.

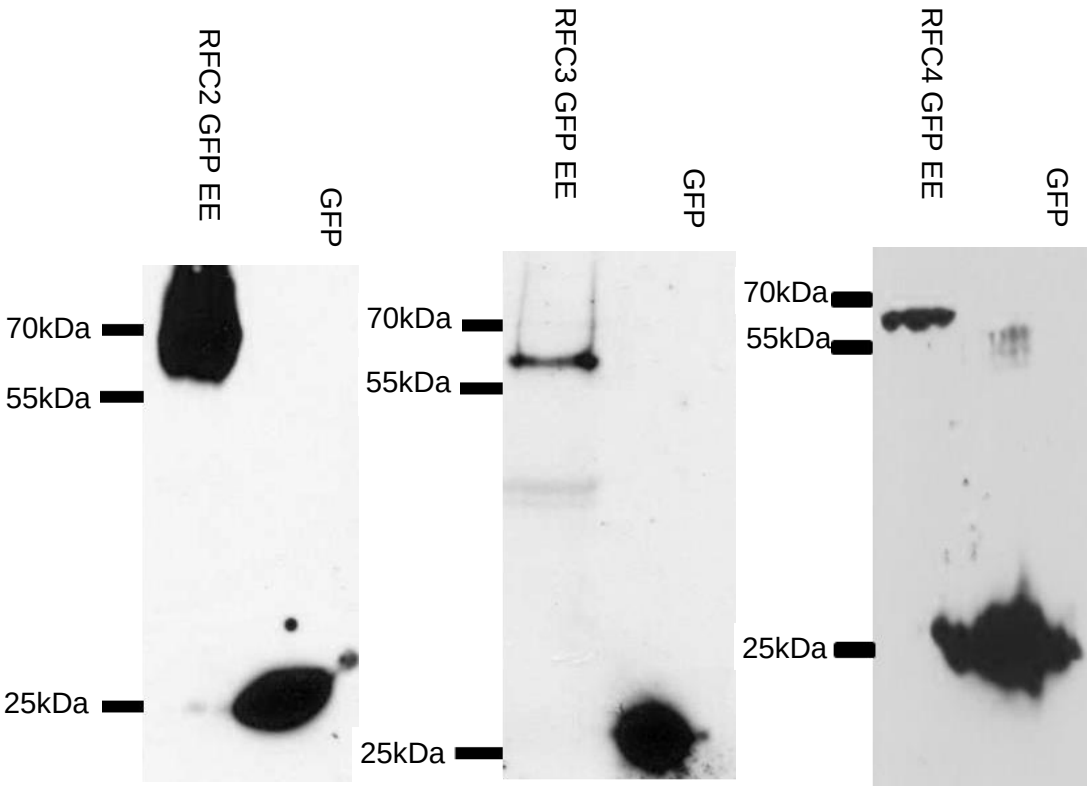


Figure 4-1 Biochemical evidence of successful GFP fusion to the small RFC subunits: RFC2, RFC3 and RFC4.

Embryo extracts of 0-3 h RFC2, 3 and 4-GFP were subjected to SDS-PAGE and Western Blotting, probing with an antibody to GFP. In all three cases a band of the expected molecular weight (~65kD is visible. ~3.5µg of bacterially expressed and purified GFP was used as a loading control.

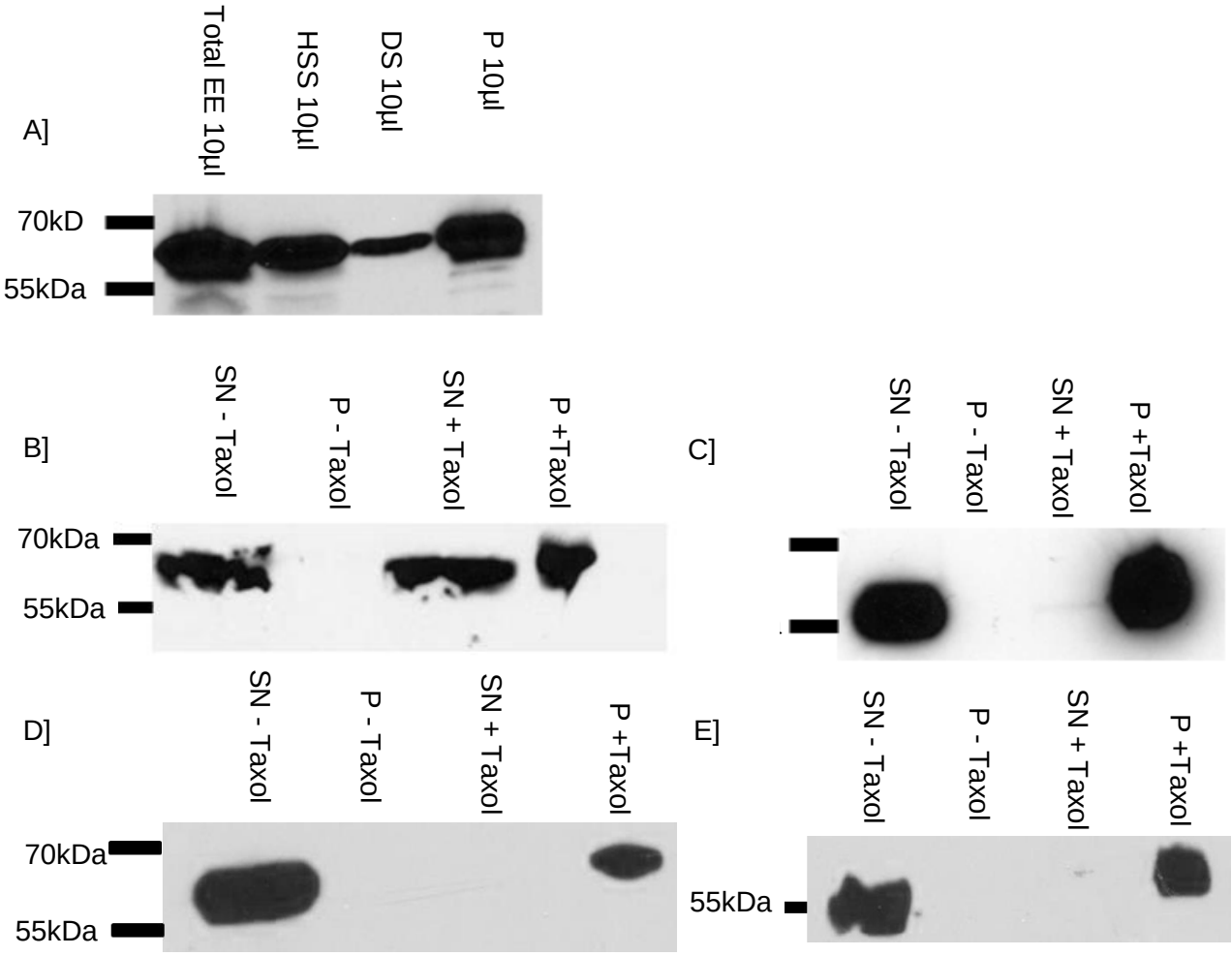


Figure 4-2 Biochemical analysis of RFC3-GFP

Embryo extracts were prepared from 0-3 hour RFC3GFP embryos, then probed using antiGFP or anti tubulinDM1A.

**A]** RFC3GFP immunoprecipitation. Total EE – total embryo extract; HSS – high speed supernatant; DS – depleted supernatant; P-pellet (containing proteins that specifically bind to the GFP-TRAP-A beads) **B]** MT spin down of RFC3GFP probed for GFP. **C]** MT spin down [B] probed for tubulin. **D]** MT spin down of RFC3 using nuclease probed for GFP. **E]** MT spin down D] probed for tubulin.

SN- Taxol – supernatant minus Taxol; P- Taxol – pellet minus Taxol. SN + Taxol – supernatant plus Taxol; P + Taxol; pellet plus Taxol.

In each case 12µL of sample was loaded.

The presence of a band in the pellet + Taxol, when probing for both GFP and tubulin would indicate that RFC3 is biochemically associating with MTs.

### 4.2.1 Affinity Purification Mass Spectrometry of RFC3-GFP verifies its association with the RFC complex

To determine whether the RFC-GFP subunits are incorporated into the RFC complex in vivo, and to determine additional interacting proteins, GFP-TRAP-A based affinity purification of 0-3 hour mitotic RFC3-GFP embryos (Figure 4-2), followed by MS analysis was carried out. The results of the MS (Table 5) were subject to the same data analysis as described in Chapter 3. When sorting for peptide/protein abundance (i.e. Area Under the Curve (AUC)), the top hit was our bait protein RFC3, followed by the other four archetypal RFC subunits. This strongly suggests that the RFC3-GFP expressed in the early embryo retains the ability to complex with the endogenous RFC.

| Name | Area | Score | Coverage (%) | Peptides |
|---|---|---|---|---|
| RFC3 | 6.422E9 | 605.73 | 91.27 | 34 |
| RFC4 | 3.624E9 | 481.82 | 87.61 | 37 |
| RFC2 | 3.603E9 | 435.05 | 85.84 | 31 |
| RFC38 | 2.926E9 | 505.07 | 83.43 | 35 |
| RFC1 (Gnf1) | 1.803E9 | 681.93 | 59.53 | 65 |
| Cutlet (Ctf18) | 4.304E8 | 582.41 | 65.36 | 60 |
| Ctf8 (CG34001) | 2.934E8 | 471.02 | 55.25 | 53 |
| His2A | 2.926E8 | 49.21 | 37.10 | 4 |
| Dcc1 (CG11788) | 2.879E8 | 85.24 | 61.74 | 7 |
| RAD17 | 2.745E8 | 295.82 | 78.88 | 34 |
| Elg1 | 2.697E8 | 196.87 | 77.88 | 29 |
| SesB | 1.044E8 | 58.76 | 52.51 | 19 |
| EB1 | 1.039E8 | 88.61 | 66.55 | 17 |
| Hoip | 9.985E7 | 33.37 | 54.33 | 5 |
| Yps | 7.483E7 | 73.98 | 50.00 | 13 |
| Larp | 7.081E7 | 168.92 | 33.59 | 37 |

Table 6: MS result for affinity purification of RFC3.

The top scoring proteins were the 5 RFC subunits, with our bait protein scoring highest. The screen also highlighted the three RLCs – Cutlet-RFC, RAD17-RFC and Elg1-RFC.

The other proteins identified are histone 2A (His2A), stress-sensitive B (SesB), End Binding protein 1 (EB1), Hoi-polloi (Hoip), Ypsilon schachtel (Yps) and La related protein (Larp).

The Data has been sorted by area under curve.

### 4.2.2 RFC3-GFP associates with four known distinct RFC-containing complexes

Three RFC1 paralogues exist in eukaryotic cells - Ctf18, Rad17 and Elg1 (Figure 4-3). *Drosophila* Cutlet is the homologue of *S.cerevisiae* Ctf18 so henceforth in this thesis CTF18 will be referred to as Cutlet. These paralogues function as the large subunit of three alternative clamp loaders in association with RFC2-5 (2-38 in *Drosophila*), known as RFC like complexes (RLC) (Majka and Burgers 2004; Kim and MacNeill 2003). These loaders target the PCNA or the Rad9-Hus1-Rad1 (9-1-1) alternative clamp (Murakami *et al*., 2010). These complexes contribute to a number of cellular processes related to DNA replication including chromosome cohesion (Cutlet-RFC), DNA damage responses (Rad17-RFC) and maintaining genome stability (Elg1-RFC) (Bermudez *et al*., 2003; Ellison and Stillman 2003). Each of these alternative RFC complex subunits, and their associated proteins, were identified as RFC3-GFP interactors.

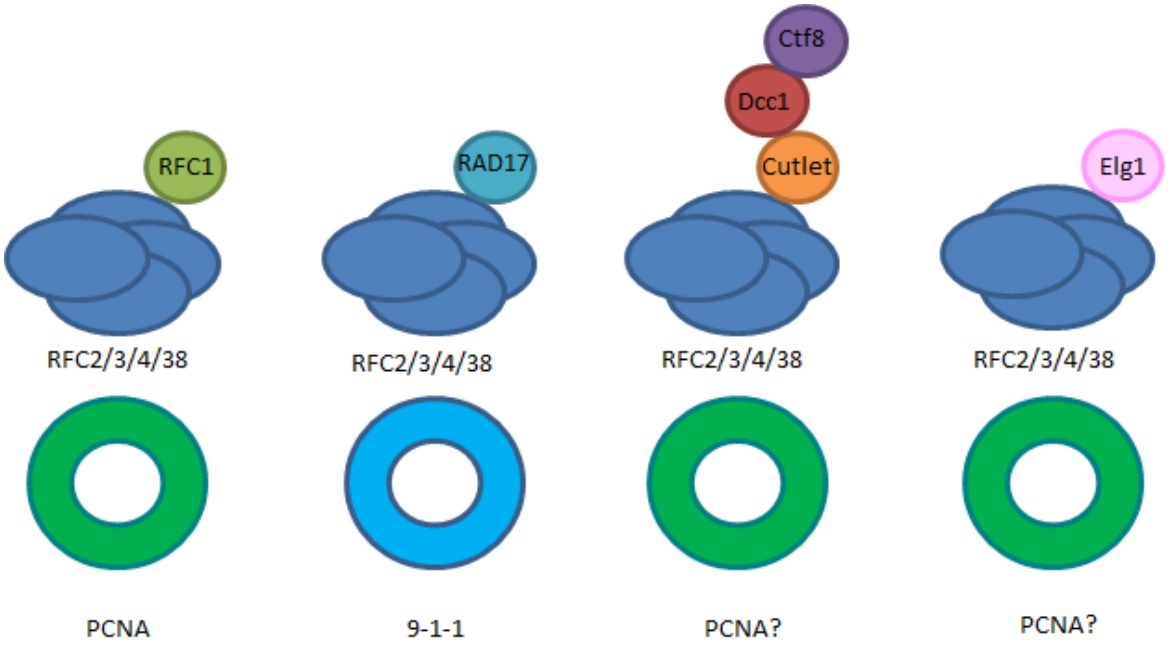


Figure 4-3 Alternative RFC complexes (RLCs) and their associated clamps.

Figure adapted from Mayer *et al.,* 2001. The Rad17-RFC complex and its associated clamp the Rad9-Hus1-Rad1 complex (9-1-1) functions in a similar fashion to the RFC PCNA, as part of the DNA damage response. The chromatid cohesion RFC complex Cutlet-RFC and the Elg1-RFC complex are both thought to associate with the PCNA based on their structural similarities to the RFC complex subunits, however this interaction is still to be established in *Drosophila*.

### 4.2.3 The Cutlet-RFC complex

The RFC1-like protein Cutlet functions with two additional co-factors, Dcc1 and CTF8 (Mayer *et al.,* 2001). Second to the archetypal RFC1, Cutlet was the most highly abundant protein in the proteomic analysis, while Dcc1 and CTF8 were also identified as interacting proteins. Cutlet contains a region of sequence homology with all 5 RFC subunits and genetically interacts with the small subunits RFC4 and RFC38 (Jaffe and Jongens, 2001). To investigate the interaction between the RFC subunits and Cutlet, Jaffe and Jongens (2001) examined if mutating one of the RFC subunits that interacts with Cutlet would enhance a Cutlet mutant phenotype. Cutlet mutants produce a number of phenotypes, one of which causes irregularity in adult eye shape and inappropriate placement of bristles. Sections of adult eye tissue taken from homozygote cutlet mutants with an RFC4 loss of function, showed a strongly enhanced phenotype when compared to homozygous cutlet mutants carrying functional RFC4. This observation was also true for RFC38 loss of function mutants, indicating that RFC4 and RFC38 both interact with Cutlet to ensure correct function.

Cutlet, Dcc1 and CTF8 are all essential for sister chromatid cohesion in yeast (Mayer *et al*., 2001). As outlined in the previous chapter, sister chromatids produced during chromosome replication remain attached until the metaphase/anaphase transition, ensuring faithful segregation to opposite spindle poles (Skibbens 2005). Cohesion resists the pulling forces generated by the spindle upon chromatids and so prevents premature chromatid separation. This process is also responsible for creating tension at the interface between the MTs and kinetochores, important in signalling the mitotic checkpoint (Nicklaes 1997). The cohesin complex associates with the chromatids from late G1 until the metaphase-anaphase transition (Michaelis *et al*., 1997; Toth *et al*., 1999), preferentially binding to regions of high AT content and to the centromeres (Tanaka *et al*., 1999). The anaphase promoting complex (APC) catalyses the degradation of securin Pds1p (Cohen-Fix *et al*., 1996) at the metaphase anaphase transition, releasing the separase Esp1p (Ciosk *et al.,* 1998). This in turn cleaves the cohesin Scc1 and so initiates chromatid separation at the onset of anaphase (Uhlmann et al., 1999; 2000).

Despite it having an important role in chromosome segregation, the interaction between the establishment of cohesion and the DNA replication machinery is poorly

understood. It has been suggested by Wang *et al* (2000) that a polymerase switch occurs prior to the cohesin complex associating with DNA during S phase. This model is comparable to the polymerase switch (from polymerase α to polymerase δ) that is mediated by the RFC complex during replication. Like the RFC complex, it is thought that the clamp for Cutlet-RFC is PCNA, as Ohta *et al*., (2002) identified cutlet as a PCNA associating protein; this association has not however been tested in *Drosophila*.

It has also been suggested that Cutlet-RFC may also act outside of its role in sister chromatid cohesion, functioning to maintain genome stability. In a paper by Gellon *et al* (2011) it was shown that Cutlet-RFC aided the replication of trinucleotide (triplicate repeats). DNA trinucleotide repeats are naturally occurring runs of 3 identical base pairs. Mutations can cause these repeats to expand and can result in a number of neurological diseases such as Huntington's. Mutations in Cutlet-RFC showed an increased level of expansion, contraction and fragility of these triplicate repeats. This information led the authors to suggest that Cutlet-RFC acts to stabilise triplicate repeats by assisting the replication machinery through the repeats and helping to repair any damaged DNA (Gellen *et al*., 2011).

Cutlet was also identified in our original QC-MAP proteomic data, showing a significant increase in MT association in mitosis. This increase could be related to its function as part of the Cutlet-RFC complex, as all five RFC subunits also showed a similar level of up-regulation. However, Dcc1 and Ctf8 were not present in the QC-MAP data, which could suggest a novel mitotic role for Cutlet, or it could suggest a link between the mitotic spindle and the Cutlet-RFC complex during sister chromatid cohesion.

In order to further investigate the Cutlet-RFC complex in mitosis, RNAi against Dcc1 was carried out to see if by disrupting the Cutlet-Dcc1-Ctf8 portion of this RLC results in any mitotic phenotype. The results of this experiment are discussed in section 4.2.8.

### 4.2.4 The Rad17-RFC complex

The second RLC identified in the screen was the Rad17-RFC complex. Rad17, in budding yeast, is involved in DNA damage and replication arrest responses (Zhou and Elledge 2000; O'Connell *et al*., 2000; Boddy and Russell 2001). In humans the

Rad17-RFC and Rad9-Rad1-Hus1 (9-1-1) checkpoint complex have been shown to be structurally similar to the RFC and PCNA respectively (Bermudez *et al*., 2003), and are predicted to function like the PCNA and RFC complex as a clamp and clamp loader; both sharing similarities in their amino acid sequences (Shiomi 2002). In the Rad17-RFC complex RFC1 is replaced by Rad17, which shows significant sequence homology to the other RFC subunits (Griffiths *et al*., 1995; Venclovas and Thalen 2000; Lindsey-Boltz *et al*., 2001). A number of studies have suggested Rad17 is also able to interact with the small RFC subunits (Naiki *et al*., 2000; Kai *et al*., 2001). In 2002, Shiomi co expressed Rad17 with the four small RFC subunits and found that a 240kDa complex was formed. This complex was oval in structure, 26x22nm in size, with a cleft reminiscent of the structure of RFC. However it was shown by Bermudez *et al* (2003) that unlike the RFC PCNA clamp loader, Rad17-RFC binding to DNA occurs independently of ATP and that the recruitment of the 9-1-1 complex depends on ATP but does not require ATP hydrolysis. So although the mechanism of action is slightly different, the Rad17-RFC does appear load the 9-1-1 complex onto DNA as part of the DNA damage response (Bermudez *et al*., 2003).

Like Cutlet, Rad17 was also identified in the QC-MAP proteomics data set as being a MAP, however its score fell below the cut off of 30 and so it was not analysed further. However the fact that it was present could suggest a potential link between the RFC complex subunits and the MTs.

### 4.2.5 The Elg1-RFC complex

The final alternative clamp loader complex identified by the MS of RFC3 was the Elg1-RFC complex. Elg1 was first identified in yeast as a mutant that causes genome instability (Kolodner, Putnam and Myung, 2002; Aroya and Kupiec, 2005; Bellaoui *et al.,* 2003). The Elg1 protein shares sequence homology with RFC subunit RFC1 and with the additional RFC proteins involved in checkpoint function and genome maintenance: Rad17 and Cutlet (Parnas *et al.,* 2009).

In 2003 it was proposed by Bellaoui and colleagues that the Elg1-RFC complex functions in both DNA replication and in the DNA damage response. Elg1 mutants show DNA replication defects and genome instability, increased levels of recombination and minichromosome maintenance defects. These mutants also show

interactions with pathways required for processing stalled replication forks, and are unable to recover from DNA damage in S phase.

In a study by Parnas *et al* (2009) it was reported that in yeast Elg1-RFC works in conjunction with the Cutlet-RFC complex to ensure sister chromatid cohesion, Elg1 having been suggested to assist in the localisation of Cutlet to the chromatin. The authors reported that Elg1 activity is important in the establishment of cohesin but not in the maintenance or cleavage, suggesting a direct role in sister chromatid cohesion; Elg1 mutants exhibiting a sister chromatid separation phenotype, as well as those detailed above.

Unlike the other RFC1 paralogues, Elg1 was not identified as a MAP in our QC-MAP screen. This information would suggest that in terms of following up the RLCs, their potential roles in mitosis and at the MT, this particular complex may have limited function in these areas. Although thought to act in a similar fashion to the Cutlet-RFC complex, the Elg1-RFC is much less characterised therefore the Cutlet-RFC complex has become the focus of the remainder of this section.

### 4.2.6 RFC3-GFP associates with a small number of additional proteins, including the MT associated protein, End Binding Protein 1 (EB1)

The MS analysis also identified six proteins not previously known to interact with any RFC complex, a number of which have reported roles related to DNA and chromatin. Given time limitations, the interactions between RFC3-GFP and the interacting proteins were not verified by reverse immuno-precipitation and Western blotting. Therefore, it remains possible that at least some of these could be false positives. However, they are briefly discussed below.

Histone 2A (His2A) is a core histone protein and so its interaction with the RFC complex is unsurprising. Hoi-polloi (Hoip) and Ypsilon schachtel (Yps) are both mRNA binding proteins (Prokopenko et al., 2000); Yps is also able to bind DNA (Johnstone and Lesko 2001). Again, given what is known about the RFC complex it is likely that the interaction here lies with its functions as a clamp loader, and in the DNA damage response. La related protein (Larp) is another protein that could be linked more specifically to the Cutlet-RFC complex as it is reported to play a role in a number of cellular processes such as centrosome separation, chromosome

condensation and spindle assembly (Blagden *et al*., 2009). Stress-sensitive B (SesB) also has a number of cellular roles this time related to ATP/ADP transport (Sardiello *et al*., 2003), mitochondrial transport (Hutter and Karch 1994; Nelson *et al*., 2000) and calcium ion homeostasis (Terhzaz *et al*., 2010). A report by Crabbé *et al*., (2010) stated that the Cutlet-RFC may have a role in the yeast replication stress response, therefore potentially explaining why we see SesB as an RFC interactor. The final protein identified via MS of RFC3-GFP was the MAP End Binding protein 1 (EB1). EB1 was first discovered in a yeast 2 hybrid screen for proteins that interacted with the human adenomatous polyposis coil (APC) tumour suppressor protein (Su *et al* 1995), and over the years subsequent proteins homologous to EB1 have been identified in a number of organisms, including *Drosophila* (Tirnauer and Bierer 2000). EB1 is known as the master regulator of MT plus ends, because it directly binds to MTs via its N-terminus in order to recruit a number of cargo proteins such as Cytoplasmic linker proteins (CLIPs), CLASP and Kinesin-13/Klp10A via its C terminal (Akhmanova and Steinmetz 2008; Slep 2010). EB1 localises specifically to growing MT plus ends and is necessary for a number of mitotic cellular functions including correct chromosome segregation, spindle elongation during anaphase and mitotic spindle positioning (Rogers *et al*., 2002). In S2 cells it was reported by Rogers et al (2002) that a loss of EB1 causes MTs to pause, no longer showing phases of rapid growth and shrinkage. A possible hypothesis for a functional relationship between the RFC complex and EB1 is described towards the end of this Chapter.

### 4.2.7 The RFC complex subunits localise weakly to syncytial mitotic spindles and biochemically associate with MTs

To investigate the cell cycle dependent localisation of the RFC-GFP subunits, 0-2 hour embryos expressing GFP fusions of RFC2, RFC3 and RFC4 were imaged using spinning disc laser confocal microscopy (Figure 4-4). Each subunit localised essentially identically, supporting the conclusion that RFC-GFP subunits can incorporate into functional RFC complexes, provided by the RFC3-GFP MS data. As expected, the RFC is nuclear during interphase. At nuclear envelope breakdown (NEB), at mitotic onset, the subunits weakly localise to the region of the mitotic spindle, until the nuclear envelope reforms just prior to the next interphase.

In order to verify both the weak localisation to the MTs of the spindle, and the original MAP proteomic data, MT co-sedimentation assays were carried out using extracts from 0-3 h embryos expressing the RFC3-GFP subunits (Figure 4-2 B]-E]). Two independent assays were carried out: one using a population of embryos actively cycling through the cell cycle and the other using a population of embryos treated with MG132, to arrest them at the metaphase-anaphase transition. The MT co-sedimentation assay shown in Figure 4-2 B and C, when probed for both GFP and Tubulin demonstrates that RFC3-GFP in mitotic embryos strongly co-sediments with MTs. In order to distinguish between an interaction with MTs, or contaminating nuclear/chromatin derived material co-sedimenting along with MTs, the assay was repeated on extracts that had been treated with Benzonase- a non-specific endonuclease. Again, western blotting then probing again for both GFP and Tubulin (Figure 4- D] and E]) revealed that the interaction between the RFC complex and the MTs was still present in the presence of the nuclease. Thus, RFC3-GFP biochemically associates with MTs, in both mitotic and cycling embryos, supporting the weak spindle localisation of the RFC subunits.

Given what is known about the RFC complex and its associated RLCs we would perhaps expect to see the subunits localising preferentially to the chromatin or kinetochores during mitosis. However, the fluorescence appears to be uniform over the entire spindle. In order to obtain further information on the relevance of the localisation of the RFC and any functional relevance of its ability to associate with MTs, I next attempted to disrupt the function of the RFC subunits in the early embryo.

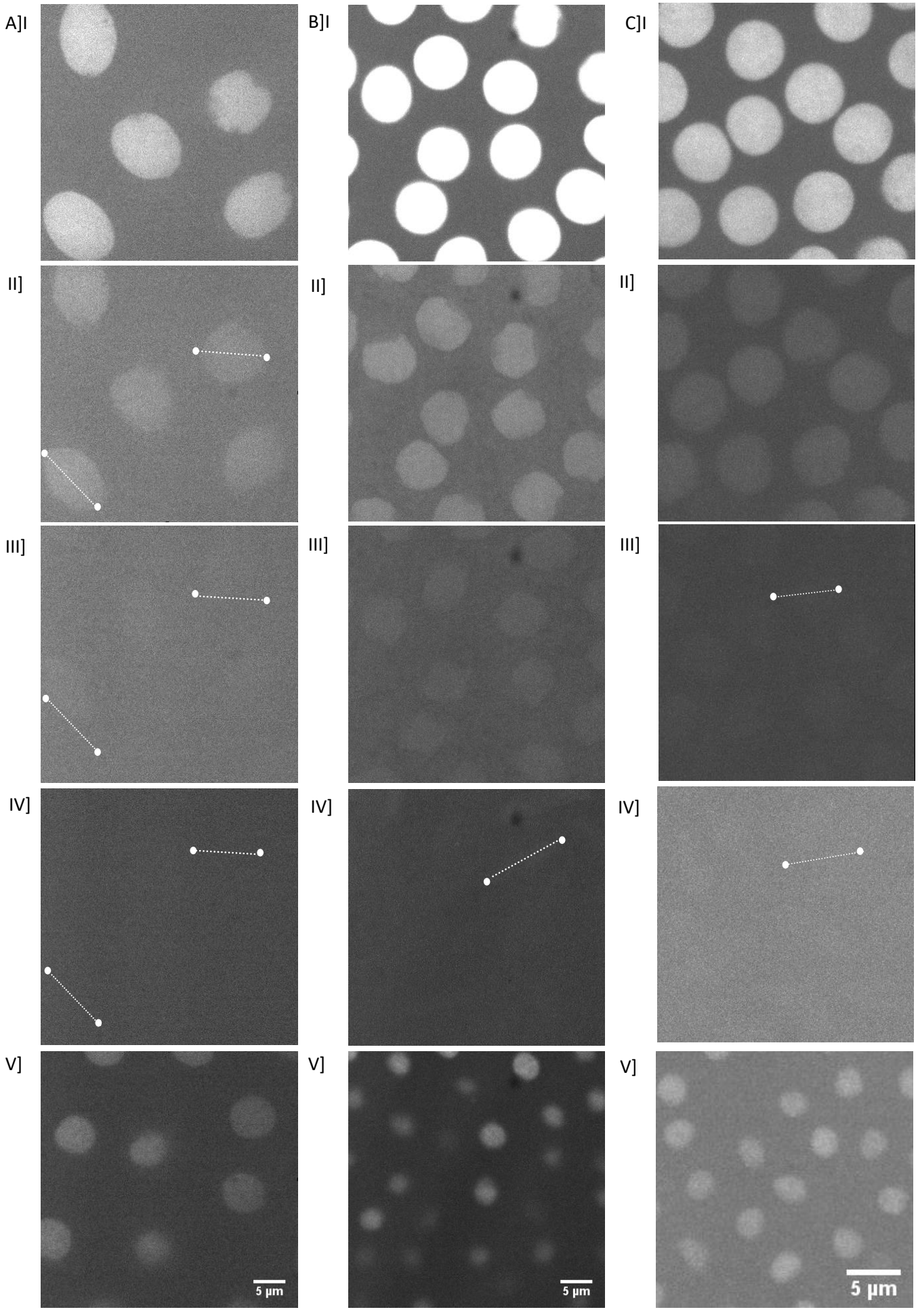
A]I
B]I
C]I
II]
II]
II]
III]
III]
III]
IV]
IV]
IV]
V]
V]
V]
5 µm
5 µm
5 µm

Figure 4-4 Localisation of [A] RFC2-GFP, [B] RFC3-GFP and [C] RFC4-GFP during mitosis in the early *Drosophila* embryo.

A] Localisation of RFC2-GFP: I] Nuclear envelope breakdown (NEB) II] 60 seconds post NEB III] 2 minutes post NEB IV] 4 minutes post NEB V] Interphase.

B] Localisation of RFC3-GFP: I] Interphase II] NEB IV] 2.5 minutes post NEB V] Interphase.

C] Localisation of RFC4-GFP I] Interphase II] NEB III] 60 seconds post NEB IV] 5.5 minutes post NEB V] Interphase

In all cases the RFC subunits are nuclear in interphase. Then as NEB occurs there appears to be a weak localisation to the spindle. Timings have been given relative to interphase and NEB as the localisation was not clear enough to accurately predict the mitotic stages.

Stills are from movies taken as follows: 200 time points, one image taken every 2 seconds. Each image is composed of a z stack, made up of 5 stacks 1 micron between each. Exposure was 200 ms with the 488 laser set at 20%

Scale bar = 5µm

### 4.2.8 Knock down of RFC subunit RFC2 or Dcc1 causes embryonic arrest prior to cellularisation

The original biochemical screen that identified *Drosophila* RFC2 (CG8142) as MT associated demonstrated that RNAi against the gene in S2 cells led to defects in mitotic spindle formation and chromosome alignment (Hughes *et al*., 2008). In addition, a chromosomal phenotype has also been observed in larval brain squashes of RFC4 mutants, this time presenting as a segregation defect (Krause *et al*., 2001). However no functional analysis of any RFC subunit in embryos has been undertaken.

I therefore sought to investigate how a knock down of the RFC subunits would impact mitosis in the early embryo. *Drosophila* lines carrying short hairpin RNAs (shRNAs) to specifically target the RFC2 gene, were crossed with a line carrying histone RFP and EB1 GFP on the 2$^{nd}$ chromosome and a maternal α tubulin GAL4-driver on the 3$^{rd}$ chromosome to create a RFC2 knock down line. 0-2 hour embryos were then imaged using a spinning disc laser confocal microscope. Fly maintenance and embryo collected were initially carried out at 25°C. However when imaging the embryos using spinning disc confocal microscopy, nuclei and MTs were not visible. Two different shRNA lines were tested and, even when flies were raised and embryo collected at 18°C, to reduce the expression of the GAL-4 driver, and therefore expression of the shRNA, embryos failed to develop past this stage. Hatch rates for this line when the RNAi was driven at both 25°C and 18°C revealed that less than 1% of embryos hatched (Supplementary Table 4). When hatch rates were counted for controls (RNAi not driven) on average 98% of all embryos hatched, this again suggesting that the RNAi is preventing the embryos from developing.

Similarly, in order to investigate whether knock-down of the chromosome cohesion-specific Cutlet-RFC complex in embryos led to mitotic defects, I used shRNA to target the subunit Dcc1 (CG11788 in *Drosophila*). Again, even at 18°C, spindles and chromatin were absent from the embryonic cortex. Hatch rates for this line again showed that less than 1% of embryos hatched when the RNAi was being driven, compared to the 97% hatch rate seen in controls (Supplementary Table 5).

The most likely explanation of these results is that reducing the expression of RFC2 or Dcc1 leads to chromosome-based defects very early on in embryogenesis or prior

to fertilisation - shRNA expression driven by the maternal a tubulin GAL-4 takes effect in the latter stages of oogenesis. Visualisation of MTs and nuclei in the early *Drosophila* embryo using confocal spinning disc microscopy relies on the presence of these structures at the embryonic cortex. The first 8 nuclear divisions occur deep inside the embryo, prior to cortical migration. Thus, phenotypes that arrest embryo development prior to cycle 9 will not be visible using this technique. Unfortunately, due to time limitations, I was unable to collect, fix and stain RFC2 or Dcc1-RNAi embryos and assess the very early embryonic phenotype. As such, the actual cause of developmental arrest remains to be explored.

### 4.3 Conclusions and further work

In summary, this Chapter has shown that a GFP-tagged version of the RFC subunit, RFC3, is capable of incorporating into endogenous RFC complexes, that it co-sediments with MTs, independently of chromatin and that RFC2 RFC2,3 and 4-GFP show identical subcellular localisations, weakly localising to mitotic spindles during metaphase. The identification of all subunits of all three RFC-like complexes, via affinity purification and MS of RFC3-GFP, strongly suggests that all three variants are present in the early embryo and, when taken in conjunction with the original QC-MAP data, suggest the Cutlet-RFC complex, containing Dcc1 and CTF8 increases its affinity to MTs during these mitoses.

Unfortunately, a preliminary functional analysis of reducing Dcc1 or RFC2 gene function has not provided any data on the precise role of this complex in mitosis; shRNA-driven knockdown of either gene appears to arrest oogenesis or embryonic development at a very early stage.

It is known that the RFC complex can exist in a number of forms, one of which is required for sister chromatid cohesion. The interaction between these two proteins could therefore be based around a shared function at the chromatids.

In order to investigate this hypothesis further, the next step would be to assess the phenotype produced by depleting subunits of the Cutlet-RFC subunits via antibody injection. As presented in this thesis knocking down levels of both RFC2 and Dcc1 via RNAi prevented embryos from developing far enough to observe a mitotic phenotype. By injecting antibodies that sterically interfere with RFC function,

embryos would be able to develop normally to a stage amenable for imaging, and then the resulting phenotypes could be imaged following injection of an RFC specific antibodies.

The interaction between the RFC complex and EB1 is also of interest, as it could present the link between the RFC complex and MTs. In a study by Rogers *et al*., paper (2002) it was shown that inhibiting EB1 in *Drosophila* S2 cells caused chromosome segregation to fail. One explanation behind this phenotype could be that EB1 mediates the interactions between MTs and kinetochores, through localising specific factors to the interface between these structures. It could, therefore, be hypothesised that the interaction between EB1 and the Cutlet-RFC complex, as highlighted by MS, is required to load Cutlet-RFC on to kinetochores, maintaining chromosome cohesion until the metaphase anaphase transition.

Several future experiments will be required to further investigate the putative interaction between EB1 and the RFC complex and the role of the RFC complex in mitosis. The first step would be to carry out a reciprocal affinity purification of EB1 to see if the RFC subunits appear as an interactor, and if any RLC complexes are interacting. By highlighting the specific RFC complex that is interacting with EB1, it will allow further experimentation to be directed more specifically to the RFC1 paralogue subunits alongside the archetypal RFC2-38, in order to further develop our understanding of this complex in mitosis.

## 5. Investigating two MAPs of known mitotic function - Abnormal spindle protein (Asp) and *Drosophila* Transforming Acid Coiled Coil (DTACC)

### 5.1 Introduction

Although much is already known about the localisation and function of a number of *Drosophila* MAPs during mitosis, recent advances in technology have resulted in new approaches to further investigate gene function. By combining biochemistry techniques with proteomics we are able to identify both known and novel protein interactors. We are also able to observe the dynamic nature of the mitotic spindle, using embryos carrying GFP fusions of our protein of interest, via cold treatment. Cold treatment of mitotic embryos at 4°C results in mitotic spindle disassembly (Hayward et al., 2014). Upon subsequent return to room temperature, MTs do not regrow from centrosomes; instead they are generated in the region of the mitotic chromatin, where they are sorted in a bipolar array capable of chromosome segregation (Hayward et al., 2014).

The aim of this chapter was to perform high temporal and spatial resolution imaging of GFP-fusions to two such previously characterised MAPs, Asp and DTACC during both centrosome-driven spindle formation and chromatin-driven spindle self-organisation, combining this analysis with proteomics, in order to uncover new interactors of these proteins and to potentially uncover further roles for them in spindle formation and mitosis.

#### 5.1.1 Abnormal Spindle Protein (Asp)

The Abnormal spindle protein (Asp) locus was first identified as a late larval mutation presenting defects in both mitosis and meiosis, making it the first MAP to be identified using a genetics based approach (Ripoll *et al*., 1985). Asp is a basic, hydrophilic protein with an alpha helical secondary structure. Sequence analysis of the Asp protein revealed the presence of a short sequence showing a significant similarity to the actin binding domains of a series of actin binding proteins, including α actinin (Saunders *et al*., 1997). Asp also carries a short sequence corresponding to a conserved calmodulin binding domain, and consensus sites for phosphorylation by $p34^{cdc2}$ and MAP kinase. It has been shown to bind MTs with high affinity, under conditions that would usually result in MAP dissociation (Saunders *et al.,* 1997)

Asp is the *Drosophila* orthologue of human ASPM. Mutations in ASPM are the most common cause of microcephaly; a disease characterised by a reduced brain size. A study carried out in larval brains show Asp mutants display defects in the neural epithelium of the optic lobe and severe microcephaly. These phenotypes would indicate that the reduced brain size seen in microcephaly cases is a result of defective spindle positioning, chromosome segregation and apoptosis (Rujano *et al*., 2013). Mutations in the Asp gene also causes mitotic and meiotic disjunction, resulting in the formation of abnormally long and wavy spindles (Gonzalez *et al.,* 1990) hence it being termed “abnormal spindle”. Spindles formed under an Asp mutation present broadened, splayed and unfocussed poles, though they are still bipolar (Wakefield et al., 2001). Depletion of Asp using RNAi in S2 cells results in a similar phenotype (Morales-Mulia and Scholey 2005). This phenotype is similar to that resulting from loss of NuMA in human cells and, in the absence of a NuMA homologue in flies, Asp has been proposed to be a functional homologue (Wakefield et al., 2001; Morales-Mulia and Scholey 2004). The reported localisation of Asp supports its role in focusing spindle poles. It is found both at the centrosome, and at the interface between the centrosome and the spindle pole during metaphase (Saunders et al., 1997; Wakefield et al., 2001). It is also present later in mitosis and meiosis at the minus ends of the central spindle (Wakefield et al., 2001). Together, the existing data is consistent with a role for Asp in cross-linking or bundling MTs at their minus ends, allowing both spindle pole and central spindle integrity.

### 5.1.2 Drosophila Transforming Acidic Coiled Coil protein (DTACC)

TACC is the *Drosophila* homologue of the human transforming acid coiled coil protein (TACC). The TACC proteins are present in a number of organisms, DTACC being the single *Drosophila* homologue (Peset and Vernos 2008). DTACC has been shown to have important roles in spindle formation during the mitotic divisions of the early *Drosophila* embryo (Gergely *et al*., 2000a). In embryos in which DTACC function has been affected, the mitotic spindle and astral MTs are much shorter and weaker leading to failure in chromosome segregation and migration of the nucleus (Gergely *et al*., 2000b). Biochemically, DTACC associates with MTs in a standard co-sedimentation assay (Gergely *et al*., 2000a). However, although the C-terminus interacts directly with MTs, it does so only very weakly, and its MT binding activity is facilitated in the embryo through a direct interaction with a further MAP, Minispindles

(Msps). Msps, the *Drosophila* homologue of XMAP215/TOG is a MT stabilising protein (Zhang and Megraw 2007), binding directly to the MTs and regulating their dynamics by influencing events occurring at the MT plus end (Cassimeris 1999). Although DTACC and Msps are thought to primarily act at the plus end of MTs GFP-fusions to both proteins are most concentrated around the centrosomes, where the MT minus ends cluster. Based upon this is has been proposed that Msps is recruited to the centrosome by TACC proteins where it is loaded onto plus ends as the MT grows, or so MT minus ends can be stabilised once released from the site of nucleation (Lee *et al*., 2001).

## 5.2 Results and Discussion

### 5.2.1 Asp localises to cortical MTs at the onset of chromatin driven spindle formation.

In order to determine the dynamic localisation of Asp during mitosis in the early embryo, 0-2 hour old embryos expressing AspGFP were imaged using spinning disc laser confocal microscopy, under conditions of both centrosome driven and chromatin driven MT formation.

As observed in Figure 5-1A at the onset of mitosis following NEB and in the early mitotic stages prophase and prometaphase, Asp localises to the spindle poles and centrosomes. In agreement with studies published by Saunders *et al* (1997) and Wakefield *et al* (2001), this localisation remains as the spindle fully forms: Asp localising to the interface between the minus ends and the centrosome. As the syncytium progresses into anaphase, Asp can now be seen at the spindle mid-body where it continues to be visualised through into telophase. During the initial stages of spindle self-organisation around chromosomes, following cold treatment (for procedure see Materials and Methods), AspGFP initially appears to localise to the ends of remaining cortical MTs (Figure 5-1B). Once the spindle has reformed and mitosis progresses the localisation then returns to that of the controls, being predominantly found at the spindle poles. Based on the observations of both control spindles, and those following cold treatment it can be concluded that Asp localises to the minus ends: both when spindle formation occurs from the centrosomes, and when spindle formation is chromatin driven.

One other interesting observation is that, when comparing controls and the cold treated embryos, there is a noticeable difference between the spindle orientation post cold treatments. In many instances the spindle poles seem to have “stuck” together forming a chain like appearance, potentially suggesting that expression of the GFP-Asp transgene has dominant effects specifically during mitotic spindle self-assembly.

Figure 5-1

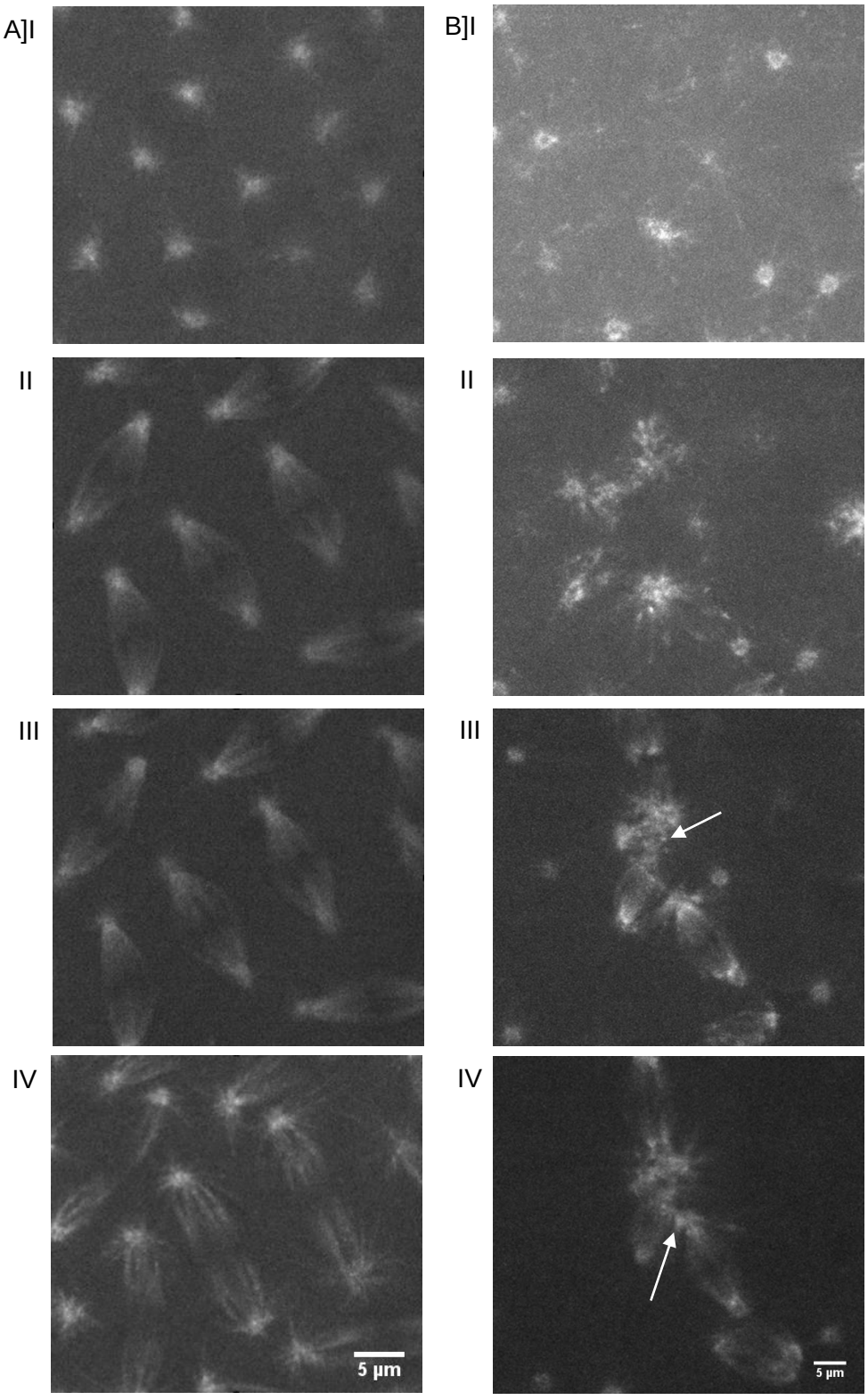

Figure 5-1: AspGFP localisation in early *Drosophila* embryos. A] Control images: I] Prophase II] Metaphase III] Anaphase IV] Telophase.

In the early stages of mitosis Asp localisation is predominantly centrosomal. As mitosis progresses this localisation shifts towards the spindle mid body.

B] Cold treated images: I] 2 seconds II] 74 seconds III] 166 seconds IV] 236 seconds.

Times represent seconds post return to room temperature. Asp can be initially visualised on astral microtubules, then as the spindles begin to reform Asp can be seen at the centrosome.

Note the re orientation of the spindles towards one another (arrows).

### 5.2.2 DTACC can be seen at the ends of astral MTs following cold treatment

In control embryos (Figure 5-2A) DTACC shows a strong centrosomal localisation throughout the entirety of mitosis. It has been reported that the TACC family of proteins can be considered a centrosomal component; however this does not restrict its localisation to this organelle as many of the TACC proteins can also form MT associations (Peset and Vernos 2008). DTACC is required for MT stabilization and the centrosome and at the minus ends (Zhang and Megraw 2007; Gergely *et al.,* 2000a). In our imaging we cannot conclude that DTACC is present at the minus ends however it is clearly at the centrosome.

When observing spindle formation driven by chromatin mediated MT nucleation, the localisation of DTACC appears to differ slightly from when the spindle forms at the centrosome (Figure 5-2B). Although we still see DTACC at the centrosomes, the intensity of the fluorescence and hence the concentration of the protein appears to be greatly increased (all imaging settings and image processing parameters remained consistent throughout). We can now also see DTACC concentrating in “blobs” at the ends of nucleating astral MTs until anaphase, where this localisation appears to fade: something that was not observed under conditions of centrosome driven spindle formation. As reported by Lee *et al* (2001) DTACC and its binding partner Msps (see section 5.2.4) are thought to act at the plus ends of MTs, however GFP fusions of both appear to localise to the minus ends. It has been suggested that DTACC recruits Msps to the centrosome where it is loaded onto plus ends. Based upon this notion, it could be suggested that the DTACC we are seeing on the ends of the astral MTs is there because of its role in Msps transportation.

Figure 5-2

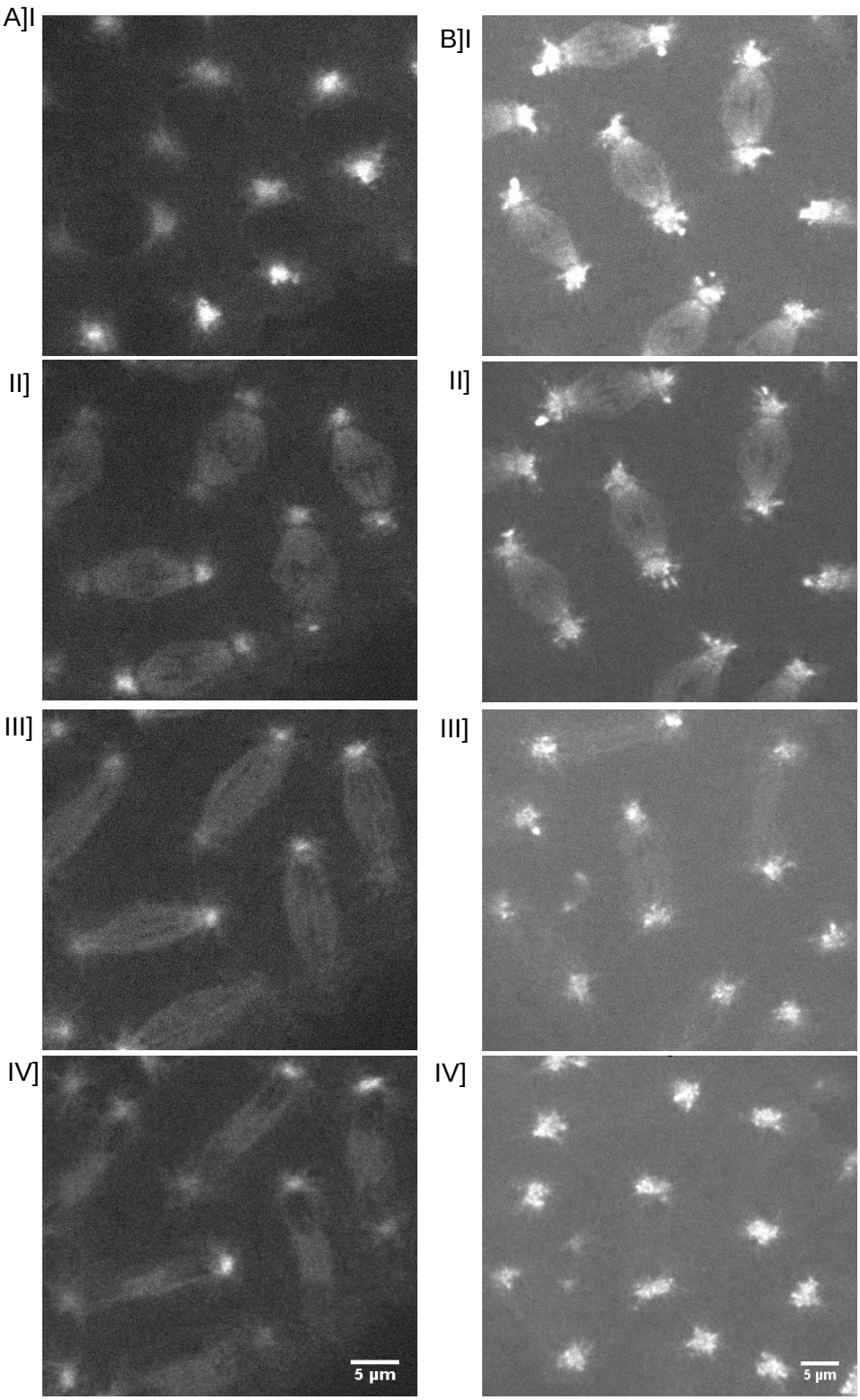

Figure 5-2: Localisation of DTACC-GFP in early *Drosophila* embryos. A] Control images: I] Prophase II] Metaphase III] Anaphase IV] Telophase.

B] Cold treated images: I] 2 seconds II] 52 seconds III] 110seconds IV] 160 seconds.

Times represent seconds post return to room temperature.

Scale bar = 5µm

### 5.2.3. Identification of Asp-GFP interacting proteins

GFP-TRAP-A based affinity purification, in combination with mass spectrometry and proteomic analysis, was used in order to identify interactors of Asp in the early embryo. This analysis was carried out in both cycling and mitotic (MG132-treated) AspGFP embryos and the results compared. As predicted, our bait protein was the top hit in both cases when analysing the mass spectrometry data, indicative of a successful purification. Following the data filtration guidelines as applied to all other data sets presented in this thesis, 10 potential mitotic interactors of Asp were identified (Table 7).

| Protein name | % coverage | MW (KDa) | Score |
|---|---|---|---|
| Asp | 19.75 | 230.0 | 1452.26 |
| PP2A-B' | 31.59 | 64.4 | 151.87 |
| SET | 21.56 | 31.0 | 116.88 |
| NLP | 23.68 | 17.0 | 102.53 |
| ATMS | 18.40 | 60.8 | 71.58 |
| CaM | 22.15 | 16.8 | 65.46 |
| CG6453 | 15.88 | 61.5 | 63.46 |
| CG2061 | 16.95 | 47.6 | 63.17 |
| Widerborst | 20.61 | 59.7 | 56.59 |
| MLC-C | 42.18 | 16.6 | 37.90 |

Table 7: Asp interacting proteins identified via MS.

Data has been sorted by score with a cut off of 30. Any proteins with less than 3 peptides (data not shown) were also removed from the list. As expected, the bait protein scored highest.

Known interactors of Asp, Calmodulin (CaM) and Myosin light chain C (MLC-C) were also present in the screen (red). Novel interactors (highlighted in blue) of particular interest include a subset of proteins associated with the protein phosphatase PP2A.

Among the mitotic interactors were proteins already known to interact with Asp - Calmodulin (CaM) and Myosin Light Chain (MLC-C) (Goshima et al., 2007). During an RNAi screen of S2 cells carried out by Goshima et al., (2007), knockdown of calmodulin (CaM) phenocopied loss of Asp. Subsequent analysis showed that Asp and CaM co-localise to the minus ends of spindle K-fibres, even when disconnected from the centrosome and that both proteins equally rely on the other for their localisation. Asp features a number of CaM binding IQ motifs and these are required for both localisation and function. It was suggested in this study that based on the specificity of the CaM phenotype produced by RNAi and its similarity to Asp RNAi that the main function of CaM during mitosis is to act as a cofactor of Asp mediated focusing of the spindle poles (Goshima *et al.,* 2007).

Analysis of the mass spectrometry data also revealed interactions with a subset of proteins related to protein phosphatase 2A (PP2A), including a PP2A inhibitor and other targeting subunits (Table 7).The PP2A holoenzyme consists of three subunits: a catalytic and a structural subunit making up the core enzyme, and a regulatory subunit. There are four distinct groups of regulatory subunit: B, B', B'' and B'''. Unlike the catalytic subunits, the regulatory subunits are diverse and likely to be involved in localisation and substrate specificity of PP2A (Janssens and Goris 2001).
The *Drosophila* genome contains 4 B type PP2A regulatory subunits: Twins (B subtype), Widerborst, PP2A-B' (both B' subtypes) and PP2A-B'' (B'' subtype) (Chen *et al*., 2007). In this screen both B' subtypes were identified as interacting with Asp. There is genetic evidence to suggest that in *Drosophila* the PPP family protein phosphatases PP1 and PP2A regulate spindle organisation and segregation of sister chromatids (Axton et al., 1990; Snaith *et al.,* 1996) In *Drosophila,* reducing PP2A activity has been reported to cause an increase in unbundled MTs, a phenotype that is further enhanced by reducing the activity of PP2A-B' (Viquez *et al*., 2006). The B' subtype protein Widerborst was has also been implicated in the segregation of chromosomes and like Asp, mitotic spindle formation (Chen *et al*., 2007). A study by Chen *et al* (2007) showed that in *Drosophila* S2 cells, Widerborst co-localised to the centromeric marker CENP-A. Following spindle formation Widerborst localises adjacent to and external to the centromeres, this localisation remaining during anaphase but less pronounced.

The final PP2A related novel interactor of Asp identified in the MS was SET. Very little is known about SET in *Drosophila.* However, in humans the homologue is a known inhibitor of PP2A (also called I2PP2A). Alignment of the amino acid sequences of both human and *Drosophila* SET showed that they are 55% identical, indicating that SET is highly conserved. SET is also the homologue of the *Xenopus laevis* Nucleosome Assembly Protein 1 (Nap1) which interacts with B type cyclins (Kellogg *et al.*, 1995). The set gene was originally identified as part of an oncogene formed by its fusion of the nuclear pore complex protein Can, in a case of acute myeloid leukemagenesis (Von Lindern *et al*., 1992). In HeLa cells SET has been reported to be predominantly nuclear (Adachi *et al*., 1994). As with the other PP2A related proteins identified as being potential novel interactors of Asp there is no direct evidence linking the cellular roles of Asp and SET. However, the identification of three separate PP2A-linked proteins as Asp interactors opens up a potential new avenue of research into the regulation of this important MAP.

### 5.2.4 Identification of DTACC-interacting proteins

Similarly to the above work carried out on Asp, in order to develop our understanding of DTACC in mitosis, 0-3 hour mitotic (MG132 treated) *Drosophila* embryos expressing DTACC-GFP were subjected to GFP-TRAP-A based affinity purification followed by MS was used to identify protein interactions. Following the data filtering procedure we were left with 7 interactors (Table 8).

| Name | % coverage | MW (kDa) | Score |
|---|---|---|---|
| Msps | 62.92 | 229.4 | 3977.55 |
| Msps | 62.82 | 230.3 | 3959.81 |
| DTACC | 68.98 | 136.4 | 3652.63 |
| Map205 | 11.26 | 124.1 | 55.97 |
| Dgt6 | 15.75 | 72.8 | 36.64 |
| Lok | 18.95 | 52.3 | 36.02 |
| Dgt5 | 10.22 | 77.9 | 33.36 |

Table 8: DTACC interacting proteins identified in MG123 treated embryos via MS.

The top scoring proteins in the MS of mitotic DTACC-GFP embryos were DTACC and Msps, which are known to bind in a 1:1 ratio. The screen also identified Map205, Lok, and the two Augmin subunits Dgt5 and Dgt6.

The top scoring proteins, present at roughly stoichiometric amounts, were two isoforms of the known DTACC interactor Msps and DTACC itself (Table 8). As explained earlier in the Chapter, Msps belongs to the Tog family of proteins; the Tog family being a subset of non-motor MAPs that are highly conserved from yeast to humans (Ohkura *et al*., 2001). XMAP215, the *Xenopus* homologue of Msps has been well characterised as a MT plus end growth regulator (Gard and Kirschner 1987; Vasquez *et al*., 1994). For many years the Tog family of proteins have been regarded as MT stabilising proteins however more recently reports have shown that under certain conditions these proteins, specifically XMAP215, and Stu2 the budding yeast homologue may also act to destabilise MTs (Shirosu-Hiza *et al*., 2003). Msps is a known interactor of DTACC, this interaction strongly influencing MT behaviour in the *Drosophila* embryo. Changing the levels of DTACC in the embryo alters the localisation of Msps; reducing DTACC levels prevents Msps from efficiently accumulating at the centrosome resulting in clearly destabilised MTs. Conversely increasing levels causes both DTACC and Msps to concentrate at the spindle poles, the centrosomal MTs now stabilised (Lee *et al* 2001).

Four other proteins were highlighted as potential interactors of DTACC in mitotic embryo extracts; Map205, Loki (Lok) and the Augmin subunits Dgt5 and Dgt6.

Map205 is a well characterised mitotic MAP with roles in the mitotic cell cycle (Archambault *et al.,* 2008). Although there is currently no evidence to suggest an interaction with either DTACC or Msps.Map205 is responsible for recruiting the mitotic kinase Polo to the spindle. (Tavares *et al.,* 1996). The MT associated population of Polo is kept inactive through this association, unless phosphorylated by Aurora B kinase (Kachaner *et al*., 2014). Given the high levels of Map205 on mitotic MTs (as highlighted in Chapter 3 of this Thesis), it is possible that Map205, similarly to Msps, increases the affinity of DTACC for MTs in the embryo, independently of, or in combination with, Msps.

Lok, the *Drosophila* orthologue of Checkpoint Protein 2 (Chk2) is essential for the embryonic DNA damage response (Takada *et al*., 2003; Sakurai *et al*., 2011). The DNA damage response includes processes such as mitotic centrosome inactivation, cell cycle delay and nuclear dropping from the cortex occur to maintain genomic integrity in syncytial embryos (Takada, Collins and Kurahashi 2015). As DTACC is

known to localise to the centrosome it could be hypothesised that the process of centrosome inactivation is the common factor between these two proteins; there is however currently no evidence to support this idea.

Perhaps most interesting result is the presence of Augmin complex subunits, Dgt5 and Dgt6, in DTACC mitotic, but not cycling, immunoprecipitates. Augmin, as described in Chapter 1, is a hetero-octomeric protein complex that associates with MTs and the γ-TuRC, facilitating MT-dependent MT nucleation. It could be hypothesised that the association of Augmin subunits and DTACC is due to the specific MG132 treatment of embryos causing a number of small MTs to be nucleated, which then recruit the Augmin complex, and which are pulled down non-specifically. If this were the case however we would expect to see the Augmin subunits appearing at a low level for all MS analysis carried out on MG132 treated samples, which we do not. This would therefore suggest that this is a true interaction. The presence of only two of the eight subunits could reflect a specific interaction between DTACC and these two proteins. Indeed, the interaction between Dgt6 and DTACC has been previously reported by Bucciarelli et al (2009). In this study they showed that depleting Dgt6 resulted in a strong reduction in the accumulation of DTACC and Msps at the centrosome (Cullen *et al*., 1999; Gergely *et al*., 2000; Brouhard *et al.,* 2008). In the reverse experiment depleting either DTACC or Msps in S2 cells prevented Dgt6 from accumulating at the poles; however its spindle localisation remained intact. It was also shown that in S2 cells Dgt6 co-precipitates with DTACC and Msps suggesting that *in vivo* Dgt6 interacts with the DTACC-Msps complex (Bucciorelli *et al.,* 2009). Thus, Dgt6, and other Augmin subunits, might have Augmin-independent roles during mitosis.

Alternatively, the lack of other Augmin subunits in the DTACC-GFP purification may reflect the stringent cut-off - indeed, Dgt3 was also present in the MS however its score was below the cut-off threshold and so was excluded.

## 5.3 Conclusions and further work

In summary, the work presented here provides new information with regards to both Asp and DTACC. It has been shown that when the spindle is depolymerised by cold treatment, inducing chromatin mediated MT regrowth, changes occur in either protein localisation or spindle orientation. It cannot yet be said that the phenotype following cold treatment of Asp is due to over expression of Asp because of the GFP tag. In order to assess this further the cold treatment would need to be repeated multiple times more to see if the same result occurs.

Using affinity purification we were able to identify a novel subset of Asp interactors related to PP2A. Only one of the interactors identified had a current mitotic functional GO, Widerborst having been implicated in spindle formation (Chen *et al.,* 2007). In order to investigate these interactions further the next step would again be to do the reciprocal affinity purifications in order to establish if the interaction remains. It may also be advantageous to investigate the PP2A interactions in Asp mutant lines in order develop an understanding of potential phosphorylation and dephosphorylation functions of Asp in mitosis.

To follow up the localisation following cold treatment of DTACC embryos, particularly to see if the astral MT “blobs” are due to Msps the most logical step would be to image DTACC-GFP under these conditions in embryos in which Msps function has been perturbed. In addition it would be advantageous to generate a *Drosophila* line expressing DTACC-GFP and for instance Msps red fluorescent protein (RFP) together and then undertaking cold treatment to examine the localisations of both proteins.

Carrying out the same affinity purification techniques, this time using DTACCGFP embryos revealed that DTACC-Msps does indeed bind to one another in a 1:1 ratio; both proteins producing an incredibly similar MS score. This analysis also revealed that the Augmin complex constituents Dgt3 (although scoring below 30), Dgt5 and Dgt6 as interactors with DTACC. The interaction between Dgt6 and DTACC-Msps has been shown previously by Bucciorelli *et al.,* (2009), however the interaction between DTACC-Msps and the other Augmin subunits appears to be novel. With regards to further investigation, the next step would be again to firstly perform reciprocal affinity purification assays and MS on the Augmin complex proteins

identified to see whether DTACC appears as an interactor. Secondly it may be interesting to combine fluorescence imaging and antibody injection to gain further information on the localisation behaviours surrounding the Dgt proteins and DTACC-Msps.

In brief, the further analyses we have carried out on these mitotic MAPs has led the way for a series of potential new experiments that could further elucidate their importance in the assembly of the bipolar mitotic spindle.

## 6. Discussion

The aim of this Masters by Research was to investigate and characterise the role of a number of MAPs during mitosis. By combining proteomics, fluorescent imaging and biochemical techniques I have been able to study the localisation and protein interactions of the RFC complex during mitosis in the early *Drosophila* syncytial embryo. By applying these techniques to the known MAPs, Asp and DTACC, I have been able to identify novel protein interactors and observe changes in protein localisation following a change in the spatial regulation of mitotic MT nucleation.

### 6.1 Potential mitotic functions for the RFC complex

Initial analysis of MT co-sedimentation assays, carried out using samples produced from both cycling and mitotic populations of *Drosophila* embryos, presented over 700 MT-associated proteins. Statistical analysis comparing both populations revealed 209 proteins that showed a significantly increased association with MTs in mitosis in comparison to the cycling population. Analysis of the GOs of these proteins assigned them into a number of complexes, including the cohesion and condensin complexes, the RISC, P granules and the RFC complex: the latter becoming the focus of this research project.

The RFC complex is a five subunit protein complex, made up of the large RFC1 subunit and the four small RFC2-38 subunits (Tsuchiya *et al*., 2007). The primary function of the RFC complex is in DNA replication, as the PCNA sliding clamp loader, first identified for its role in the replication of SV40 (Fairman *et al.,* 1988). In the initial stages of this investigation, I generated GFP fusions of the three small RFC subunits RFC2, RFC3 and RFC4. Using these fusions, I was then able to assess the localisation of the RFC complex during mitosis. Prior to this study, there was no evidence to suggest that the RFC complex localises to the mitotic spindle; however, there is evidence of mitotic function for the small subunits RFC2 and RFC4. RNAi against RFC2 presents a chromosome misalignment phenotype (Hughes *et al.,* 2008) and mutations in the rfc4 gene result in chromosome segregation defects (Krause *et al.,* 2001). The RFC complex has a number of functions outside of its role as the PCNA clamp loader, which are facilitated by the replacement of the large RFC1 subunit. For instance, RFC1 can be replaced with the *Drosophila* homologue of CTF18, Cutlet. Cutlet functions with two additional co-

factors, DCC1 and CTF8, and is essential for sister chromatid cohesion in yeast (Meyer *et al.,* 2001). Based upon the information presented above, when imaging the RFC subunits we expected to see the RFC complex localising strongly to the nucleus during interphase, then localising to the chromatin or kinetochores as part of the Cutlet-RFC complex during mitosis. Concordantly, my imaging (Figure 4-4) showed a strong nuclear localisation for all 3 GFP-tagged RFC subunits during interphase; however what was observed during mitosis differed from this prediction. Following NEB, a weak GFP signal is present in the region of the mitotic spindle. Based on imaging alone the results are inconclusive, and the potential interaction between MTs and the RFC complex in mitosis was therefore investigated biochemically. A MT spin-down using 0-3 hour RFC3GFP *Drosophila* embryos probed for both GFP and tubulin revealed that RFC3 pelleted with MTs (Figure 4-2), a novel finding that had only previously been inferred (Hughes *et al*., 2008).

Having confirmed that the RFC complex localises to MTs in mitosis I next sought to identify interacting proteins, achieved by combining biochemistry with MS. This analysis highlighted the presence of the alternative RFC complexes; Cutlet-RFC, Elg1-RFC and Rad17-RFC, as well as a number of other potential interactors, including the well-characterised MAP EB1. Having identified EB1 as an interacting protein with RFC, it can be hypothesised that it is this link joining the RFC complex to the MTs; the Cutlet-RFC complex more specifically. It has been revealed in *Drosophila* S2 cells that inhibition of EB1 results in failed chromosome segregation (Rogers *et al.,* 2001), similar to that observed following RNAi of RFC4 (Krause *et al.,* 2001) again demonstrated in S2 cells. Prior to any further investigation I hypothesise that EB1 is acting as a mediator between the MT and kinetochores, and therefore is required to load Cutlet-RFC onto the kinetochores to maintain sister chromatid cohesion (see Chapter 4.7).

By way of investigating the role of the Cutlet-RFC complex in mitosis, RNAi against the small RFC subunit RFC2, and the associate protein DCC1 was carried out in *Drosophila* embryos. An RNAi phenotype has already been observed for RFC2 in S2 cells (Hughes *et al.,* 2008) but not in the early embryo. I was unable to observe a spindle phenotype in either knockdown as the embryos arrested prior to formation of a spindle monolayer in cycle 10 (Karr and Alberts, 1986). As previously described

(Chapter 4.5), this occurrence is likely to be due to a failure at the DNA level during the first few rounds of division.

To summarise the progress made with regard to investigating the RFC complex in mitosis, the work presented here indicates that firstly the RFC complex binds to MTs during mitosis, and that there is a weak spindle localisation during the early mitotic divisions in the *Drosophila* embryo. We have also confirmed the presence of the three alternative RFC complexes, as well as the archetypal complex in embryos that have been chemically arrested in mitosis. The most promising candidate for future work is the Cutlet-RFC complex, as this seems to have the most likely mitotic function. Further work will investigate this protein complex in greater detail, aiming to identify a mitotic phenotype for this complex with regard to the spindle and spindle formation, both at the centrosomal and chromatin levels.

## 6.2 Chromatin driven spindle formation alters the localisation of MAPs in mitosis.

In addition to aiming to characterise the mitotic role of a subset of novel MAPs, our attention was also focused upon re-addressing and developing our understanding of the functions of the previously well-characterised MAPs. One such MAP was Asp; it is established that mutations in the asp gene result in the formation of broadened, splayed and unfocused spindles (Wakefield *et al.,* 2001), which would indicate that Asp is vital for focusing the spindle pole. This function is supported by its localisation; as reported by Saunders *et al.,* (1997) and Wakefield *et al.,* (2001), Asp localises both to the centrosome and at the interface between the centrosome and the spindle poles. This localisation is true for centrosome-mediated spindle formation, but the localisation of Asp during chromatin-driven spindle formation remained unresolved. Using temperature to depolymerise the mitotic spindle, we were able to observe the localisation of Asp as the mitotic spindle reformed under a different nucleation pathway. The localisation with regard to position relative to the spindle was consistent between the two pathways; however, as the spindle was regenerating Asp, was now observed on the ends of cortical MTs. This localisation subsequently disappeared as Asp returned to the poles of the newly formed spindle. Notably, the spindles that regenerated following the cold treatment changed orientation and "stuck" together, forming an apparent chain of individual spindles. We are reluctant to postulate that this occurrence is simply an artefact of the cold treatment process

as Asp is the only protein background we have observed this in; we could not generalise from these results alone as to what is causing this shift, making this grounds for further investigation.

The second protein we investigated in this manner was DTACC. Like Asp, DTACC localises to the centrosome and MT minus ends, where it is required for MT stabilisation (Zhang and Megraw, 2007; Gergely *et al.,* 2000a). Again, this localisation is well-characterised, yet DTACC localisation during chromatin-mediated MT localisation was previously unknown. Following cold treatment, the signal intensity of DTACC at the centrosome increased compared to the control, despite all imaging parameters remaining the same. We also observed "blobs" of DTACC accumulating at the end of nucleating astral MTs until anaphase. Again, no further investigation has been done to identify as to why this shift in localisation may be occurring but we can hypothesise that DTACC is being observed, particularly at the ends of asters, as part of its role in Msps transportation for the stabilisation of the newly nucleated MTs (Lee *et al.,* 2001).

### 6.3 Novel interactors identified for known mitotic MAPs

As well as re-addressing protein localisation during mitosis, we also aimed to investigate the protein interactions of Asp and DTACC in mitosis. As with the RFC complex, biochemical assays followed by proteomics analysis highlighted proteins that specifically interacted with our bait proteins in mitosis. With regards to DTACC this analysis confirmed the binding relationship between DTACC and the Drosophila homologue of XMAP215, Msps (Gard and Kirschner 1987; Vasquez *et al.,* 1994), with both DTACC and Msps being required for MT stabilisation at the spindle poles (Lee *et al.,* 2001). Interestingly amongst the other four proteins identified as mitotic interactors with DTACC were the Augmin subunits Dgt5 and Dgt6. The interaction between Dgt6 and DTACC was reported originally in 2009 by Bucciarelli *et al* (2009), but there was no evidence to suggest this interaction extended to other subunits. We hypothesise that this is a true interaction that required further investigation.

The biochemical and MS analyses again reinforced our knowledge of the binding of Asp to established interactors CaM and MLC-C, as reported by Goshima *et al.* (2007). A subset of the remaining mitotic interactors share a common relationship

with PP2A and there is genetic evidence to suggest that PP1 and PP2A protein families regulate spindle organisation and chromatid segregation (Axton *et al.,* 1990; Snaith *et al.,* 1996). Given what we know about Asp function in mitosis, these proteins may share a common function in the organisation of the mitotic spindle; however, further study will provide the necessary evidence to support this notion. There is also the possibility of a secondary Asp function in protein phosphorylation, therefore explaining why 2 of the 4 *Drosophila* B-type PP2A regulatory subunits (Widerborst and PP2A-B') (Chen *et al*., 2007) appear to be interactors of Asp. Again, further work is required to investigate this hypothesis.

## 6.4 Summary

In summary, the work carried out in this Masters by Research project has used a combination of proteomics, combined with fluorescence imaging and biochemical techniques, to enhance our knowledge of the mitotic MAP. This work has demonstrated that MS is a highly valuable tool for identifying both protein interactors on a small scale, and as a way of investigating protein levels between populations. By subsequently applying biochemistry-based approaches, these interactions can be investigated more thoroughly allowing us to better understand protein function. We have further demonstrated, particularly in reference to the known MAPs, that the specific MT nucleation pathway used by the embryo to generate a bipolar spindle correlates with differential protein localisation, thereby potentially revealing novel detail into roles of previously well characterised MAPs.

Supplementary Information

S1 – Fly food recipe (11L)

11kg Yeast

400g Glucose

400g Molasses

500g Flour

110g Agar

60ml Propionic Acid

220ml 10% Nipagin

1) Add yeast, glucose and molasses to 7L hot water and boil for 15min while mixing
2) Add flour and agar to 4L hot water, dissolve, and add to the main mix and boil for a further 15min while mixing
3) Turn heat off and cool to 60°C while constantly mixing
4) Add propionic acid and nipagin
5) Pour into bottles and vials
6) Leave to set and then plug the tops with bungs when cold

S2 Sequences

S2-1 pDONRzeo entry vector:

CTTTCCTGCGTTATCCCCTGATTCTGTGGATAACCGTATTACCGCCTTTGAGTGAGCTG
ATACCGCTCGCCGCAGCCGAACGACCGAGCGCAGCGAGTCAGTGAGCGAGGAAGCG
GAAGAGCGCCCAATACGCAAACCGCCTCTCCCCGCGCGTTGGCCGATTCATTAATGCA
GCTGGCACGACAGGTTTCCCGACTGGAAAGCGGGCAGTGAGCGCAACGCAATTAATAC
GCGTACCGCTAGCCAGGAAGAGTTTGTAGAAACGCAAAAAGGCCATCCGTCAGGATGG
CCTTCTGCTTAGTTTGATGCCTGGCAGTTTATGGCGGGCGTCCTGCCCGCCACCCTCC
GGGCCGTTGCTTCACAACGTTCAAATCCGCTCCCGGCGGATTTGTCCTACTCAGGAGA
GCGTTCACCGACAAACAACAGATAAAACGAAAGGCCCAGTCTTCCGACTGAGCCTTTC
GTTTTATTTGATGCCTGGCAGTTCCCTACTCTCGCGTTAACGCTAGCATGGATGTTTTCC
CAGTCACGACGTTGTAAAACGACGGCCAGTCTTAAGCTCGGGCCCCAAATAATGATTTT
ATTTTGACTGATAGTGACCTGTTCGTTGCAACACATTGATGAGCAATGCTTTTTTATAAT
GCCAACTTTGTACAAAAAAGCTGAACGAGAAACGTAAAATGATATAAATATCAATATATT
AAATTAGATTTTGCATAAAAAACAGACTACATAATACTGTAAAACACAACATATCCAGTCA
CTATGAATCAACTACTTAGATGGTATTAGTGACCTGTAGTCGACCGACAGCCTTCCAAA
TGTTCTTCGGGTGATGCTGCCAACTTAGTCGACCGACAGCCTTCCAAATGTTCTTCTCA
AACGGAATCGTCGTATCCAGCCTACTCGCTATTGTCCTCAATGCCGTATTAAATCATAAA
AAGAAATAAGAAAAAGAGGTGCGAGCCTCTTTTTTGTGTGACAAAATAAAAACATCTACC
TATTCATATACGCTAGTGTCATAGTCCTGAAAATCATCTGCATCAAGAACAATTTCACAA
CTCTTATACTTTTCTCTTACAAGTCGTTCGGCTTCATCTGGATTTTCAGCCTCTATACTTA
CTAAACGTGATAAAGTTTCTGTAATTTCTACTGTATCGACCTGCAGACTGGCTGTGTATA
AGGGAGCCTGACATTTATATTCCCCAGAACATCAGGTTAATGGCGTTTTTGATGTCATTT
TCGCGGTGGCTGAGATCAGCCACTTCTTCCCCGATAACGGAGACCGGCACACTGGCCA
TATCGGTGGTCATCATGCGCCAGCTTTCATCCCCGATATGCACCACCGGGTAAAGTTCA
CGGGAGACTTTATCTGACAGCAGACGTGCACTGGCCAGGGGGATCACCATCCGTCGC
CCGGGCGTGTCAATAATATCACTCTGTACATCCACAAACAGACGATAACGGCTCTCTCT
TTTATAGGTGTAAACCTTAAACTGCATTTCACCAGCCCCTGTTCTCGTCAGCAAAAGAG
CCGTTCATTTCAATAAACCGGGCGACCTCAGCCATCCCTTCCTGATTTTCCGCTTTCCA
GCGTTCGGCACGCAGACGACGGGCTTCATTCTGCATGGTTGTGCTTACCAGACCGGAG
ATATTGACATCATATATGCCTTGAGCAACTGATAGCTGTCGCTGTCAACTGTCACTGTAA
TACGCTGCTTCATAGCATACCTCTTTTTGACATACTTCGGGTATACATATCAGTATATATT
CTTATACCGCAAAAATCAGCGCGCAAATACGCATACTGTTATCTGGCTTTTAGTAAGCC
GGATCCACGCGGCGTTTACGCCCCGCCCTGCCACTCATCGCAGTACTGTTGTAATTCA
TTAAGCATTCTGCCGACATGGAAGCCATCACAGACGGCATGATGAACCTGAATCGCCA
GCGGCATCAGCACCTTGTCGCCTTGCGTATAATATTTGCCCATGGTGAAAACGGGGGC

GAAGAAGTTGTCCATATTGGCCACGTTTAAATCAAAACTGGTGAAACTCACCCAGGGAT
TGGCTGAGACGAAAAACATATTCTCAATAAACCCTTTAGGGAAATAGGCCAGGTTTTCA
CCGTAACACGCCACATCTTGCGAATATATGTGTAGAAACTGCCGGAAATCGTCGTGGTA
TTCACTCCAGAGCGATGAAAACGTTTCAGTTTGCTCATGGAAAACGGTGTAACAAGGGT
GAACACTATCCCATATCACCAGCTCACCGTCTTTCATTGCCATACGGAATTCCGGATGA
GCATTCATCAGGCGGGCAAGAATGTGAATAAAGGCCGGATAAAACTTGTGCTTATTTTT
CTTTACGGTCTTTAAAAAGGCCGTAATATCCAGCTGAACGGTCTGGTTATAGGTACATT
GAGCAACTGACTGAAATGCCTCAAAATGTTCTTTACGATGCCATTGGGATATATCAACG
GTGGTATATCCAGTGATTTTTTTCTCCATTTTAGCTTCCTTAGCTCCTGAAAATCTCGATA
ACTCAAAAAATACGCCCGGTAGTGATCTTATTTCATTATGGTGAAAGTTGGAACCTCTTA
CGTGCCGATCAACGTCTCATTTTCGCCAAAAGTTGGCCCAGGGCTTCCCGGTATCAAC
AGGGACACCAGGATTTATTTATTCTGCGAAGTGATCTTCCGTCACAGGTATTTATTCGG
CGCAAAGTGCGTCGGGTGATGCTGCCAACTTAGTCGACTACAGGTCACTAATACCATCT
AAGTAGTTGATTCATAGTGACTGGATATGTTGTGTTTTACAGTATTATGTAGTCTGTTTTT
TATGCAAAATCTAATTTAATATATTGATATTTATATCATTTTACGTTTCTCGTTCAGCTTTC
TTGTACAAAGTTGGCATTATAAGAAAGCATTGCTTATCAATTTGTTGCAACGAACAGGTC
ACTATCAGTCAAAATAAAATCATTATTTGCCATCCAGCTGATATCCCCTATAGTGAGTCG
TATTACATGGTCATAGCTGTTTCCTGGCAGCTCTGGCCCGTGTCTCAAAATCTCTGATG
TTACATTGCACAAGATAAAATAATATCATCATGATCAGTCCTGCTCCTCGGCCACGAAGT
GCACGCAGTTGCCGGCCGGGTCGCGCAGGGCGAACTCCCGCCCCCACGGCTGCTCG
CCGATCTCGGTCATGGCCGGCCCGGAGGCGTCCCGGAAGTTCGTGGACACGACCTCC
GACCACTCGGCGTACAGCTCGTCCAGGCCGCGCACCCACACCCAGGCCAGGGTGTTG
TCCGGCACCACCTGGTCCTGGACCGCGCTGATGAACAGGGTCACGTCGTCCCGGACC
ACACCGGCGAAGTCGTCCTCCACGAAGTCCCGGGAGAACCCGAGCCGGTCGGTCCAG
AACTCGACCGCTCCGGCGACGTCGCGCGCGGTGAGCACCGGAACGGCACTGGTCAAC
TTGGCCATGGTTTAGTTCCTCACCTTGTCGTATTATACTATGCCGATATACTATGCCGAT
GATTAATTGTCAACACGTGCTGATCATGACCAAAATCCCTTAACGTGAGTTACGCGTCG
TTCCACTGAGCGTCAGACCCCGTAGAAAAGATCAAAGGATCTTCTTGAGATCCTTTTTTT
CTGCGCGTAATCTGCTGCTTGCAAACAAAAAAACCACCGCTACCAGCGGTGGTTTGTTT
GCCGGATCAAGAGCTACCAACTCTTTTTCCGAAGGTAACTGGCTTCAGCAGAGCGCAG
ATACCAAATACTGTTCTTCTAGTGTAGCCGTAGTTAGGCCACCACTTCAAGAACTCTGTA
GCACCGCCTACATACCTCGCTCTGCTAATCCTGTTACCAGTGGCTGCTGCCAGTGGCG
ATAAGTCGTGTCTTACCGGGTTGGACTCAAGACGATAGTTACCGGATAAGGCGCAGCG
GTCGGGCTGAACGGGGGGTTCGTGCACACAGCCCAGCTTGGAGCGAACGACCTACAC
CGAACTGAGATACCTACAGCGTGAGCTATGAGAAAGCGCCACGCTTCCCGAAGGGAGA
AAGGCGGACAGGTATCCGGTAAGCGGCAGGGTCGGAACAGGAGAGCGCACGAGGGA
GCTTCCAGGGGGAAACGCCTGGTATCTTTATAGTCCTGTCGGGTTTCGCCACCTCTGA

CTTGAGCGTCGATTTTTGTGATGCTCGTCAGGGGGGCGGAGCCTATGGAAAAACGCCA
GCAACGCGGCCTTTTTACGGTTCCTGGCCTTTTGCTGGCCTTTTGCTCACATGTT

S2-2 pDONR RFC2 Entry Clone:

AATGCTTTTTTATAATGCCAACTTTGTACAAAAAAGCAGGCTTCATGCAAGCCTTTTTGA
AAACGGGAAAATCAACGGCGGGATCCGGAGACAAGAGCCAGGGTACTCCGGCGGCGC
GTCGCAAGCCACCGGCACCGTGGGTGGAGAAATACCGGCCACGCAATGTGGATGATG
TGGTGGAGCAGTCCGAAGTGGTGGCCGTGCTGCGCAAGTGCGTTGAAGGCGGGGACC
TGCCCAACATGCTGCTCTACGGACCGCCCGGCACGGGCAAGACCAGCACGATCCTGG
CTGCCAGCCGACAGATCTTCGGCGACATGTTCAAGGACCGCATCCTCGAGCTGAACGC
CTCCGACGAGCGTGGCATCAATGTGGTGCGCACCAAGATCAAAAACTTCTCGCAGCTG
TCGGCCAGCAGTGTGCGTCCGGACGGTAAGCCGTGTCCGCCCTTCAAGATCATCATTC
TGGACGAGGCCGATTCGATGACCCATGCCGCACAGTCTGCGCTGCGTCGCACCATGG
AGAAGGAGAGCCGGAGCACCCGTTTTTGCCTGATCTGCAACTATGTGTCCCGAATTATC
GTGCCAATCACGTCGCGTTGCTCTAAATTTCGCTTCAAGGCGCTGGGCGAAGACAAGG
TGATCGATCGTTTGAAGTACATTTGCGAGATGGAGGGAGTAAAGATAGAGGACGATGC
CTATAAATCCATTGTCAAAATTTCCGGCGGAGATCTGCGACGCGCTATCACCACCTTGC
AGTCCTGCTACCGCCTTAAAGGGCCCGAGCACATCATCAACACTGCTGATCTGTTCGA
GATGTCGGGCGTTATACCGGAGTACTATCTGGAGGATTACCTGGAGGTCTGTCGCTCT
GGGAACTACGAGCGCCTGGAGCAGTTCGTGCGGGAGATTGGCTTCTCCGCCTACAGC
GTTGGCCAAATGATGGAACAGTTCGTCGAGTTCATTGTCCATCATCCGGGGCTGAATGA
TCCGCAAAAGGCCACGATCTGCGATAAGCTGGGCGAATGCTGCTTTCGACTGCAGGAC
GGCGGCTCCGAGTATCTGCAGATCATGGACCTTGGCTGCTGCATCATCTTAGCTTTAAA
GGACCCAGCTTTCTTGTACAAAGTTGGCATTATAAGAAAGCATT

S2-3 FASTA CDS RFC2:

ATGCAAGCCTTTTTGAAAACGGGAAAATCAACGGCGGGATCCGGAGACAAGAGCCAGG
GTACTCCGGCGGCGCGTCGCAAGCCACCGGCACCGTGGGTGGAGAAATACCGGCCAC
GCAATGTGGATGATGTGGTGGAGCAGTCCGAAGTGGTGGCCGTGCTGCGCAAGTGCG
TTGAAGGCGGGGACCTGCCCAACATGCTGCTCTACGGACCGCCCGGCACGGGCAAGA
CCAGCACGATCCTGGCTGCCAGCCGACAGATCTTCGGCGACATGTTCAAGGACCGCAT
CCTCGAGCTGAACGCCTCCGACGAGCGTGGCATCAATGTGGTGCGCACCAAGATCAAA
AACTTCTCGCAGCTGTCGGCCAGCAGTGTGCGTCCGGACGGTAAGCCGTGTCCGCCC
TTCAAGATCATCATTCTGGACGAGGCCGATTCGATGACCCATGCCGCACAGTCTGCGC
TGCGTCGCACCATGGAGAAGGAGAGCCGGAGCACCCGTTTTTGCCTGATCTGCAACTA
TGTGTCCCGAATTATCGTGCCAATCACGTCGCGTTGCTCTAAATTTCGCTTCAAGGCGC
TGGGCGAAGACAAGGTGATCGATCGTTTGAAGTACATTTGCGAGATGGAGGGAGTAAA

GATAGAGGACGATGCCTATAAATCCATTGTCAAAATTTCCGGCGGAGATCTGCGACGC
GCTATCACCACCTTGCAGTCCTGCTACCGCCTTAAAGGGCCCGAGCACATCATCAACA
CTGCTGATCTGTTCGAGATGTCGGGCGTTATACCGGAGTACTATCTGGAGGATTACCTG
GAGGTCTGTCGCTCTGGGAACTACGAGCGCCTGGAGCAGTTCGTGCGGGAGATTGGC
TTCTCCGCCTACAGCGTTGGCCAAATGATGGAACAGTTCGTCGAGTTCATTGTCCATCA
TCCGGGGCTGAATGATCCGCAAAAGGCCACGATCTGCGATAAGCTGGGCGAATGCTG
CTTTCGACTGCAGGACGGCGGCTCCGAGTATCTGCAGATCATGGACCTTGGCTGCTGC
ATCATCTTAGCTTTAAAGTAA

S2-4 pDONR RFC3 Entry clone:

AATGCTTTTTTATAATGCCAACTTTGTACAAAAAAGCAGGCTTCATGTCGGAAACCAGTG
GACCCGCAGTGCGCATGCCTTGGGTGGAAAAGTACAGACCAAGCGGTCTCGATGATTT
GATATCTCACGAGGAAATAATATCAACAATAACCCGCTTTATAAGCCGCAAGCAGCTGC
CCCATTTGCTGTTCTACGGACCACCTGGCACGGGAAAAACGAGTACAATCCTGGCCTG
CGCTCGCCAATTGTATTCCCCTCAGCAGTTTAAGTCCATGGTCCTGGAGCTGAATGCCT
CGGATGACCGAGGCATTGGGATTGTGCGCGGTCAAATCCTTAACTTCGCGTCCACACG
CACCATTTTCTGCGACACCTTTAAGCTGATCATTTTGGACGAGGCCGATGCCATGACCA
ACGATGCCCAGAATGCCCTGCGCCGCATAATTGAGAAATATACGGACAACGTGCGCTT
CTGTGTGATTTGCAATTATTTGAGCAAAATCATTCCGGCGCTGCAGTCGCGTTGCACCC
GTTTTCGGTTCGCTCCATTATCCCAGGATCAGATGATGCCGCGACTGGAAAAAATCATC
GAAGCCGAAGCCGTTCAGATAACTGAGGACGGCAAGCGGGCACTGCTGACCCTGGCC
AAAGGTGATATGAGAAAGGTCTTGAACGTCCTGCAGAGTACCGTGATGGCATTTGATAC
GGTAAACGAGGATAACGTCTACATGTGCGTGGGCTATCCGTTGAGGCAGGATATTGAA
CAGATATTGAAGGCCTTGCTATCCGGCAGTAGCTTGGAGGACTCCTTCAAAACTGTCGA
AAGTGCCAAGTACGCAAGAGGTCTCGCTTTGGAAGACATCATTACAGAATTGCATTTGT
TTGTTATGAGACTTGAGCTGCCTATGTCGGTCATGAACAAGCTTATTGTAAAGCTAGCT
CAGATCGAGGAGAGATTGGCCAAAGGATGTACAGAAGTGGCTCAAACTGCAGCTCTGG
TAGCCGCCTTCTTTATTTGCCGAGATATGGTTTCAATGGAGAAGGACCCAGCTTTCTTG
TACAAAGTTGGCATTATAAGAAAGCATT

S2-5 FASTA CDS RFC3:

ATGTCGGAAACCAGTGGACCCGCAGTGCGCATGCCTTGGGTGGAAAAGTACAGACCAA
GCGGTCTCGATGATTTGATATCTCACGAGGAAATAATATCAACAATAACCCGCTTTATAA
GCCGCAAGCAGCTGCCCCATTTGCTGTTCTACGGACCACCTGGCACGGGAAAAACGAG
TACAATCCTGGCCTGCGCTCGCCAATTGTATTCCCCTCAGCAGTTTAAGTCCATGGTCC
TGGAGCTGAATGCCTCGGATGACCGAGGCATTGGGATTGTGCGCGGTCAAATCCTTAA

CTTCGCGTCCACACGCACCATTTTCTGCGACACCTTTAAGCTGATCATTTTGGACGAGG
CCGATGCCATGACCAACGATGCCCAGAATGCCCTGCGCCGCATAATTGAGAAATATAC
GGACAACGTGCGCTTCTGTGTGATTTGCAATTATTTGAGCAAAATCATTCCGGCGCTGC
AGTCGCGTTGCACCCGTTTTCGGTTCGCTCCATTATCCCAGGATCAGATGATGCCGCG
ACTGGAAAAAATCATCGAAGCCGAAGCCGTTCAGATAACTGAGGACGGCAAGCGGGCA
CTGCTGACCCTGGCCAAAGGTGATATGAGAAAGGTCTTGAACGTCCTGCAGAGTACCG
TGATGGCATTTGATACGGTAAACGAGGATAACGTCTACATGTGCGTGGGCTATCCGTTG
AGGCAGGATATTGAACAGATATTGAAGGCCTTGCTATCCGGCAGTAGCTTGGAGGACT
CCTTCAAAACTGTCGAAAGTGCCAAGTACGCAAGAGGTCTCGCTTTGGAAGACATCATT
ACAGAATTGCATTTGTTTGTTATGAGACTTGAGCTGCCTATGTCGGTCATGAACAAGCTT
ATTGTAAAGCTAGCTCAGATCGAGGAGAGATTGGCCAAAGGATGTACAGAAGTGGCTC
AAACTGCAGCTCTGGTAGCCGCCTTCTTTATTTGCCGAGATATGGTTTCAATGGAGAAG
TGA

S2-6 pDONR RFC4 Entry clone:

CGAATTGGCGGAAGGCCGTCAAGGCCACGTGTCTTGTCCAGAGCTCACAAGTTTGTAC
AAAAAAGCAGGCTTCATGCCGGAAGAACCAGAGAAAACGGCGGACGACAAGCGCAGT
CACTTGCCGTGGATTGAGAAGTACCGCCCCGTGAAGTTCAAGGAGATAGTGGGCAATG
AGGATACCGTAGCAAGACTATCCGTATTCGCCACCCAGGGAAATGCACCCAATATTATT
ATTGCTGGTCCTCCTGGCGTGGGCAAGACAACCACCATCCAGTGTCTGGCCAGGATTC
TCCTGGGAGACAGCTACAAGGAGGCTGTCCTCGAGCTGAATGCCTCCAATGAACGAGG
AATCGATGTGGTCCGCAACAAGATCAAGATGTTTGCTCAGCAGAAGGTGACACTGCCG
CGGGGCAGGCACAAGATTGTGATTCTGGACGAGGCGGACAGCATGACGGAGGGTGCC
CAGCAGGCACTGCGCCGGACCATGGAGATCTACAGCAGCACCACTCGTTTTGCCCTGG
CCTGCAACACCAGCGAGAAGATCATAGAGCCTATCCAGTCCCGCTGCGCCATGCTACG
ATTCACCAAGCTGTCCGATGCGCAAGTTCTGGCCAAGCTCATCGAGGTGGCCAAGTGG
GAGAAGCTTAACTACACGGAGGACGGACTTGAGGCCATCGTATTCACTGCCCAAGGTG
ATATGCGACAGGGACTGAACAACCTGCAGTCCACCGCTCAGGGATTTGGCGACATCAC
CGCTGAGAACGTCTTTAAGGTCTGCGACGAGCCGCACCCAAAGCTCCTAGAGGAGATG
ATCCACCATTGCGCTGCTAACGACATACACAAGGCCTACAAAATCCTGGCCAAGCTGTG
GAAGCTGGGATACTCGCCGGAGGACATCATTGCGAACATATTCCGTGTCTGCAAGCGC
ATCAACATCGATGAGCATTTGAAGCTGGACTTTATCCGTGAGATCGGAATCACCCACAT
GAAGATTATCGATGGTATCAACTCGCTGCTGCAGCTCACCGCCCTTCTGGCCAAACTCT
GCATTGCCGCCGAGAAGCATGACCCAGCTTTCTTGTACAAAGTGGTGGTACCTGGAGC
ACAAGACTGGCCTCATGGGCCTTCCGCTCACTGC

S2-7 FASTA CDS RFC4:

ATGCCGGAAGAACCAGAGAAAACGGCGGACGACAAGCGCAGTCACTTGCCGTGGATT
GAGAAGTACCGCCCCGTGAAGTTCAAGGAGATAGTGGGCAATGAGGATACCGTAGCAA
GACTATCCGTATTCGCCACCCAGGGAAATGCACCCAATATTATTATTGCTGGTCCTCCT
GGCGTGGGCAAGACAACCACCATCCAGTGTCTGGCCAGGATTCTCCTGGGAGACAGC
TACAAGGAGGCTGTCCTCGAGCTGAATGCCTCCAATGAACGAGGAATCGATGTGGTCC
GCAACAAGATCAAGATGTTTGCTCAGCAGAAGGTGACACTGCCGCGGGGCAGGCACAA
GATTGTGATTCTGGACGAGGCGGACAGCATGACGGAGGGTGCCCAGCAGGCACTGCG
CCGGACCATGGAGATCTACAGCAGCACCACTCGTTTTGCCCTGGCCTGCAACACCAGC
GAGAAGATCATAGAGCCTATCCAGTCCCGCTGCGCCATGCTACGATTCACCAAGCTGT
CCGATGCGCAAGTTCTGGCCAAGCTCATCGAGGTGGCCAAGTGGGAGAAGCTTAACTA
CACGGAGGACGGACTTGAGGCCATCGTATTCACTGCCCAAGGTGATATGCGACAGGGA
CTGAACAACCTGCAGTCCACCGCTCAGGGATTTGGCGACATCACCGCTGAGAACGTCT
TTAAGGTCTGCGACGAGCCGCACCCAAAGCTCCTAGAGGAGATGATCCACCATTGCGC
TGCTAACGACATACACAAGGCCTACAAAATCCTGGCCAAGCTGTGGAAGCTGGGATAC
TCGCCGGAGGACATCATTGCGAACATATTCCGTGTCTGCAAGCGCATCAACATCGATG
AGCATTTGAAGCTGGACTTTATCCGTGAGATCGGAATCACCCACATGAAGATTATCGAT
GGTATCAACTCGCTGCTGCAGCTCACCGCCCTTCTGGCCAAACTCTGCATTGCCGCCG
AGAAGCATTAG

S2-8 69-pUBQ-mGFP-CDest Destination vector:

CATGATGAAATAACATAAGGTGGTCCCGTCGAAAGCCGAAGCTTACCGAAGTATACACT
TAAATTCAGTGCACGTTTGCTTGTTGAGAGGAAAGGTTGTGTGCGGACGAATTTTTTTTT
GAAAACATTAACCCTTACGTGGAATAAAAAAAAATGAAATGTAACCGGACCGGATCATTA
ATCAGTGGTATATAAATTTGTTCAAACAGCTCTCCAGCTTAGTTTACACATTAAACGACT
CAATTATTTTTAAAACATTTAATTCACTATGTATATATAAACAAATTAACAAATAAAATCGT
CATTTTAAATGCTTAACTAGTTCTAGAGCGGCCGCCACCGCGGTGGCGGCCGCTCTAG
ATTATTTGTATAGTTCATCCATGCCATGTGTAATCCCAGCAGCTGTTACAAACTCAAGAA
GGACCATGTGGTCTCTCTTTTCGTTGGGATCTTTCGAAAGGGCAGATTGTGTGGACAG
GTAATGGTTGTCTGGTAAAAGGACAGGGCCATCGCCAATTGGAGTATTTTGTTGATAAT
GATCAGCGAGTTGCACGCCGCCGTCTTCGATGTTGTGGCGGGTCTTGAAGTTGGCTTT
GATGCCGTTCTTTTGCTTGTCGGCCATGATGTATACGTTGTGGGAGTTGTAGTTGTATT
CCAACTTGTGGCCGAGGATGTTTCCGTCCTCCTTGAAATCGATTCCCTTAAGCTCGATC
CTGTTGACGAGGGTGTCTCCCTCAAACTTGACTTCAGCACGTGTCTTGTAGTTCCCGTC
GTCCTTGAAGAAGATGGTCCTCTCCTGCACGTATCCCTCAGGCATGGCGCTCTTGAAG
AAGTCGTGCCGCTTCATATGATCAGGGTAACGGGAGAAGCACTGCACGCCGTAGGTCA

GGGTGGTGACCAGGGTTGGCCATGGAACAGGTAGTTTTCCAGTAGTGCAAATAAATTTA
AGGGTAAGTTTTCCGTATGTTGCATCACCTTCACCCTCTCCACTGACAGAAAATTTGTG
CCCATTAACATCACCATCTAATTCAACAAGAATTGGGACAACTCCAGTGAAAAGTTCTTC
TCCTTTACTCATCACCACTTTGTACAAGAAAGCTGAACGAGAAACGTAAAATGATATAAA
TATCAATATATTAAATTAGATTTTGCATAAAAAACAGACTACATAATACTGTAAAACACAA
CATATCCAGTCACTATGGTCGACCTGCAGACTGGCTGTGTATAAGGGAGCCTGACATTT
ATATTCCCCAGAACATCAGGTTAATGGCGTTTTTGATGTCATTTTCGCGGTGGCTGAGA
TCAGCCACTTCTTCCCCGATAACGGAGACCGGCACACTGGCCATATCGGTGGTCATCA
TGCGCCAGCTTTCATCCCCGATATGCACCACCGGGTAAAGTTCACGGGAGACTTTATCT
GACAGCAGACGTGCACTGGCCAGGGGGATCACCATCCGTCGCCCGGGCGTGTCAATA
ATATCACTCTGTACATCCACAAACAGACGATAACGGCTCTCTCTTTTATAGGTGTAAACC
TTAAACTGCATTTCACCAGTCCCTGTTCTCGTCAGCAAAAGAGCCGTTCATTTCAATAAA
CCGGGCGACCTCAGCCATCCCTTCCTGATTTTCCGCTTTCCAGCGTTCGGCACGCAGA
CGACGGGCTTCATTCTGCATGGTTGTGCTTACCAGACCGGAGATATTGACATCATATAT
GCCTTGAGCAACTGATAGCTGTCGCTGTCAACTGTCACTGTAATACGCTGCTTCATAGC
ACACCTCTTTTTGACATACTTCGGGTATACATATCAGTATATATTCTTATACCGCAAAAAT
CAGCGCGCAAATACGCATACTGTTATCTGGCTTTTAGTAAGCCGGATCCACGCGTTTAC
GCCCCGCCCTGCCACTCATCGCAGTACTGTTGTAATTCATTAAGCATTCTGCCGACATG
GAAGCCATCACAGACGGCATGATGAACCTGAATCGCCAGCGGCATCAGCACCTTGTCG
CCTTGCGTATAATATTTGCCCATGGTGAAAACGGGGGCGAAGAAGTTGTCCATATTGGC
CACGTTTAAATCAAAACTGGTGAAACTCACCCAGGGATTGGCTGAGACGAAAAACATAT
TCTCAATAAACCCTTTAGGGAAATAGGCCAGGTTTTCACCGTAACACGCCACATCTTGC
GAATATATGTGTAGAAACTGCCGGAAATCGTCGTGGTATTCACTCCAGAGCGATGAAAA
CGTTTCAGTTTGCTCATGGAAAACGGTGTAACAAGGGTGAACACTATCCCATATCACCA
GCTCACCGTCTTTCATTGCCATACGGAATTCCGGATGAGCATTCATCAGGCGGGCAAG
AATGTGAATAAAGGCCGGATAAAACTTGTGCTTATTTTTCTTTACGGTCTTTAAAAAGGC
CGTAATATCCAGCTGAACGGTCTGGTTATAGGTACATTGAGCAACTGACTGAAATGCCT
CAAAATGTTCTTTACGATGCCATTGGGATATATCAACGGTGGTATATCCAGTGATTTTTT
TCTCCATTTTAGCTTCCTTAGCTCCTGAAAATCTCGCCGGATCCTAACTCAAAATCCACA
CATTATACGAGCCGGAAGCATAAAGTGTAAAGCCTGGGGTGCCTAATGCGGCCGCCAT
AGTGACTGGATATGTTGTGTTTTACAGTATTATGTAGTCTGTTTTTTATGCAAAATCTAAT
TTAATATATTGATATTTATATCATTTTACGTTTCTCGTTCAGCTTTTTTGTACAAACTTGTG
ATGACCTCGAGGGGGGGCCCGGTACCGATGGATTATTCTGCGGGCAAAATAGAGATGT
GGAAAATTAGTACGAAATCAAATGAGTTTCGTTGAAATTACAAAACTATTGAAACTAACT
TCCTGGCTGGGGAATAAAAATGGGAAACTTATTTATCGACGCCAACTTTGTTGAGAAAC
CCCTATTAACCCTCTACGAATATTGGAACAAAGGAAAGCGAAGAAACAGGAACAAAGGT
AGTTGAGAAACCTGTTCCGTTGCTCGTCATCGTTTTCATAATGCGAGTGTGTGCATGTA

TATATACACAGCTGAAACGCATGCATACACATTATTTTGTGTGTATATGGTGACGTCACA
ACTACTAAGCAATAAGAAATTTTCCAGACGTGGCTTTCGTTTCAAGCAACCTACTCTATT
TCAGCTAAAAATAAGTGGATTTCGTTGGTAAAATACTTCAATTAAGCAAAGAACTAACTA
ACTAATAACATGCACACAAATGCTCGAGTGCGTTCGTGATTTCTCGAATTTTCAAATGCG
TCACTGCGAATTTCACAATTTGCCAATAAATCTTGGCGAAAATCAACACGCAAGTTTTAT
TTATAGATTTGTTTGCGTTTTGATGCCAATTGATTGGGAAAACAAGATGCGTGGCTGCC
AATTTCTTATTTTGTAATTACGTAGAGCGTTGAATAAAAAAAAAATGGCCGAACAAAGAC
CTTGAAATGCAGTTTTTCTTGAAATTACTCAACGTCTTGTTGCTCTTATTACTAATTGGTA
ACAGCGAGTTAAAAACTTACGTTTCTTGTGACTTTCGAGAATGTTCTTTTAATTGTACTTT
AATCACCAACAATTAAGTATAAATTTTTCGCTGATTGCGCTTTACTTTCTGCTTGTACTTG
CTGCTGCAAATGTCAATTGGTTTTGAAGGCGACCGTTCGCGAACGCTGTTTATATACCT
TCGGTGTCCGTTGAAAATCACTAAAAAATACCGTAGTGTTCGTAACACTTTAGTACAGAG
AAAAAAAATTGTGCCGAAATGTTTTTGATACGTACGAATACCTTGTATTAAAATTTTTTAT
GATTTCTGTGTATCACTTTTTTTTTGTGTTTTTCGTTTAAACTCACCACAGTACAAAACAA
TAAAATATTTTTAAGACAATTTCAAATTGAGACCTTTCTCGTACTGACTTGACCGGCTGA
ATGAGGATTTCTACCTAGACGACCTACTTCTTACCATGACATTGAATGCAATGCCACCTT
TGATCTAAACTTACAAAAGTCCAAGGCTTGTTAGGATTGGTGTTTTGGAATTTAAGACCC
TTGTTAGTTTGCTTTTGAAATAGCACTGTCTTCTCTACCGGCTATAATTTTGAAACTCGC
AGCTTGACTGGAAATTTAAAATGGAGCTATCTGGCAACGCTGCGCATAATCTTACACAA
GCTTTTCTTAATCCATTTTTTAAGTGAAATTTGTTTATACTCTTTCGGCAAATAATTGTTAA
ATCGCTTTAAGTGGGCTTACATCTGGATAAGTAATGAAAACCTGCATATTATAATATTAA
AACATATAATCCACTGTGCTTTCCCCGTGTGTGGCCATATACCTAAAAAAGTTTATTTTC
GCAGAGCCCCGCACGTCACACTACGGTTCGGCGATTTTCGATTTTGGACAGTACTGATT
GCAAGCGCACCGAAAGCAAAATGGAGCTGGAGATTTTGAACGCGAAGAACAGCAAGCC
AGATCCTCTAGAGTCGACGTCACGCGTCCATGGAGATCCTAGTATGTATGTAAGTTAAT
AAAACCCTTTTTTGGAGAATGTAGATTTAAAAAAACATATTTTTTTTTTATTTTTTACTGCA
CTGGACATCATTGAACTTATCTGATCAGTTTTAAATTTACTTCGATCCAAGGGTATTTGA
AGTACCAGGTTCTTTCGATTACCTCTCACTCAAAATGACATTCCACTCAAAGTCAGCGCT
GTTTGCCTCCTTCTCTGTCCACAGAAATATCGCCGTCTCTTTCGCCGCTGCGTCCGCTA
TCTCTTTCGCCACCGTTTGTAGCGTTACCTAGCGTCAATGTCCGCCTTCAGTTGCACTT
TGTCAGCGGTTTCGTGACGAAGCTCCAAGCGGTTTACGCCATCAATTAAACACAAAGTG
CTGTGCCAAAACTCCTCTCGCTTCTTATTTTTGTTTGTTTTTTGAGTGATTGGGGTGGTG
ATTGGTTTTGGGTGGGTAAGCAGGGGAAAGTGTGAAAAATCCCGGCAATGGGCCAAGA
GGATCAGGAGCTATTAATTCGCGGAGGCAGCAAACACCCATCTGCCGAGCATCTGAAC
AATGTGAGTAGTACATGTGCATACATCTTAAGTTCACTTGATCTATAGGAACTGCGATTG
CAACATCAAATTGTCTGCGGCGTGAGAACTGCGACCCACAAAAATCCCAAACCGCAATC
GCACAAACAAATAGTGACACGAAACAGATTATTCTGGTAGCTGTGCTCGCTATATAAGA

CAATTTTTAAGATCATATCATGATCAAGACATCTAAAGGCATTCATTTTCGACTACATTCT
TTTTTACAAAAAATATAACAACCAGATATTTTAAGCCTAGATGCACAAAAAATAAATAAAA
GTATAAACCTACTTCGTAGGATACTTCGTTTTGTTCGGGGTTAGATGAGCATAACGCTT
GTAGTTGATATTTGAGATCCCCTATCATTGCAGGGTGACAGCGGACGCTTCGCAGAGC
TGCATTAACCAGGGCTTCGGGCAGGCCAAAAACTACGGCACGCTCCTGCCACCCAGTC
CGCCGGAGGACTCCGGTTCAGGGAGCGGCCAACTAGCCGAGAACCTCACCTATGCCT
GGCACAATATGGACATCTTTGGGGCGGTCAATCAGCCGGGCTCCGGATGGCGGCAGC
TGGTCAACCGGACACGCGGACTATTCTGCAACGAGCGACACATACCGGCGCCCAGGA
AACATTTGCTCAAGAACGGTGAGTTTCTATTCGCAGTCGGCTGATCTGTGTGAAATCTT
AATAAAGGGTCCAATTACCAATTTGAAACTCAGTTTGCGGCGTGGCCTATCCGGGCGAA
CTTTTGGCCGTGATGGGCAGTTCCGGTGCCGGAAAGACGACCCTGCTGAATGCCCTTG
CCTTTCGATCGCCGCAGGGCATCCAAGTATCGCCATCCGGGATGCGACTGCTCAATGG
CCAACCTGTGGACGCCAAGGAGATGCAGGCCAGGTGCGCCTATGTCCAGCAGGATGA
CCTCTTTATCGGCTCCCTAACGGCCAGGGAACACCTGATTTTCCAGGCCATGGTGCGG
ATGCCACGACATCTGACCTATCGGCAGCGAGTGGCCCGCGTGGATCAGGTGATCCAG
GAGCTTTCGCTCAGCAAATGTCAGCACACGATCATCGGTGTGCCCGGCAGGGTGAAAG
GTCTGTCCGGCGGAGAAAGGAAGCGTCTGGCATTCGCCTCCGAGGCACTAACCGATC
CGCCGCTTCTGATCTGCGATGAGCCCACCTCCGGACTGGACTCATTTACCGCCCACAG
CGTCGTCCAGGTGCTGAAGAAGCTGTCGCAGAAGGGCAAGACCGTCATCCTGACCATT
CATCAGCCGTCTTCCGAGCTGTTTGAGCTCTTTGACAAGATCCTTCTGATGGCCGAGG
GCAGGGTAGCTTTCTTGGGCACTCCCAGCGAAGCCGTCGACTTCTTTTCCTAGTGAGTT
CGATGTGTTTATTAAGGGTATCTAGCATTACATTACATCTCAACTCCTATCCAGCGTGGG
TGCCCAGTGTCCTACCAACTACAATCCGGCGGACTTTTACGTACAGGTGTTGGCCGTT
GTGCCCGGACGGGAGATCGAGTCCCGTGATCGGATCGCCAAGATATGGCGACAATTTT
GCTATTAGCAAAGTAGCCCGGGATATGGAGCAGTTGTTGGCCACCAAAAATTTGGAGA
AGCCACTGGAGCAGCCGGAGAATGGGTACACCTACAAGGCCACCTGGTTCATGCAGTT
CCGGGCGGTCCTGTGGCGATCCTGGCTGTCGGTGCTCAAGGAACCACTCCTCGTAAAA
GTGCGACTTATTCAGACAACGGTGAGTGGTTCCAGTGGAAACAAATGATATAACGCTTA
CAATTCTTGGAAACAAATTCGCTAGATTTTAGTTAGAATTGCCTGATTCCACACCCTTCT
TAGTTTTTTTCAATGAGATGTATAGTTTATAGTTTTGCAGAAAATAAATAAATTTCATTTAA
CTCGCGAACATGTTGAAGATATGAATATTAATGAGATGCGAGTAACATTTTAATTTGCAG
ATGGTTGCCATCTTGATTGGCCTCATCTTTTTGGGCCAACAACTCACGCAAGTGGGCGT
GATGAATATCAACGGAGCCATCTTCCTCTTCCTGACCAACATGACCTTTCAAAACGTCTT
TGCCACGATAAATGTAAGTCTTGTTTAGAATACATTTGCATATTAATAATTTACTAACTTT
CTAATGAATCGATTCGATTTAGGTGTTCACCTCAGAGCTGCCAGTTTTTATGAGGGAGG
CCCGAAGTCGACTTTATCGCTGTGACACATACTTTCTGGGCAAAACGATTGCCGAATTA
CCGCTTTTTCTCACAGTGCCACTGGTCTTCACGGCGATTGCCTATCCGATGATCGGACT

GCGGGCCGGAGTGCTGCACTTCTTCAACTGCCTGGCGCTGGTCACTCTGGTGGCCAAT
GTGTCAACGTCCTTCGGATATCTAATATCCTGCGCCAGCTCCTCGACCTCGATGGCGCT
GTCTGTGGGTCCGCCGGTTATCATACCATTCCTGCTCTTTGGCGGCTTCTTCTTGAACT
CGGGCTCGGTGCCAGTATACCTCAAATGGTTGTCGTACCTCTCATGGTTCCGTTACGC
CAACGAGGGTCTGCTGATTAACCAATGGGCGGACGTGGAGCCGGGCGAAATTAGCTG
CACATCGTCGAACACCACGTGCCCCAGTTCGGGCAAGGTCATCCTGGAGACGCTTAAC
TTCTCCGCCGCCGATCTGCCGCTGGACTACGTGGGTCTGGCCATTCTCATCGTGAGCT
TCCGGGTGCTCGCATATCTGGCTCTAAGACTTCGGGCCCGACGCAAGGAGTAGCCGA
CATATATCCGAAATAACTGCTTGTTTTTTTTTTTACCATTATTACCATCGTGTTTACTGTTT
ATTGCCCCCTCAAAAAGCTAATGTAATTATATTTGTGCCAATAAAAACAAGATATGACCT
ATAGAATACAAGTATTTCCCCTTCGAACATCCCCACAAGTAGACTTTGGATTTGTCTTCT
AACCAAAAGACTTACACACCTGCATACCTTACATCAAAAACTCGTTTATCGCTACATAAA
ACACCGGGATATATTTTTTATATACATACTTTTCAAATCGCGCGCCCTCTTCATAATTCAC
CTCCACCACACCACGTTTCGTAGTTGCTCTTTCGCTGTCTCCCACCCGCTCTCCGCAAC
ACATTCACCTTTTGTTCGACGACCTTGGAGCGACTGTCGTTAGTTCCGCGCGATTCGGT
TCGCTCAAATGGTTCCGAGTGGTTCATTTCGTCTCAATAGAAATTAGTAATAAATATTTG
TATGTACAATTTATTTGCTCCAATATATTTGTATATATTTCCCTCACAGCTATATTTATTCT
AATTTAATATTATGACTTTTTAAGGTAATTTTTTGTGACCTGTTCGGAGTGATTAGCGTTA
CAATTTGAACTGAAAGTGACATCCAGTGTTTGTTCCTTGTGTAGATGCATCTCAAAAAAA
TGGTGGGCATAATAGTGTTGTTTATATATATCAAAAATAACAACTATAATAATAAGAATAC
ATTTAATTTAGAAAATGCTTGGATTTCACTGGAACTAGGATCTCGAGGTCGAATTATGAG
TTAATTCAAACCCCACGGACATGCTAAGGGTTAATCAACAATCATATCGCTGTCTCACTC
AGACTCAATACGACACTCAGAATACTATTCCTTTCACTCGCACTTATTGCAAGCATACGT
TAAGTGGATGTCTCTTGCCGACGGGACCACCTTATGTTATTTCATCATGGTCTGGGTAA
CCGCCGTCCCGTCAAGTCAGCGTAATGCTCTGCCAGTGTTACAACCAATTAACCAATTC
TGATTAGAAAAACTCATCGAGCATCAAATGAAACTGCAATTTATTCATATCAGGATTATC
AATACCATATTTTTGAAAAAGCCGTTTCTGTAATGAAGGAGAAAACTCACCGAGGCAGTT
CCATAGGATGGCAAGATCCTGGTATCGGTCTGCGATTCCGACTCGTCCAACATCAATAC
AACCTATTAATTTCCCCTCGTCAAAAATAAGGTTATCAAGTGAGAAATCACCATGAGTGA
CGACTGAATCCGGTGAGAATGGCAAAAGCTTATGCATTTCTTTCCAGACTTGTTCAACA
GGCCAGCCATTACGCTCGTCATCAAAATCACTCGCATCAACCAAACCGTTATTCATTCG
TGATTGCGCCTGAGCGAGACGAAATACGCGATCGCTGTTAAAAGGACAATTACAAACA
GGAATCGAATGCAACCGGCGCAGGAACACTGCCAGCGCATCAACAATATTTTCACCTG
AATCAGGATATTCTTCTAATACCTGGAATGCTGTTTTCCCGGGGATCGCAGTGGTGAGT
AACCATGCATCATCAGGAGTACGGATAAAATGCTTGATGGTCGGAAGAGGCATAAATTC
CGTCAGCCAGTTTAGTCTGACCATCTCATCTGTAACATCATTGGCAACGCTACCTTTGC
CATGTTTCAGAAACAACTCTGGCGCATCGGGCTTCCCATACAATCGATAGATTGTCGCA

CCTGATTGCCCGACATTATCGCGAGCCCATTTATACCCATATAAATCAGCATCCATGTT
GGAATTTAATCGCGGCCTCGAGCAAGACGTTTCCCGTTGAATATGGCTCATAACACCCC
TTGTATTACTGTTTATGTAAGCAGACAGTTTTATTGTTCATGATGATATATTTTTATCTTGT
GCAATGTAACATCAGAGATTTTGAGACACTGAGCGTCAGACCCCGTAGAAAAGATCAAA
GGATCTTCTTGAGATCCTTTTTTTCTGCGCGTAATCTGCTGCTTGCAAACAAAAAAACCA
CCGCTACCAGCGGTGGTTTGTTTGCCGGATCAAGAGCTACCAACTCTTTTTCCGAAGGT
AACTGGCTTCAGCAGAGCGCAGATACCAAATACTGTTCTTCTAGTGTAGCCGTAGTTAG
GCCACCACTTCAAGAACTCTGTAGCACCGCCTACATACCTCGCTCTGCTAATCCTGTTA
CCAGTGGCTGCTGCCAGTGGCGATAAGTCGTGTCTTACCGGGTTGGACTCAAGACGAT
AGTTACCGGATAAGGCGCAGCGGTCGGGCTGAACGGGGGGTTCGTGCACACAGCCCA
GCTTGGAGCGAACGACCTACACCGAACTGAGATACCTACAGCGTGAGCATTGAGAAAG
CGCCACGCTTCCCGAAGGGAGAAAGGCGGACAGGTATCCGGTAAGCGGCAGGGTCG
GAACAGGAGAGCGCACGAGGGAGCTTCCAGGGGGAAACGCCTGGTATCTTTATAGTC
CTGTCGGGTTTCGCCACCTCTGACTTGAGCGTCGATTTTTGTGATGCTCGTCAGGGGG
GCGGAGCCTATGGAAAAACGCCAGCAACGTCGACC

S3 pDonr Entry maps from GeneArt

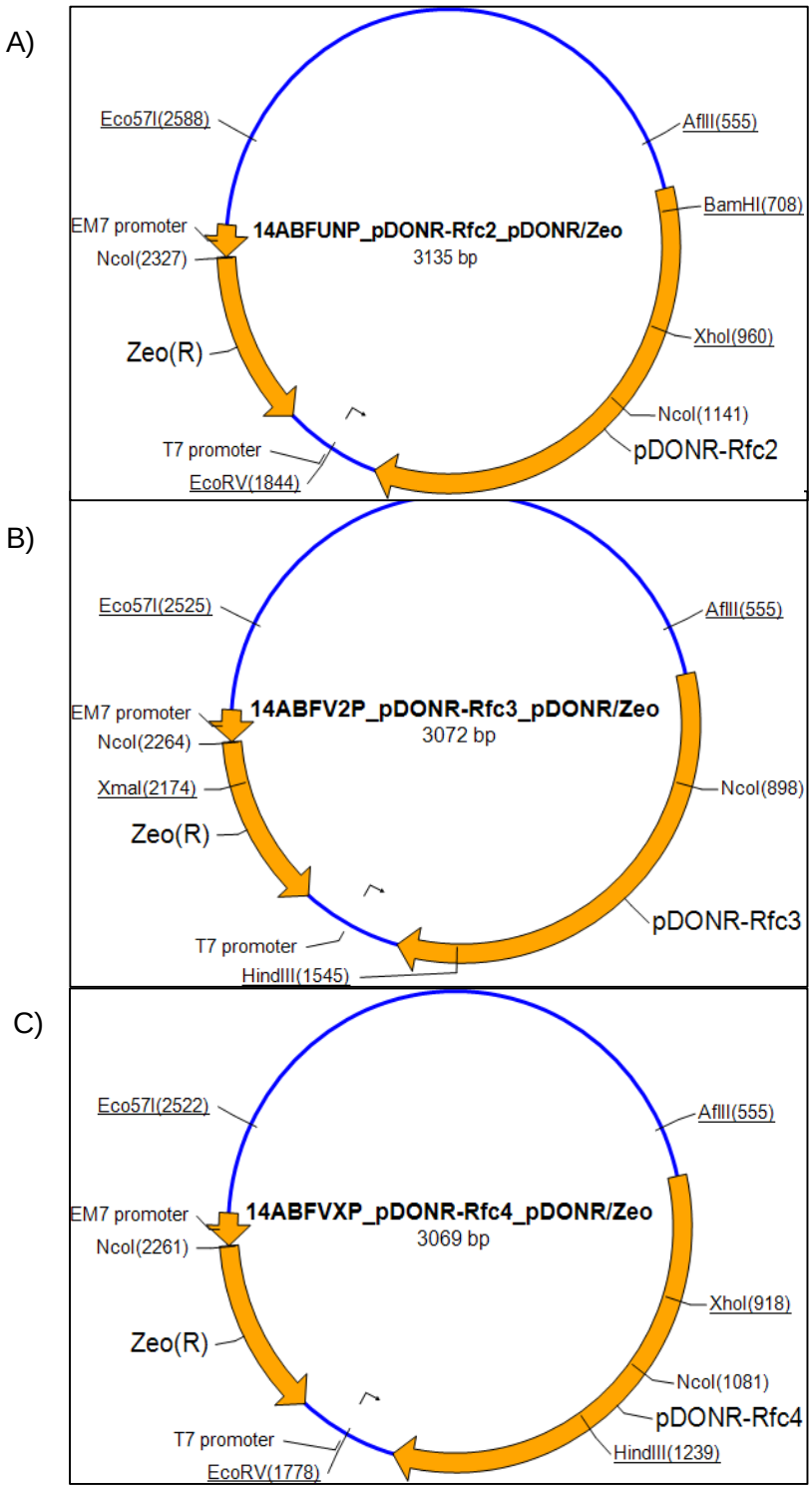


S3 - Plasmid maps for pDONR entry clone RfC2 (A) RfC3 (B) and RfC4 (C). Maps produced by GeneArt.

## S4 Entry and destination vector maps

### S4-1 Entry vector

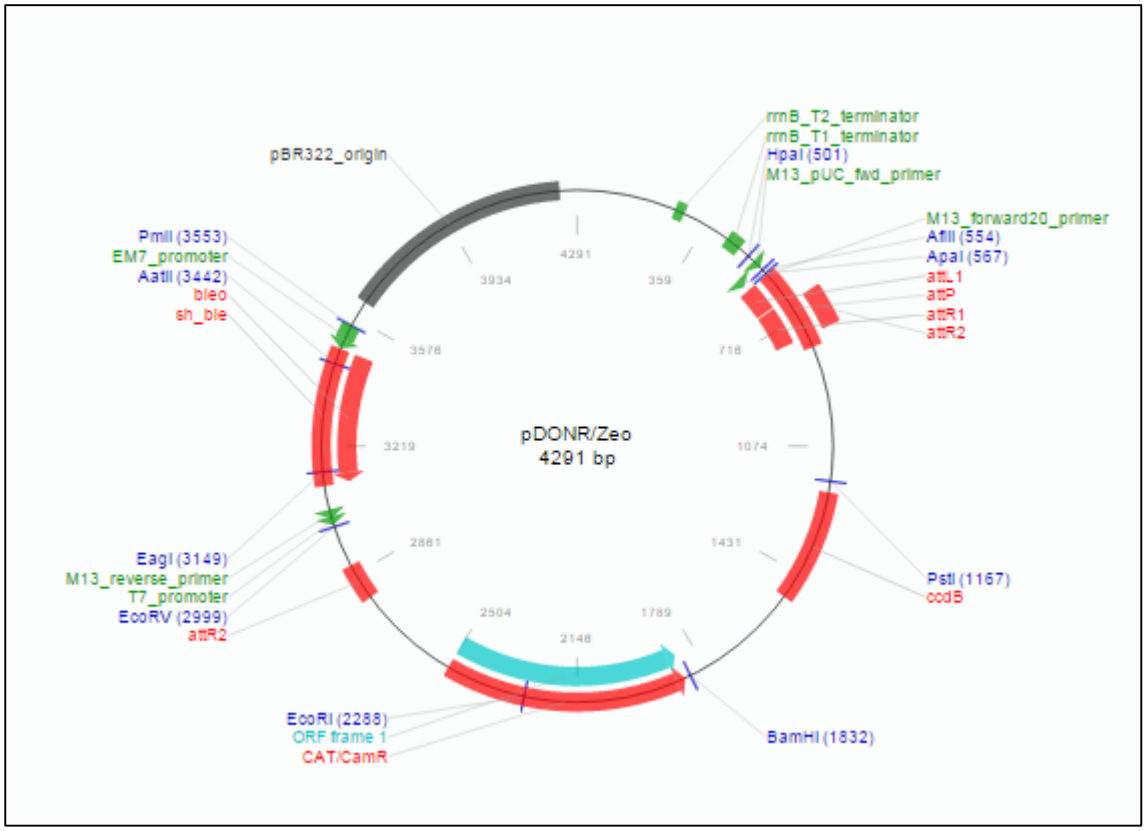


pDONR/Zeo entry vector map; image and information taken from addgene.

S4-2 Destination vector

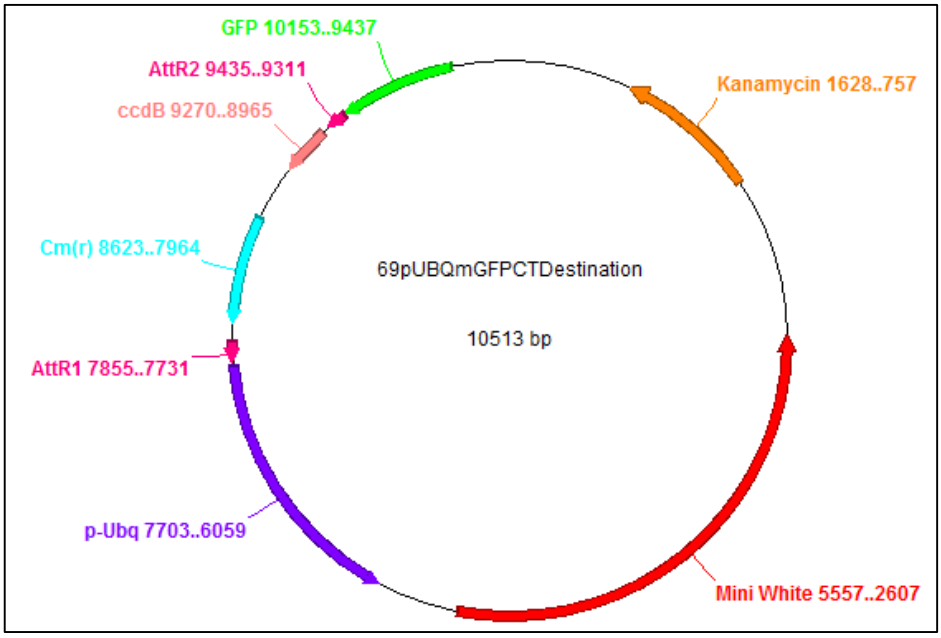


69pUBQmGFPCTDest destination vector map produced using ApE software. Vector kindly given by Jordan Raff (University of Oxford).

Vector contains AttR1/AttR2 sites for LR cloning. Coding sequence between these sites will be removed and replaced with a gene of interest.

Vector also carries a poly ubiquitin promotor, and the coding sequence for C terminal GFP.

To aid selection, the vector also contains the following; kanamycin and chloramphenicol resistance, a ccdB and the mini white gene. Antibiotic resistance will allow for the detection of a successful recombination reaction; if the gene of interest has been successfully inserted into the vector backbone the chloramphenicol resistance will be lost. The ccdB produces a toxin that targets *E.coli*. If recombination has not been successful (in a successful reaction the ccdB is replaced by the gene of interest); further transformation into *E.coli* competent cells will result in colonies failing to grow. The mini white gene allows for selection at a phenotypic level. Flies possessing the mini white gene will have eyes ranging from mid orange to red, depending on the level of expression.

## S5 Destination vector containing RFC inserts

### S5-1 RFC2

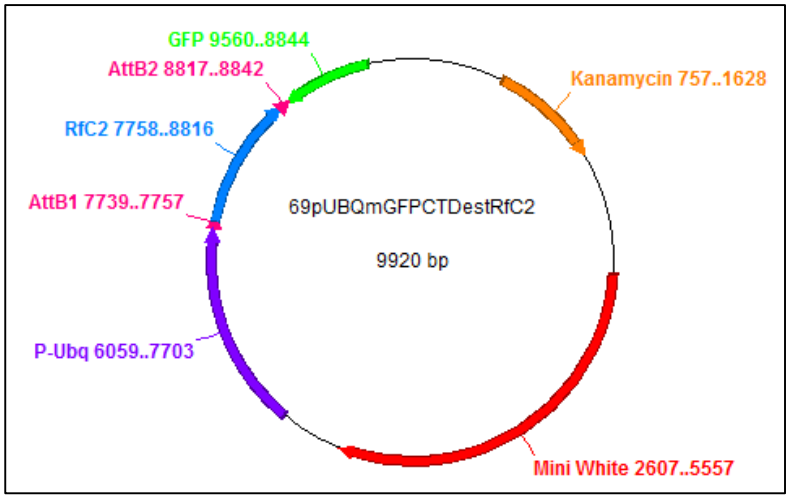


### S5-2 RFC3

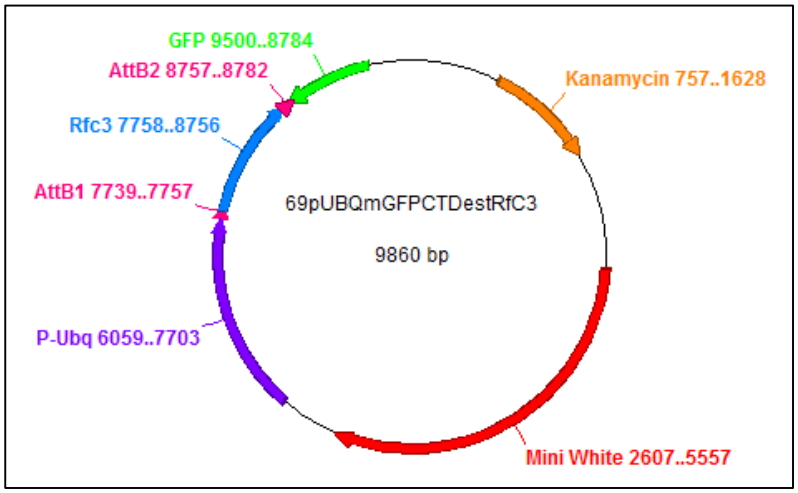


### S5-3 RFC4

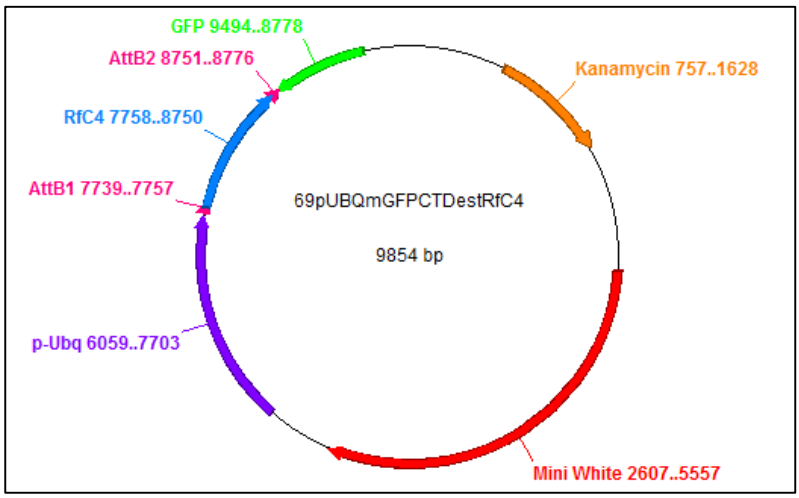

## S6 Levenes test example:

A]

**Test of Homogeneity of Variances**

Score

| Levene Statistic | df1 | df2 | Sig. |
|---|---|---|---|
| 8.090 | 1 | 4 | .047 |

B]

**Independent Samples Test**

| | | t-test for Equality of Means | | | | | | |
|---|---|---|---|---|---|---|---|---|
| | | | | | | | 95% Confidence Interval of the Difference | |
| | | t | df | Sig. (2-tailed) | Mean Difference | Std. Error Difference | Lower | Upper |
| Score | Equal variances assumed | -2.501 | 4 | .067 | -3.02000 | 1.20759 | -6.37280 | .33280 |
| | Equal variances not assumed | -2.501 | 2.263 | .115 | -3.02000 | 1.20759 | -7.67814 | 1.63814 |

C]

**Independent Samples Test**

| | | t-test for Equality of Means | | | | | | |
|---|---|---|---|---|---|---|---|---|
| | | | | | | | 95% Confidence Interval of the Difference | |
| | | t | df | Sig. (2-tailed) | Mean Difference | Std. Error Difference | Lower | Upper |
| Score | Equal variances assumed | -10.785 | 3 | .002 | -4.18950 | .38845 | -5.42572 | -2.95328 |
| | Equal variances not assumed | -13.888 | 2.031 | .005 | -4.18950 | .30167 | -5.46869 | -2.91031 |

Equal variance cannot be assumed for mitotic data set.

Using the scores for known mitotic MAP Abnormal spindle protein:

A] Levenes test for homogeneity of variance for the complete mitotic data set. Test shows that there is a significant difference between the data points and hence homogeneity cannot be assumed.

B] Independent samples t-test comparing the cycling and mitotic values for Asp. Equal variance cannot be assumed $p>0.05$ therefore no significant difference between cycling and mitotic values for Asp. This result goes against what is known for this protein; Asp is a known mitotic MAP and hence should show a significant increase in association with MTs during mitosis.

C] Independent samples t-test repeated, having removed 3rd mitotic repeat. Homogeneity of variance can now be assumed (data not shown) therefore $p<0.05$. Test now showing that there is a significant increase in Asp association with MTs during mitosis.

## Supplementary Table 1 – Full data set

| Name/GO | Score | Mean | SD | Mean Edit | SD | MFI | p value | p value edit |
|---|---|---|---|---|---|---|---|---|
| **msps** | **1475.34** | **1.512** | **0.486** | **2.971** | **3.621** | **0.243** | **1.965** | 0.111 | 0.021 |
| Hsc70-4 | 1150.29 | 1.118 | 0.107 | 1.543 | 1.965 | 0.264 | 1.380 | 0.388 | 0.013 |
| **Dhc64C** | **1137.62** | **1.549** | **0.546** | **3.883** | **5.265** | **0.147** | **2.507** | **0.23** | **0.003** |
| Ef1alpha48D | 1048.82 | 1.682 | 0.802 | 3.855 | 5.071 | 1.680 | 2.291 | 0.214 | 0.05 |
| CLIP-190 | 838.89 | 1.844 | 1.054 | 6.669 | 8.787 | 0.546 | 3.616 | 0.095 | 0.004 |
| **Map205 -1** | **836.79** | **1.543** | **0.544** | **0.787** | **1.041** | **0.095** | **0.510** | **0.136** | **0.307** |
| **Map205- 2** | **802.20** | **1.314** | **0.277** | **1.202** | **1.500** | **0.148** | **0.915** | **0.762** | **0.497** |
| Aats-glupro | 796.44 | 1.526 | 0.497 | 1.378 | 1.237 | 0.413 | 0.903 | 0.747 | 0.601 |
| **Hsp83** | **728.99** | **1.684** | **0.867** | **1.294** | **1.717** | **0.475** | **0.768** | **0.598** | **0.966** |
| **Klp61F** | **705.65** | **1.841** | **0.885** | **1.204** | **1.414** | **0.424** | **0.654** | **0.333** | **0.583** |
| **Klp3A** | **690.24** | **1.619** | **0.627** | **3.629** | **4.384** | **0.972** | **2.241** | **0.096** | **0.028** |
| Ef1alpha100E | 656.48 | 1.580 | 0.593 | 3.511 | 4.663 | 1.526 | 2.222 | 0.227 | 0.044 |
| TppII | 593.30 | 1.007 | 0.119 | 0.615 | 0.554 | 0.102 | 0.610 | 0.017 | 0.022 |
| ens | 570.68 | 0.925 | 0.320 | 0.452 | 0.576 | 0.065 | 0.489 | 0.103 | 0.245 |
| Rfabg | 556.69 | 1.367 | 0.325 | 1.649 | 2.170 | 0.540 | 1.206 | 0.662 | 0.121 |
| **tacc** | **539.00** | **1.648** | **0.635** | **2.627** | **3.235** | **0.224** | **1.594** | 0.244 | 0.047 |
| Yp3 | 535.44 | 1.146 | 0.233 | 0.522 | 0.670 | 0.108 | 0.456 | 0.038 | 0.081 |
| Aats-ile | 523.43 | 1.547 | 0.511 | 1.309 | 1.176 | 0.371 | 0.846 | 0.541 | 0.45 |
| **EF2** | **519.13** | **1.327** | **0.329** | **0.898** | **0.925** | **0.137** | **0.677** | 0.099 | 0.215 |
| RpL4 | 508.83 | 1.107 | 0.115 | 0.636 | 0.709 | 0.013 | 0.575 | 0.719 | 0.085 |
| Hsp27 | 488.30 | 1.618 | 0.660 | 3.500 | 4.990 | 2.344 | 2.162 | 0.358 | 0.085 |
| Hsp26 | 482.17 | 1.562 | 0.569 | 3.856 | 5.602 | 2.606 | 2.468 | 0.33 | 0.067 |
| blw | 479.55 | 1.702 | 0.721 | 2.709 | 3.530 | 1.591 | 1.592 | 0.421 | 0.164 |
| RpL22 | 452.71 | 1.138 | 0.123 | 0.976 | 1.118 | 0.051 | 0.858 | 0.369 | 0.847 |
| Hsc70-3 | 449.32 | 1.093 | 0.096 | 1.825 | 2.419 | 0.124 | 1.669 | 0.289 | 0.001 |
| Yp1 | 447.18 | 1.142 | 0.176 | 0.496 | 0.637 | 0.103 | 0.434 | 0.023 | 0.038 |
| RpL23A | 409.98 | 1.014 | 0.063 | 0.567 | 0.584 | 0.088 | 0.559 | 0.001 | 0.007 |
| Yp2 | 405.84 | 1.147 | 0.181 | 0.468 | 0.573 | 0.055 | 0.408 | 0.011 | 0.025 |
| RpL5 | 367.41 | 1.057 | 0.077 | 0.567 | 0.603 | 0.065 | 0.536 | 0.001 | 0.006 |
| Act5C | 356.98 | 1.666 | 0.892 | 3.363 | 4.403 | 2.229 | 2.019 | 0.314 | 0.136 |
| **Cctgamma** | **351.13** | **1.622** | **0.628** | **1.653** | **2.246** | **1.387** | **1.019** | 0.974 | 0.524 |
| Nup358 | 349.21 | 1.598 | 0.563 | 5.604 | 6.620 | 0.130 | 3.507 | 0.02 | 0.001 |
| CG15100 | 338.22 | 1.575 | 0.596 | 1.330 | 1.111 | 0.348 | 0.845 | 0.601 | 0.406 |
| RpS3 | 336.12 | 1.396 | 0.366 | 1.016 | 1.117 | 0.023 | 0.728 | 0.18 | 0.382 |
| Gapdh1 | 332.93 | 1.928 | 1.178 | 0.423 | 0.525 | 0.039 | 0.220 | 0.094 | 0.208 |
| glu | 327.12 | 1.599 | 0.607 | **3.561** | **4.721** | **1.375** | **2.226** | 0.216 | 0.035 |
| **Klp10A** | **320.10** | **1.512** | **0.553** | **5.603** | **6.349** | **0.258** | **3.705** | 0.007 | 0.002 |

| | | | | | | | | | |
|---|---|---|---|---|---|---|---|---|---|
| CG33123 | 319.93 | 1.184 | 0.160 | 1.018 | 0.864 | 0.259 | 0.860 | 0.47 | 0.176 |
| **eIF3-S10** | 318.49 | 1.473 | 0.435 | **1.180** | **1.276** | **0.002** | **0.801** | 0.338 | 0.587 |
| Aats-lys | 317.73 | 1.219 | 0.190 | 1.035 | 0.844 | 0.240 | 0.849 | 0.382 | 0.143 |
| RpS27A | 314.88 | 1.294 | 0.293 | 1.466 | 1.800 | 0.187 | 1.133 | 0.665 | 0.122 |
| Gapdh2 | 312.64 | 1.960 | 1.281 | 0.471 | 0.602 | 0.084 | 0.240 | 0.119 | 0.251 |
| **eIF4G** | 307.77 | 1.578 | 0.542 | **3.486** | **4.688** | **1.249** | **2.209** | 0.228 | 0.028 |
| Msp-300 | 303.36 | 0.984 | 0.178 | 1.758 | 2.113 | 1.895 | 1.787 | 0.417 | 0.344 |
| poe | 300.58 | 1.793 | 0.836 | 2.310 | 2.808 | 1.052 | 1.288 | 0.561 | 0.311 |
| **Tcp-1zeta** | **297.73** | **1.543** | **0.559** | **1.747** | **2.350** | **1.143** | **1.132** | 0.818 | 0.351 |
| RpL7A | 293.79 | 1.039 | 0.085 | 0.563 | 0.596 | 0.072 | 0.542 | 0.002 | 0.009 |
| RpS6 | 283.17 | 1.195 | 0.173 | 0.714 | 0.759 | 0.035 | 0.598 | 0.012 | 0.044 |
| RpL3 | 282.50 | 1.138 | 0.148 | 0.564 | 0.619 | 0.029 | 0.495 | 0.005 | 0.019 |
| DNApol-delta | 278.79 | 1.646 | 0.764 | 5.283 | 7.216 | 1.855 | 3.209 | 0.162 | 0.016 |
| **CG8258** | **275.76** | **1.528** | **0.711** | **1.670** | **2.265** | **1.134** | **1.093** | 0.877 | 0.424 |
| RpL7 | 275.40 | 1.089 | 0.106 | 0.595 | 0.646 | 0.022 | 0.547 | 0.003 | 0.01 |
| Nc73EF | 272.58 | 1.022 | 0.071 | 0.807 | 0.976 | 0.055 | 0.790 | 0.288 | 0.503 |
| ATPsyn-beta | 271.92 | 1.574 | 0.695 | 3.130 | 4.049 | 1.250 | 1.989 | 0.239 | 0.06 |
| TER94 | 269.69 | 1.339 | 0.328 | 0.930 | 1.185 | 0.093 | 0.694 | 0.27 | 0.58 |
| **CG7033** | **267.00** | **1.510** | **0.569** | **1.168** | **1.544** | **0.786** | **0.774** | 0.596 | 0.957 |
| **Klp67A** | **266.94** | **1.809** | **0.939** | **5.183** | **6.393** | **2.780** | **2.865** | 0.125 | 0.239 |
| **T-cp1** | **260.02** | **1.586** | **0.608** | **0.967** | **1.226** | **0.646** | **0.610** | 0.291 | 0.571 |
| RpS19a | 256.72 | 1.140 | 0.123 | 0.756 | 0.772 | 0.068 | 0.664 | 0.008 | 0.033 |
| l(1)G0156 | 256.13 | 1.784 | 0.909 | 3.183 | 4.368 | 1.504 | 1.785 | 0.384 | 0.089 |
| RpS4 | 255.52 | 1.172 | 0.151 | 0.609 | 0.614 | 0.013 | 0.519 | 0.003 | 0.016 |
| **polo** | **252.99** | **1.442** | **0.385** | **1.849** | **2.451** | **0.134** | **1.283** | 0.561 | 0.042 |
| RpS3A | 252.82 | 1.272 | 0.242 | 0.881 | 0.911 | 0.077 | 0.693 | 0.056 | 0.147 |
| RpL14 | 249.18 | 1.085 | 0.101 | 0.597 | 0.643 | 0.076 | 0.550 | 0.004 | 0.014 |
| Rpn3 | 247.84 | 1.302 | 0.282 | 1.085 | 1.299 | 0.363 | 0.833 | 0.518 | 0.99 |
| RpS2 | 247.60 | 1.151 | 0.131 | 0.669 | 0.686 | 0.036 | 0.581 | 0.004 | 0.018 |
| Hop | 246.68 | 1.248 | 0.246 | 2.670 | 3.137 | 0.268 | 2.139 | 0.047 | 0.004 |
| Mtpalpha | 246.43 | 1.437 | 0.430 | 2.985 | 3.979 | 2.324 | 2.078 | 0.33 | 0.139 |
| sle | 237.33 | 1.467 | 0.536 | 2.988 | 3.935 | 1.096 | 2.036 | 0.236 | 0.039 |
| RpL28 | 236.50 | 1.070 | 0.113 | 0.518 | 0.536 | 0.048 | 0.484 | 0.001 | 0.009 |
| RpL13A | 235.09 | 1.156 | 0.168 | 0.578 | 0.669 | 0.040 | 0.500 | 0.012 | 0.031 |
| Aats-arg | 234.14 | 1.526 | 0.477 | 1.252 | 1.145 | 0.312 | 0.821 | 0.443 | 0.403 |
| PyK | 230.78 | 1.588 | 0.598 | 3.060 | 3.895 | 1.217 | 1.927 | 0.226 | 0.06 |
| Aats-gln | 230.36 | 1.393 | 0.361 | 1.257 | 1.113 | 0.288 | 0.902 | 0.652 | 0.432 |
| RpS9 | 229.96 | 1.239 | 0.208 | 0.710 | 0.762 | 0.095 | 0.573 | 0.018 | 0.061 |
| 26-29-p | 228.40 | 1.606 | 0.621 | 2.567 | 3.317 | 0.759 | 1.599 | 0.339 | 0.068 |
| **skap** | **227.77** | **1.718** | **0.772** | **3.602** | **4.810** | **2.127** | **2.096** | 0.292 | 0.091 |

| | | | | | | | | | |
|---|---|---|---|---|---|---|---|---|---|
| Iva | 224.70 | 1.597 | 0.558 | 2.601 | 3.360 | 0.543 | 1.628 | 0.305 | 0.04 |
| RpL13 | 220.11 | 1.083 | 0.112 | 0.516 | 0.532 | 0.059 | 0.476 | 0.001 | 0.009 |
| Drp1 | 219.43 | 1.875 | 1.100 | 5.388 | 7.232 | 3.044 | 2.874 | 0.208 | 0.065 |
| RpL6 | 219.03 | 1.072 | 0.109 | 0.585 | 0.637 | 0.014 | 0.546 | 0.004 | 0.013 |
| tral | 218.06 | 1.415 | 0.390 | 3.259 | 4.133 | 1.095 | 2.303 | 0.141 | 0.025 |
| RpLP0 | 216.68 | 1.051 | 0.093 | 0.524 | 0.567 | 0.032 | 0.498 | 0.002 | 0.007 |
| Tudor-SN | 215.14 | 1.126 | 0.110 | 1.384 | 1.501 | 0.034 | 1.230 | 0.127 | 0.021 |
| Chc | 214.43 | 1.856 | 0.854 | 1.064 | 1.284 | 0.269 | 0.573 | 0.447 | 0.816 |
| RpL26 | 213.57 | 1.091 | 0.103 | 0.633 | 0.703 | 0.040 | 0.580 | 0.008 | 0.017 |
| RpL8 | 212.29 | 1.129 | 0.140 | 0.603 | 0.658 | 0.029 | 0.534 | 0.006 | 0.021 |
| vig2 | 209.35 | 1.193 | 0.171 | 0.739 | 0.843 | 0.052 | 0.619 | 0.035 | 0.075 |
| Khc | 206.90 | 1.578 | 0.566 | 0.773 | 0.997 | 0.190 | 0.490 | 0.117 | 0.273 |
| **CG5525** | **204.32** | **1.564** | **0.539** | **1.249** | **1.624** | **0.728** | **0.799** | 0.661 | 0.92 |
| RpS7 | 200.34 | 1.250 | 0.216 | 0.734 | 0.765 | 0.005 | 0.588 | 0.016 | 0.058 |
| **sta** | **199.93** | **1.081** | **0.083** | **0.670** | **0.720** | **0.067** | **0.620** | 0.009 | 0.015 |
| **mars** | **199.80** | **1.431** | **0.379** | **3.033** | **3.246** | **0.080** | **2.120** | 0.006 | 0.003 |
| r | 198.04 | 1.656 | 0.704 | 1.799 | 2.277 | 0.762 | 1.086 | 0.857 | 0.421 |
| **asp** | **197.98** | **1.538** | **0.520** | **4.558** | **5.727** | **0.037** | **2.964** | 0.067 | 0.005 |
| Pen | 197.86 | 1.681 | 0.757 | 2.667 | 3.742 | 2.331 | 1.586 | 0.547 | 0.255 |
| RpL10 | 197.39 | 1.309 | 0.267 | 0.715 | 0.775 | 0.034 | 0.546 | 0.023 | 0.076 |
| RpS18 | 193.85 | 1.263 | 0.229 | 0.773 | 0.826 | 0.009 | 0.612 | 0.026 | 0.083 |
| zip | 191.67 | 1.716 | 0.831 | 1.679 | 2.280 | 0.883 | 0.979 | 0.968 | 0.519 |
| Nap1 | 191.39 | 1.685 | 0.780 | 3.232 | 4.326 | 0.619 | 1.917 | 0.27 | 0.029 |
| CG6439 | 191.09 | 1.846 | 0.974 | 3.719 | 5.222 | 2.868 | 2.014 | 0.339 | 0.138 |
| **Tcp-1eta** | **191.07** | **1.363** | **0.365** | **1.298** | **1.735** | **1.297** | **0.952** | 0.932 | 0.665 |
| Rpn2 | 188.25 | 1.357 | 0.324 | 0.898 | 0.988 | 0.248 | 0.662 | 0.117 | 0.271 |
| **Cam** | **187.29** | **1.163** | **0.147** | **3.892** | **5.006** | **0.430** | **3.346** | 0.037 | 0.001 |
| Vps4 | 186.36 | 1.730 | 0.912 | 6.088 | 8.217 | 5.273 | 3.518 | 0.229 | 0.108 |
| sesB | 183.25 | 1.646 | 0.728 | 9.576 | 12.631 | 3.349 | 5.817 | 0.078 | 0.009 |
| **bel** | **182.66** | **1.641** | **0.639** | **3.592** | **4.896** | **0.955** | **2.189** | 0.239 | 0.018 |
| CG42232 | 181.87 | 1.629 | 0.804 | 6.214 | 8.089 | 2.030 | 3.816 | 0.095 | 0.013 |
| CG5028 | 181.43 | 1.863 | 0.979 | 3.667 | 5.082 | 2.195 | 1.969 | 0.365 | 0.1 |
| RpS13 | 179.58 | 1.152 | 0.132 | 0.634 | 0.667 | 0.026 | 0.550 | 0.003 | 0.017 |
| pAbp | 178.96 | 1.540 | 0.486 | 2.303 | 2.949 | 0.431 | 1.495 | 0.35 | 0.044 |
| **me31B** | **178.58** | **1.414** | **0.362** | **3.242** | **4.126** | **0.884** | **2.292** | 0.135 | 0.015 |
| Rpn1 | 177.95 | 1.367 | 0.350 | 1.192 | 1.410 | 0.486 | 0.872 | 0.649 | 0.915 |
| **Gl** | **177.62** | **1.520** | **0.480** | **2.086** | **2.919** | **0.577** | **1.373** | 0.567 | 0.059 |
| **feo** | **177.24** | **1.497** | **0.461** | **3.142** | **3.773** | **0.009** | **2.099** | 0.074 | 0.007 |
| Ef1gamma | 176.82 | 1.164 | 0.148 | 1.183 | 1.533 | 0.211 | 1.016 | 0.962 | 0.1 |

| | | | | | | | | | |
|---|---|---|---|---|---|---|---|---|---|
| RpL35A | 175.51 | 1.048 | 0.116 | 0.523 | 0.545 | 0.074 | 0.499 | 0.002 | 0.013 |
| **SMC2** | **174.73** | **1.607** | **0.616** | **3.833** | **5.045** | **1.733** | **2.385** | 0.199 | 0.044 |
| Rpt1 | 174.33 | 1.325 | 0.324 | 1.099 | 1.285 | 0.309 | 0.830 | 0.483 | 0.899 |
| stai | 173.33 | 1.537 | 0.705 | 7.314 | 10.718 | 6.491 | 4.758 | 0.253 | 0.293 |
| **cmet** | **173.29** | **1.687** | **0.637** | **2.687** | **3.450** | **0.452** | **1.593** | 0.313 | 0.045 |
| Rack1 | 172.85 | 1.188 | 0.173 | 0.992 | 1.055 | 0.028 | 0.835 | 0.174 | 0.381 |
| Rpt6 | 172.47 | 1.445 | 0.399 | 1.217 | 1.446 | 0.428 | 0.842 | 0.57 | 0.999 |
| CG8858 | 172.27 | 1.624 | 0.697 | 3.439 | 4.697 | 3.407 | 2.118 | 0.394 | 0.197 |
| Prosalpha6 | 171.53 | 1.016 | 0.171 | 0.627 | 0.677 | 0.148 | 0.617 | 0.037 | 0.107 |
| eIF-4a | 170.67 | 1.771 | 0.836 | 0.606 | 0.791 | 0.167 | 0.342 | 0.091 | 0.221 |
| **dgt5** | **170.42** | **1.595** | **0.635** | **6.889** | **7.468** | **0.221** | **4.320** | 0.002 | 0.001 |
| RpL24 | 170.27 | 1.085 | 0.082 | 0.526 | 0.537 | 0.080 | 0.485 | 0.001 | 0.005 |
| RpL18A | 169.39 | 1.094 | 0.117 | 0.586 | 0.642 | 0.028 | 0.535 | 0.005 | 0.014 |
| Gnf1 | 169.18 | 1.505 | 0.459 | 1.904 | 2.350 | 0.243 | 1.265 | 0.493 | 0.104 |
| RpL17 | 167.85 | 1.113 | 0.133 | 0.550 | 0.577 | 0.050 | 0.494 | 0.003 | 0.014 |
| RpS16 | 167.60 | 1.215 | 0.187 | 0.740 | 0.776 | 0.026 | 0.609 | 0.014 | 0.052 |
| alpha-Spec | 166.50 | 1.430 | 0.425 | 2.453 | 3.159 | 0.961 | 1.716 | 0.292 | 0.063 |
| eIF-2gamma | 165.40 | 1.458 | 0.448 | 1.556 | 1.980 | 0.717 | 1.067 | 0.872 | 0.377 |
| RpS5a | 164.88 | 1.176 | 0.162 | 0.771 | 0.812 | 0.051 | 0.656 | 0.018 | 0.061 |
| lic | 164.41 | 1.752 | 0.870 | 3.253 | 4.536 | 1.955 | 1.857 | 0.619 | 0.144 |
| Pep | 163.48 | 1.289 | 0.253 | 1.539 | 2.100 | 0.180 | 1.194 | 0.691 | 0.031 |
| tud | 162.77 | 1.506 | 0.490 | 3.957 | 5.344 | 1.661 | 2.627 | 0.194 | 0.027 |
| RpS12 | 161.47 | 1.601 | 0.545 | 0.784 | 0.860 | 0.056 | 0.490 | 0.066 | 0.166 |
| RpS11 | 161.41 | 1.126 | 0.110 | 0.641 | 0.659 | 0.030 | 0.570 | 0.002 | 0.011 |
| Rm62 | 161.10 | 1.281 | 0.245 | 2.180 | 2.823 | 0.264 | 1.702 | 0.249 | 0.007 |
| Pfk | 160.39 | 1.785 | 0.890 | 3.434 | 4.675 | 3.198 | 1.924 | 0.428 | 0.209 |
| kra | 160.38 | 1.647 | 0.752 | 7.117 | 10.049 | 7.959 | 4.320 | 0.282 | 0.141 |
| CG10576 | 160.17 | 0.965 | 0.187 | 0.526 | 0.552 | 0.139 | 0.545 | 0.025 | 0.079 |
| RpL9 | 158.46 | 1.160 | 0.167 | 0.632 | 0.668 | 0.044 | 0.545 | 0.006 | 0.027 |
| Rpt4 | 157.61 | 1.343 | 0.320 | 1.083 | 1.272 | 0.384 | 0.807 | 0.446 | 0.837 |
| Pxt | 156.45 | 1.659 | 0.794 | 3.356 | 4.494 | 1.647 | 2.023 | 0.292 | 0.074 |
| **sub** | **156.25** | **1.892** | **1.012** | **4.871** | **6.323** | **2.119** | **2.574** | 0.171 | 0.046 |
| Cct5 | 155.05 | 1.505 | 0.511 | 0.582 | 0.704 | 0.149 | 0.387 | 0.044 | 0.125 |
| CG5261 | 154.73 | 1.428 | 0.417 | 2.472 | 3.321 | 0.312 | 1.731 | 0.307 | 0.013 |
| Mi-2 | 153.93 | 1.556 | 0.533 | 3.726 | 5.047 | 1.218 | 2.395 | 0.207 | 0.019 |
| **Fs(2)Ket** | **151.36** | **1.570** | **0.574** | **2.397** | **3.081** | **1.000** | **1.527** | **0.392** | **0.112** |
| **Mtor** | **150.62** | **1.815** | **0.755** | **2.387** | **3.127** | **0.197** | **1.315** | **0.543** | **0.106** |
| Aats-asp | 150.21 | 1.188 | 0.163 | 0.954 | 0.749 | 0.148 | 0.803 | 0.372 | 0.056 |
| Mcm6 | 150.16 | 1.826 | 0.897 | 0.538 | 0.703 | 0.159 | 0.295 | 0.078 | 0.194 |

| | | | | | | | | | |
|---|---|---|---|---|---|---|---|---|---|
| RpS8 | 149.92 | 1.193 | 0.178 | 0.729 | 0.741 | 0.030 | 0.611 | 0.011 | 0.043 |
| Cand1 | 149.91 | 1.829 | 1.018 | 1.882 | 2.132 | 0.953 | 1.029 | 0.947 | 0.761 |
| CG9281 | 149.70 | 1.662 | 0.690 | 2.306 | 2.854 | 0.138 | 1.388 | 0.397 | 0.105 |
| lin19 | 149.68 | 1.770 | 0.861 | 4.669 | 6.365 | 4.340 | 2.639 | 0.311 | 0.149 |
| **larp** | **149.02** | **1.250** | **0.224** | **2.299** | **2.953** | **0.081** | **1.839** | **0.191** | **0.002** |
| Iswi | 147.44 | 1.312 | 0.279 | 1.017 | 1.308 | 0.212 | 0.775 | 0.439 | 0.988 |
| **Rpt2** | **146.68** | **1.309** | **0.307** | **1.317** | **1.578** | **0.432** | **1.006** | **0.655** | **0.465** |
| Cp190 | 145.03 | 1.685 | 0.759 | 6.850 | 8.690 | 0.210 | 4.066 | 0.053 | 0.001 |
| **dpa** | **144.77** | **1.741** | **0.855** | **0.929** | **1.246** | **0.419** | **0.534** | **0.255** | **0.516** |
| **Lam** | **144.75** | **1.496** | **0.465** | **1.735** | **2.254** | **0.464** | **1.160** | **0.717** | **0.175** |
| CG2982 | 143.87 | 1.419 | 0.396 | 4.570 | 6.067 | 0.833 | 3.220 | 0.112 | 0.003 |
| fax | 141.64 | 1.814 | 0.942 | 4.659 | 6.345 | 4.139 | 2.568 | 0.31 | 0.142 |
| alt | 141.45 | 1.651 | 0.637 | 2.612 | 3.383 | 0.425 | 1.582 | 0.332 | 0.046 |
| l(1)G0334 | 139.83 | 1.765 | 1.032 | 3.974 | 5.592 | 2.405 | 2.252 | 0.328 | 0.239 |
| mbf1 | 138.69 | 1.204 | 0.177 | 1.468 | 1.706 | 0.148 | 1.219 | 0.377 | 0.047 |
| Map60 | 138.16 | 1.344 | 0.313 | 1.262 | 1.460 | 0.369 | 0.939 | 0.124 | 0.076 |
| CG17896 | 138.04 | 1.908 | 1.183 | 3.991 | 5.654 | 2.673 | 2.092 | 0.378 | 0.11 |
| RpS15Aa | 136.89 | 1.156 | 0.142 | 0.678 | 0.684 | 0.027 | 0.587 | 0.004 | 0.021 |
| lds | 135.69 | 1.652 | 0.733 | 3.723 | 5.021 | 1.394 | 2.254 | 0.234 | 0.035 |
| **Fmr1** | **135.09** | **1.349** | **0.302** | **1.900** | **2.420** | **0.114** | **1.409** | **0.372** | **0.019** |
| Gp93 | 134.62 | 1.552 | 0.663 | 4.193 | 5.821 | 0.809 | 2.701 | 0.197 | 0.007 |
| RnrL | 134.58 | 1.950 | 1.095 | 0.583 | 0.710 | 0.062 | 0.299 | 0.101 | 0.226 |
| **rept** | **134.45** | **1.500** | **0.491** | **1.503** | **1.863** | **0.358** | **1.002** | **0.994** | **0.443** |
| RpL19 | 134.33 | 1.111 | 0.132 | 0.542 | 0.567 | 0.074 | 0.488 | 0.003 | 0.014 |
| shi | 133.18 | 1.624 | 0.687 | 3.832 | 5.168 | 3.333 | 2.360 | 0.32 | 0.368 |
| CG6453 | 132.76 | 1.811 | 1.058 | 5.332 | 7.391 | 2.686 | 2.944 | 0.218 | 0.041 |
| mask | 131.55 | 1.496 | 0.450 | 1.605 | 2.012 | 0.129 | 1.073 | 0.833 | 0.228 |
| ACC | 131.25 | 1.655 | 0.652 | 2.863 | 3.762 | 2.337 | 1.730 | 0.426 | 0.21 |
| RpL18 | 130.52 | 1.147 | 0.141 | 0.529 | 0.568 | 0.027 | 0.461 | 0.002 | 0.012 |
| **Pp2A-29B** | **130.20** | **1.531** | **0.593** | **1.018** | **1.282** | **0.294** | **0.665** | **0.317** | **0.623** |
| nocte | 129.60 | 1.338 | 0.293 | 2.538 | 3.115 | 0.706 | 1.897 | 0.146 | 0.026 |
| Lsd-2 | 129.32 | 1.670 | 0.713 | 5.087 | 7.052 | 3.575 | 3.046 | 0.241 | 0.071 |
| RpL31 | 129.19 | 1.129 | 0.137 | 0.525 | 0.527 | 0.087 | 0.465 | 0.002 | 0.013 |
| baf | 129.18 | 1.573 | 0.710 | 0.448 | 0.552 | 0.028 | 0.285 | 0.056 | 0.149 |
| Thiolase | 128.51 | 1.710 | 0.726 | 2.862 | 3.828 | 1.898 | 1.673 | 0.428 | 0.159 |
| **NAT1** | **128.45** | **1.483** | **0.421** | **2.555** | **3.196** | **0.054** | **1.723** | **0.193** | **0.012** |
| smid | 128.22 | 1.696 | 0.832 | 5.392 | 7.306 | 2.935 | 3.178 | 0.185 | 0.211 |
| **Dlic** | **128.18** | **1.449** | **0.448** | **3.334** | **4.568** | **0.391** | **2.301** | **0.211** | **0.004** |
| faf | 127.73 | 1.840 | 0.918 | 2.726 | 3.670 | 1.836 | 1.482 | 0.538 | 0.22 |
| Nipped-A | 126.46 | 1.750 | 0.741 | 3.346 | 4.384 | 1.513 | 1.912 | 0.281 | 0.073 |

| | | | | | | | | | |
|---|---|---|---|---|---|---|---|---|---|
| CG30382 | 125.93 | 0.963 | 0.143 | 0.615 | 0.653 | 0.215 | 0.639 | 0.051 | 0.14 |
| **rok** | **125.43** | **1.417** | **0.439** | **2.655** | **3.558** | **0.989** | **1.874** | **0.29** | **0.04** |
| **mei-38** | **124.93** | **1.335** | **0.317** | **5.851** | **7.103** | **0.298** | **4.382** | **0.067** | **0.001** |
| RpS23 | 124.93 | 1.250 | 0.221 | 0.830 | 0.864 | 0.072 | 0.664 | 0.036 | 0.106 |
| FK506-bp1 | 124.12 | 1.377 | 0.343 | 1.135 | 1.322 | 0.002 | 0.824 | 0.424 | 0.842 |
| CG5214 | 122.38 | 1.486 | 0.471 | 1.902 | 2.353 | 0.415 | 1.280 | 0.494 | 0.127 |
| lid | 122.21 | 1.711 | 0.834 | 8.298 | 12.057 | 7.254 | 4.851 | 0.243 | 0.076 |
| scu | 121.59 | 1.425 | 0.368 | 1.626 | 1.831 | 0.418 | 1.141 | 0.589 | 0.332 |
| Msp-300 | 120.41 | 1.901 | 0.789 | 3.989 | 5.222 | 0.509 | 2.098 | 0.192 | 0.014 |
| CG17514 | 120.28 | 1.677 | 0.641 | 1.823 | 2.473 | 0.834 | 1.087 | 0.868 | 0.308 |
| **RfC4** | **120.28** | **1.597** | **0.555** | **2.918** | **3.742** | **0.398** | **1.827** | **0.233** | **0.019** |
| **chb** | **119.92** | **1.585** | **0.510** | **1.479** | **1.843** | **0.148** | **0.933** | **0.833** | **0.554** |
| Rpt5 | 119.60 | 1.288 | 0.268 | 0.938 | 1.017 | 0.194 | 0.729 | 0.14 | 0.312 |
| Jabba | 119.26 | 1.694 | 0.783 | 3.954 | 5.283 | 2.223 | 2.334 | 0.2484 | 0.072 |
| rad50 | 119.23 | 1.796 | 0.752 | 3.452 | 4.413 | 0.933 | 1.922 | 0.241 | 0.039 |
| CG8235 | 118.47 | 1.427 | 0.391 | 1.182 | 0.998 | 0.288 | 0.828 | 0.48 | 0.283 |
| Droj2 | 117.48 | 1.572 | 0.668 | 5.180 | 6.576 | 0.410 | 3.296 | 0.069 | 0.003 |
| bsf | 117.48 | 1.542 | 0.504 | 1.586 | 2.086 | 0.941 | 1.028 | 0.953 | 0.446 |
| kis | 117.00 | 1.657 | 0.630 | 3.384 | 4.421 | 0.393 | 2.042 | 0.195 | 0.013 |
| woc | 116.62 | 1.667 | 0.634 | 5.703 | 7.332 | 1.617 | 3.421 | 0.088 | 0.01 |
| row | 116.48 | 1.517 | 0.548 | 6.457 | 8.156 | 1.584 | 4.257 | 0.055 | 0.086 |
| RpL11 | 116.26 | 1.188 | 0.176 | 0.672 | 0.746 | 0.040 | 0.565 | 0.015 | 0.045 |
| GstD1 | 116.00 | 2.003 | 1.273 | 0.656 | 0.858 | 0.233 | 0.327 | 0.154 | 0.317 |
| Karybeta3 | 115.56 | 1.597 | 0.668 | 2.858 | 3.308 | 0.788 | 1.790 | 0.135 | 0.078 |
| **rod** | **115.50** | **1.704** | **0.712** | **2.190** | **2.520** | **0.877** | **1.285** | **0.488** | **0.33** |
| **eIF-2alpha** | **115.16** | **1.399** | **0.409** | **1.657** | **2.136** | **0.800** | **1.185** | **0.303** | **0.251** |
| RpS10b | 114.99 | 1.357 | 0.346 | 1.000 | 1.054 | 0.070 | 0.737 | 0.162 | 0.329 |
| porin | 114.72 | 1.857 | 0.942 | 10.301 | 13.664 | 3.543 | 5.547 | 0.085 | 0.12 |
| RpL30 | 114.51 | 1.113 | 0.135 | 0.528 | 0.548 | 0.075 | 0.474 | 0.002 | 0.014 |
| tho2 | 113.75 | 1.425 | 0.398 | 1.739 | 2.217 | 0.090 | 1.221 | 0.586 | 0.078 |
| Scsalpha | 113.19 | 1.764 | 0.900 | 4.504 | 6.326 | 2.929 | 2.553 | 0.289 | 0.256 |
| RpL27A | 112.66 | 1.033 | 0.084 | 0.516 | 0.551 | 0.061 | 0.500 | 0.001 | 0.006 |
| RpL35 | 111.60 | 1.150 | 0.148 | 0.491 | 0.515 | 0.010 | 0.427 | 0.002 | 0.011 |
| Rpn6 | 110.76 | 1.169 | 0.147 | 0.753 | 0.833 | 0.213 | 0.644 | 0.046 | 0.122 |
| RpL12 | 110.53 | 1.202 | 0.176 | 0.618 | 0.661 | 0.039 | 0.514 | 0.007 | 0.028 |
| Prosalpha4 | 110.51 | 1.033 | 0.104 | 0.850 | 1.015 | 0.346 | 0.823 | 0.463 | 0.954 |
| Dys | 110.38 | 1.887 | 0.990 | 2.079 | 2.728 | 1.306 | 1.102 | 0.859 | 0.466 |
| **dgt6** | **110.34** | **1.604** | **0.700** | **7.977** | **8.690** | **0.272** | **4.975** | **0.002** | **0.001** |
| RpS25 | 108.33 | 1.191 | 0.180 | 0.747 | 0.790 | 0.027 | 0.627 | 0.017 | 0.059 |
| kst | 107.75 | 1.445 | 0.441 | 3.556 | 4.635 | 0.188 | 2.461 | 0.185 | 0.003 |

| | | | | | | | | | |
|---|---|---|---|---|---|---|---|---|---|
| **Prosalpha3** | **107.67** | **0.989** | **0.120** | **0.777** | **0.879** | **0.207** | **0.786** | **0.23** | **0.494** |
| sw | 107.43 | 1.273 | 0.255 | 1.943 | 2.732 | 0.068 | 1.526 | 0.492 | 0.005 |
| Mcm7 | 107.28 | 1.809 | 0.903 | 0.881 | 1.148 | 0.393 | 0.487 | 0.201 | 0.417 |
| eIF3-S9 | 106.88 | 1.543 | 0.531 | 1.091 | 1.162 | 0.008 | 0.707 | 0.225 | 0.407 |
| Rpt3 | 106.74 | 1.324 | 0.293 | 1.040 | 1.197 | 0.316 | 0.786 | 0.343 | 0.674 |
| **cnn** | **106.34** | **1.825** | **0.854** | **2.625** | **3.476** | **0.193** | **1.438** | **0.083** | **0.083** |
| RpS17 | 105.98 | 1.173 | 0.171 | 0.662 | 0.688 | 0.034 | 0.564 | 0.008 | 0.033 |
| CG7461 | 105.97 | 1.594 | 0.575 | 3.358 | 4.539 | 1.890 | 2.107 | 0.29 | 0.256 |
| **Su(var)2-HP2** | **105.87** | **1.388** | **0.404** | **5.334** | **7.374** | **0.646** | **3.844** | **0.194** | **0.001** |
| **toc** | **105.72** | **1.387** | **0.390** | **3.878** | **4.882** | **0.791** | **2.796** | **0.081** | **0.006** |
| **DNApol-epsilon** | **105.66** | **1.778** | **0.828** | **3.120** | **4.292** | **2.127** | **1.755** | **0.431** | **0.144** |
| alphaCop | 105.62 | 1.686 | 0.676 | 2.437 | 2.971 | 0.841 | 1.446 | 0.37 | 0.152 |
| Nmt | 105.52 | 1.092 | 0.140 | 0.941 | 0.967 | 0.096 | 0.861 | 0.182 | 0.361 |
| **Chro** | **105.42** | **1.544** | **0.580** | **4.900** | **6.241** | **0.181** | **3.173** | **0.122** | **0.002** |
| RpS21 | 105.10 | 1.219 | 0.259 | 0.797 | 0.879 | 0.036 | 0.654 | 0.069 | 0.178 |
| DNA-ligI | 104.90 | 1.589 | 0.680 | 2.904 | 4.045 | 3.520 | 1.827 | 0.522 | 0.292 |
| Gs1 | 104.75 | 1.861 | 1.034 | 2.192 | 3.031 | 1.161 | 1.178 | 0.784 | 0.32 |
| RpII215 | 104.10 | 1.728 | 0.795 | 1.457 | 1.918 | 0.456 | 0.844 | 0.716 | 0.786 |
| rig | 103.94 | 1.727 | 0.688 | 2.446 | 3.223 | 0.518 | 1.416 | 0.468 | 0.082 |
| spag | 103.90 | 1.594 | 0.597 | 1.553 | 1.830 | 0.377 | 0.975 | 0.936 | 0.661 |
| mud | 103.83 | 1.669 | 0.703 | 5.063 | 6.935 | 0.502 | 3.034 | 0.209 | 0.003 |
| par-1 | 103.80 | 1.413 | 0.452 | 1.772 | 2.195 | 0.088 | 1.254 | 0.511 | 0.105 |
| Hsp60 | 102.90 | 1.426 | 0.437 | 1.437 | 1.888 | 0.541 | 1.008 | 0.986 | 0.364 |
| eIF3-S8 | 102.82 | 1.477 | 0.431 | 1.153 | 1.235 | 0.050 | 0.781 | 0.284 | 0.504 |
| Rpn5 | 102.80 | 1.252 | 0.219 | 0.913 | 1.037 | 0.152 | 0.729 | 0.145 | 0.322 |
| Aldh | 102.28 | 1.629 | 0.564 | 1.130 | 1.535 | 0.586 | 0.693 | 0.432 | 0.869 |
| CG12304 | 102.10 | 1.512 | 0.506 | 1.301 | 1.146 | 0.426 | 0.861 | 0.603 | 0.466 |
| CG5787 | 102.07 | 1.345 | 0.307 | 2.385 | 3.001 | 0.081 | 1.773 | 0.18 | 0.006 |
| **ncd** | **101.98** | **1.689** | **0.723** | **1.477** | **1.898** | **0.065** | **0.875** | **0.74** | **0.724** |
| **sti** | **101.91** | **1.789** | **0.822** | **3.878** | **4.611** | **0.471** | **2.167** | **0.076** | **0.025** |
| Hsc70Cb | 101.49 | 1.457 | 0.462 | 0.959 | 1.266 | 0.416 | 0.659 | 0.322 | 0.672 |
| RpS14b | 101.21 | 1.304 | 0.301 | 0.998 | 1.078 | 0.009 | 0.766 | 0.186 | 0.389 |
| **Dmn** | **101.20** | **1.189** | **0.176** | **1.661** | **2.374** | **1.004** | **1.396** | **0.6** | **0.118** |
| DNApol-alpha180 | 101.09 | 1.671 | 0.638 | 1.701 | 2.327 | 1.335 | 1.018 | 0.975 | 0.496 |
| CG8142 | 100.99 | 1.543 | 0.527 | 2.999 | 3.845 | 0.029 | 1.943 | 0.181 | 0.01 |
| Cen | 100.76 | 1.720 | 0.754 | 3.070 | 4.247 | 0.957 | 1.785 | 0.363 | 0.044 |
| CG4169 | 100.64 | 1.735 | 0.782 | 4.735 | 6.372 | 2.143 | 2.730 | 0.191 | 0.036 |
| ATPsyn-gamma | 100.57 | 1.658 | 0.712 | 3.980 | 5.157 | 1.956 | 2.401 | 0.192 | 0.057 |
| Rbcn-3A | 99.85 | 1.589 | 0.581 | 3.532 | 4.734 | 1.626 | 2.223 | 0.241 | 0.047 |
| **cana** | **99.38** | **1.707** | **0.703** | **2.970** | **3.947** | **0.832** | **1.740** | **0.319** | **0.047** |
| Nopp140 | 99.30 | 1.292 | 0.260 | 1.764 | 2.264 | 0.118 | 1.365 | 0.42 | 0.017 |

| | | | | | | | | | |
|---|---|---|---|---|---|---|---|---|---|
| Saf-B | 99.12 | 1.285 | 0.259 | 1.348 | 1.635 | 0.240 | 1.049 | 0.861 | 0.226 |
| eIF5B | 98.74 | 1.303 | 0.273 | 1.512 | 1.795 | 0.076 | 1.160 | 0.555 | 0.099 |
| ATPCL | 98.50 | 1.662 | 0.763 | 2.606 | 2.578 | 0.299 | 1.568 | 0.255 | 0.393 |
| RpL15 | 97.99 | 1.232 | 0.202 | 0.839 | 1.015 | 0.075 | 0.681 | 0.14 | 0.258 |
| CG14476 | 97.97 | 1.404 | 0.677 | 3.522 | 4.698 | 1.075 | 2.509 | 0.183 | 0.023 |
| betaCop | 97.51 | 1.759 | 0.854 | 3.034 | 3.801 | 1.803 | 1.725 | 0.338 | 0.172 |
| His3:CG33833 | 97.26 | 1.308 | 0.340 | 0.587 | 0.713 | 0.175 | 0.449 | 0.042 | 0.114 |
| CG8036 | 97.20 | 1.687 | 0.758 | 0.967 | 1.261 | 0.431 | 0.573 | 0.265 | 0.535 |
| **14-3-3epsilon** | **97.06** | **1.498** | **0.453** | **1.004** | **1.303** | **0.161** | **0.670** | 0.287 | **0.657** |
| Mcm5 | 97.04 | 1.791 | 0.842 | 0.732 | 0.954 | 0.517 | 0.409 | 0.139 | 0.309 |
| FKBP59 | 96.89 | 1.697 | 0.708 | 0.559 | 0.732 | 0.030 | 0.330 | 0.062 | 0.165 |
| hyd | 96.83 | 1.631 | 0.714 | 2.933 | 3.834 | 1.521 | 1.798 | 0.328 | 0.106 |
| Fdh | 95.91 | 1.851 | 0.961 | 0.275 | 0.339 | 0.016 | 0.149 | 0.048 | 0.125 |
| l(2)03709 | 95.51 | 1.662 | 0.720 | 10.857 | 14.009 | 2.567 | 6.534 | 0.052 | 0.08 |
| **pnut** | **95.34** | **1.612** | **0.684** | **7.906** | **10.347** | **1.495** | **4.904** | **0.069** | **0.003** |
| RfC3 | 95.15 | 1.514 | 0.505 | 2.742 | 3.503 | 0.326 | 1.811 | 0.211 | 0.017 |
| His3.3B | 94.94 | 1.378 | 0.369 | 0.484 | 0.566 | 0.129 | 0.351 | 0.019 | 0.064 |
| Spt5 | 94.34 | 1.819 | 0.903 | 3.711 | 5.229 | 2.171 | 2.041 | 0.36 | 0.083 |
| **Arp1** | **94.27** | **1.487** | **0.487** | **2.252** | **3.183** | **0.866** | **1.515** | **0.501** | **0.062** |
| emb | 94.15 | 1.772 | 0.879 | 2.579 | 2.771 | 1.738 | 1.456 | 0.417 | 0.441 |
| clu | 93.92 | 1.280 | 0.243 | 0.740 | 0.852 | 0.011 | 0.578 | 0.04 | 0.1 |
| Prp8 | 93.45 | 1.491 | 0.451 | 1.255 | 1.580 | 0.261 | 0.841 | 0.612 | 0.822 |
| RpL23 | 93.39 | 1.140 | 0.122 | 0.762 | 0.858 | 0.036 | 0.668 | 0.034 | 0.055 |
| **RpA-70** | **93.22** | **1.673** | **0.885** | **0.908** | **1.180** | **0.217** | **0.542** | **0.261** | **0.515** |
| fry | 92.84 | 1.685 | 0.837 | 6.411 | 8.922 | 3.549 | 3.806 | 0.184 | 0.202 |
| **tws** | **92.79** | **1.666** | **0.716** | **1.863** | **2.535** | **0.617** | **1.119** | **0.824** | **0.258** |
| **cup** | **92.73** | **1.409** | **0.354** | **2.988** | **3.705** | **0.260** | **2.121** | **0.104** | **0.005** |
| Ref1 | 92.27 | 1.290 | 0.253 | 1.680 | 2.204 | 0.409 | 1.302 | 0.541 | 0.053 |
| Msh6 | 91.53 | 1.892 | 1.007 | 1.257 | 1.385 | 0.360 | 0.665 | 0.359 | 0.56 |
| Df31 | 89.79 | 1.029 | 0.048 | 1.091 | 1.466 | 0.089 | 1.061 | 0.883 | 0.005 |
| SMC1 | 89.43 | 1.612 | 0.723 | 3.998 | 5.315 | 0.077 | 2.480 | 0.161 | 0.006 |
| **cdc2** | **88.69** | **1.727** | **0.740** | **1.914** | **2.524** | **1.108** | **1.108** | **0.841** | **0.394** |
| CG7337 | 88.48 | 1.560 | 0.535 | 2.479 | 3.232 | 0.073 | 1.589 | 0.323 | 0.025 |
| cathD | 88.35 | 1.852 | 1.015 | 5.451 | 7.459 | 4.427 | 2.944 | 0.263 | 0.316 |
| **Eb1** | **88.17** | **1.534** | **0.620** | **2.849** | **3.882** | **0.826** | **1.857** | **0.314** | **0.034** |
| Pkn | 87.96 | 1.707 | 0.901 | 6.022 | 8.273 | 2.281 | 3.527 | 0.158 | 0.126 |
| eIF-5A | 87.54 | 1.480 | 0.416 | 1.090 | 1.174 | 0.057 | 0.736 | 0.201 | 0.398 |
| CG12262 | 87.52 | 1.893 | 1.198 | 2.566 | 3.371 | 0.576 | 1.355 | 0.569 | 0.215 |
| Gdh | 87.36 | 1.030 | 0.230 | 0.265 | 0.283 | 0.026 | 0.258 | 0.005 | 0.023 |
| RpL21 | 87.21 | 1.004 | 0.051 | 0.507 | 0.529 | 0.055 | 0.504 | 0 | 0.002 |

| | | | | | | | | | |
|---|---|---|---|---|---|---|---|---|---|
| RpL34b | 87.07 | 1.111 | 0.144 | 0.421 | 0.443 | 0.047 | 0.379 | 0.001 | 0.009 |
| CG12264 | 86.93 | 1.733 | 0.808 | 3.713 | 5.062 | 1.581 | 2.143 | 0.275 | 0.048 |
| CG7546 | 86.88 | 1.498 | 0.569 | 2.870 | 3.834 | 0.984 | 1.915 | 0.279 | 0.04 |
| CG11876 | 86.80 | 1.633 | 0.750 | 2.635 | 3.624 | 1.213 | 1.613 | 0.446 | 0.101 |
| CG30122 | 86.04 | 1.279 | 0.258 | 2.025 | 2.827 | 1.074 | 1.584 | 0.465 | 0.281 |
| rhea | 85.90 | 1.663 | 0.692 | 1.371 | 1.789 | 0.621 | 0.824 | 0.874 | 0.677 |
| bic | 85.44 | 1.002 | 0.079 | 0.572 | 0.607 | 0.070 | 0.571 | 0.003 | 0.011 |
| CG3542 | 85.16 | 1.551 | 0.501 | 1.444 | 1.842 | 0.039 | 0.931 | 0.843 | 0.484 |
| brm | 84.87 | 1.713 | 0.670 | 2.814 | 3.616 | 1.222 | 1.643 | 0.342 | 0.102 |
| CG4452 | 84.66 | 1.692 | 0.678 | 4.482 | 5.892 | 0.013 | 2.650 | 0.129 | 0.004 |
| RpL36 | 83.89 | 1.032 | 0.109 | 0.463 | 0.472 | 0.065 | 0.449 | 0.001 | 0.008 |
| egg | 83.88 | 1.614 | 0.624 | 3.186 | 4.076 | 0.603 | 1.974 | 0.188 | 0.022 |
| spel1 | 83.65 | 1.858 | 0.989 | 1.334 | 1.559 | 0.477 | 0.718 | 0.461 | 0.726 |
| dom | 83.61 | 1.531 | 0.547 | 2.926 | 3.820 | 0.217 | 1.911 | 0.217 | 0.012 |
| Rpt4R | 83.56 | 1.611 | 0.539 | 1.048 | 1.242 | 0.441 | 0.651 | 0.24 | 0.485 |
| Top2 | 82.82 | 1.379 | 0.329 | 1.520 | 1.882 | 0.166 | 1.102 | 0.752 | 0.149 |
| CG8184 | 82.75 | 1.561 | 0.600 | 2.680 | 3.492 | 1.205 | 1.717 | 0.33 | 0.089 |
| yps | 82.58 | 1.103 | 0.111 | 1.367 | 1.601 | 0.130 | 1.239 | 0.348 | 0.019 |
| RpS20 | 82.58 | 1.333 | 0.321 | 1.231 | 1.405 | 0.277 | 0.924 | 0.733 | 0.815 |
| Pol32 | 82.50 | 1.514 | 0.712 | 12.841 | 17.912 | 5.014 | 8.482 | 0.108 | 0.132 |
| CG1516 | 82.35 | 1.652 | 0.709 | 2.215 | 2.965 | 1.375 | 1.341 | 0.611 | 0.239 |
| **Mcm3** | **82.33** | **1.701** | **0.702** | **0.662** | **0.847** | **0.317** | **0.389** | **0.089** | **0.218** |
| Akap200 | 81.99 | 1.154 | 0.352 | 2.303 | 3.020 | 0.096 | 1.996 | 0.198 | 0.006 |
| ERp60 | 81.94 | 1.471 | 0.556 | 2.309 | 3.308 | 0.258 | 1.569 | 0.472 | 0.024 |
| Klc | 81.70 | 1.757 | 0.706 | 0.623 | 0.831 | 0.015 | 0.355 | 0.068 | 0.177 |
| RpL27 | 80.63 | 1.041 | 0.050 | 0.568 | 0.604 | 0.014 | 0.545 | 0.001 | 0.001 |
| CG42724 | 79.85 | 1.426 | 0.380 | 2.393 | 3.128 | 0.451 | 1.678 | 0.287 | 0.019 |
| Akap200 | 79.52 | 1.179 | 0.187 | 2.909 | 3.854 | 0.572 | 2.468 | 0.216 | 0.078 |
| CG5590 | 79.44 | 1.683 | 0.852 | 3.211 | 4.260 | 0.179 | 1.908 | 0.258 | 0.028 |
| **Rpn12** | **78.99** | **1.242** | **0.211** | **0.859** | **0.914** | **0.256** | **0.692** | **0.087** | **0.212** |
| **Cdc27** | **78.83** | **1.715** | **0.727** | **3.228** | **4.357** | **0.471** | **1.883** | **0.282** | **0.021** |
| dre4 | 78.38 | 1.714 | 0.700 | 0.758 | 0.937 | 0.149 | 0.442 | 0.099 | 0.237 |
| CG4365 | 78.35 | 1.498 | 0.519 | 3.826 | 5.276 | 1.143 | 2.555 | 0.208 | 0.013 |
| CG17528 | 78.15 | 1.536 | 0.504 | 4.559 | 5.971 | 2.918 | 2.968 | 0.181 | 0.272 |
| pzg | 78.04 | 1.637 | 0.769 | 5.382 | 6.647 | 1.322 | 3.288 | 0.061 | 0.012 |
| **CG10932** | **77.50** | **1.779** | **0.835** | **1.199** | **1.393** | **0.309** | **0.674** | 0.339 | 0.594 |
| Atx2 | 77.24 | 1.593 | 0.681 | 4.811 | 6.607 | 0.826 | 3.021 | 0.16 | 0.005 |
| slik | 77.04 | 1.892 | 1.347 | 4.621 | 6.312 | 2.556 | 2.443 | 0.27 | 0.078 |
| **Rpn13** | **77.03** | **1.313** | **0.272** | **0.563** | **0.551** | **0.041** | **0.429** | **0.039** | **0.033** |

| | | | | | | | | | |
|---|---|---|---|---|---|---|---|---|---|
| **pds5** | **76.84** | **1.560** | **0.565** | **2.224** | **2.886** | **0.638** | **1.426** | **0.444** | **0.091** |
| His2B:CG33882 | 76.80 | 1.317 | 0.290 | 1.019 | 1.177 | 0.441 | 0.773 | 0.364 | 0.687 |
| Tm2 | 76.73 | 2.285 | 2.232 | 3.972 | 5.406 | 4.739 | 1.738 | 0.57 | 0.375 |
| WRNexo | 76.31 | 1.235 | 0.207 | 3.175 | 4.133 | 0.758 | 2.572 | 0.127 | 0.1 |
| Hsc70-5 | 76.29 | 1.147 | 0.150 | 1.083 | 1.424 | 0.174 | 0.944 | 0.868 | 0.15 |
| beta'Cop | 76.10 | 1.644 | 0.638 | 2.463 | 3.064 | 1.141 | 1.498 | 0.387 | 0.161 |
| Not1 | 76.08 | 1.613 | 0.634 | 3.440 | 4.555 | 2.500 | 2.133 | 0.305 | 0.336 |
| mRpL12 | 75.76 | 0.910 | 0.202 | 0.224 | 0.233 | 0.037 | 0.245 | 0.033 | 0.03 |
| Oscp | 75.68 | 1.632 | 0.660 | 4.181 | 5.415 | 1.735 | 2.562 | 0.157 | 0.035 |
| **gammaTub37C** | **75.28** | **1.535** | **0.501** | **3.933** | **4.824** | **0.956** | **2.563** | **0.077** | **0.013** |
| **Nat1** | **75.28** | **1.430** | **0.400** | **1.430** | **1.798** | **0.180** | **1.000** | **1** | **0.324** |
| Ef1beta | 75.22 | 1.101 | 0.095 | 1.261 | 1.640 | 0.187 | 1.146 | 0.721 | 0.021 |
| Rpn7 | 74.61 | 1.308 | 0.268 | 0.972 | 1.102 | 0.334 | 0.743 | 0.24 | 0.496 |
| Rpn13 | 74.48 | 1.158 | 0.138 | 0.525 | 0.508 | 0.026 | 0.453 | 0.012 | 0.008 |
| Prosbeta2 | 73.85 | 1.011 | 0.167 | 0.570 | 0.610 | 0.067 | 0.564 | 0.015 | 0.053 |
| Rtf1 | 73.42 | 1.695 | 0.775 | 4.187 | 5.646 | 1.385 | 2.471 | 0.2 | 0.024 |
| Torsin | 73.39 | 1.657 | 0.750 | 8.562 | 11.976 | 2.472 | 5.167 | 0.127 | 0.005 |
| Cyp1 | 73.18 | 1.409 | 0.474 | 1.072 | 1.424 | 0.179 | 0.761 | 0.498 | 0.969 |
| **l(1)dd4** | **72.95** | **1.635** | **0.627** | **3.970** | **4.786** | **1.418** | **2.429** | **0.093** | **0.037** |
| RpS28b | 72.90 | 1.213 | 0.197 | 0.827 | 0.874 | 0.086 | 0.682 | 0.039 | 0.114 |
| CG7433 | 72.74 | 1.823 | 1.154 | 2.202 | 3.032 | 1.237 | 1.208 | 0.764 | 0.344 |
| CG3800 | 72.25 | 1.637 | 0.557 | 1.567 | 1.878 | 0.302 | 0.957 | 0.887 | 0.625 |
| **dgt2** | **71.82** | **1.582** | **0.649** | **6.967** | **7.418** | **0.220** | **4.405** | **0.001** | **0.001** |
| Sra-1 | 71.77 | 1.983 | 1.239 | 4.892 | 5.959 | 0.597 | 2.467 | 0.09 | 0.027 |
| pont | 71.76 | 1.476 | 0.472 | 1.724 | 2.157 | 0.476 | 1.168 | 0.698 | 0.234 |
| Ranbp16 | 71.25 | 1.707 | 0.764 | 2.874 | 3.522 | 1.593 | 1.683 | 0.316 | 0.171 |
| WRNexo | 70.69 | 1.278 | 0.252 | 3.868 | 5.127 | 1.086 | 3.027 | 0.126 | 0.008 |
| yl | 70.47 | 1.686 | 0.623 | 4.903 | 6.555 | 0.688 | 2.909 | 0.134 | 0.004 |
| CG8478 | 70.41 | 1.440 | 0.469 | 2.961 | 3.763 | 0.483 | 2.057 | 0.155 | 0.013 |
| CaMKII | 70.39 | 1.737 | 0.775 | 10.753 | 13.571 | 1.496 | 6.192 | 0.086 | 0.001 |
| RpL37a | 70.03 | 1.039 | 0.120 | 0.484 | 0.490 | 0.096 | 0.466 | 0.002 | 0.013 |
| Tango7 | 69.91 | 1.557 | 0.533 | 1.483 | 1.777 | 0.493 | 0.953 | 0.884 | 0.674 |
| CG32165 | 69.70 | 1.782 | 0.783 | 2.104 | 2.752 | 1.001 | 1.181 | 0.735 | 0.305 |
| **RfC38** | **69.65** | **1.564** | **0.501** | **2.727** | **3.494** | **0.208** | **1.744** | **0.231** | **0.016** |
| **l(3)72Ab** | **69.57** | **1.454** | **0.398** | **1.135** | **1.419** | **0.219** | **0.781** | **0.443** | **0.917** |
| Tor | 69.53 | 1.874 | 0.851 | 3.017 | 4.002 | 0.094 | 1.610 | 0.358 | 0.044 |
| CG33129 | 69.40 | 1.604 | 0.704 | 6.349 | 8.549 | 0.745 | 3.959 | 0.162 | 0.002 |
| **Grip75** | **69.00** | **1.585** | **0.576** | **3.236** | **4.065** | **1.155** | **2.042** | **0.177** | **0.045** |
| RanGAP | 68.97 | 1.744 | 0.894 | 1.932 | 2.419 | 0.331 | 1.108 | 0.807 | 0.399 |
| Nup205 | 68.76 | 1.742 | 0.787 | 2.662 | 3.204 | 1.699 | 1.528 | 0.406 | 0.265 |

| | | | | | | | | | |
|---|---|---|---|---|---|---|---|---|---|
| Nup93-2 | 68.55 | 1.638 | 0.705 | 3.887 | 5.322 | 4.148 | 2.373 | 0.418 | 0.425 |
| Su(var)205 | 68.48 | 1.508 | 0.561 | 2.041 | 2.776 | 0.454 | 1.354 | 0.497 | 0.076 |
| CG6543 | 68.46 | 1.577 | 0.512 | 0.704 | 0.871 | 0.001 | 0.447 | 0.062 | 0.162 |
| CG6197 | 68.40 | 1.530 | 0.488 | 2.515 | 3.463 | 1.249 | 1.644 | 0.426 | 0.082 |
| RpL37a | 68.15 | 1.079 | 0.083 | 0.457 | 0.447 | 0.093 | 0.423 | 0.001 | 0.004 |
| RpII140 | 68.02 | 1.714 | 0.785 | 1.639 | 2.192 | 0.662 | 0.956 | 0.927 | 0.533 |
| Cas | 67.90 | 1.543 | 0.520 | 3.377 | 3.503 | 1.949 | 2.189 | 0.1 | 0.382 |
| CG1703 | 67.75 | 0.926 | 0.322 | 0.561 | 0.652 | 0.001 | 0.605 | 0.152 | 0.335 |
| Ssrp | 67.37 | 1.583 | 0.629 | 0.973 | 1.227 | 0.385 | 0.614 | 0.264 | 0.536 |
| Cep135 | 67.14 | 1.368 | 0.320 | 5.673 | 6.636 | 0.452 | 4.148 | 0.013 | 0.001 |
| spg | 67.09 | 1.600 | 0.521 | 3.767 | 4.577 | 0.266 | 2.354 | 0.068 | 0.005 |
| Sep1 | 67.00 | 1.554 | 0.645 | 10.109 | 13.439 | 0.260 | 6.503 | 0.122 | 0 |
| **wac** | **66.99** | **1.641** | **0.621** | **8.027** | **9.149** | **0.024** | **4.892** | **0.006** | **0.001** |
| Cul-2 | 66.24 | 1.840 | 0.951 | 2.225 | 2.859 | 1.315 | 1.209 | 0.719 | 0.38 |
| Klp31E | 66.06 | 1.653 | 0.672 | 4.436 | 6.180 | 2.136 | 2.683 | 0.237 | 0.188 |
| cutlet | 65.74 | 1.726 | 0.719 | 3.587 | 4.418 | 0.103 | 2.078 | 0.116 | 0.015 |
| CG4119 | 65.72 | 1.471 | 0.453 | 0.868 | 1.000 | 0.130 | 0.590 | 0.113 | 0.265 |
| **Prosbeta5** | **65.61** | **1.021** | **0.144** | **0.543** | **0.575** | **0.020** | **0.532** | **0.006** | **0.026** |
| gammaCop | 65.56 | 1.907 | 0.828 | 2.761 | 3.506 | 2.159 | 1.448 | 0.532 | 0.477 |
| **14-3-3zeta** | **65.18** | **1.258** | **0.224** | **0.728** | **0.944** | **0.062** | **0.578** | **0.104** | **0.162** |
| Bruce | 65.04 | 1.739 | 0.718 | 2.594 | 3.338 | 1.178 | 1.492 | 0.431 | 0.146 |
| msk | 64.94 | 1.579 | 0.577 | 3.491 | 4.159 | 2.715 | 2.212 | 0.275 | 0.402 |
| CG16935 | 64.71 | 1.485 | 0.477 | 3.886 | 5.143 | 1.859 | 2.616 | 0.183 | 0.207 |
| TfIIFbeta | 64.63 | 1.527 | 0.563 | 7.446 | 10.362 | 0.267 | 4.875 | 0.178 | 0 |
| CG7430 | 64.49 | 1.125 | 0.110 | 1.498 | 1.984 | 0.198 | 1.331 | 0.529 | 0.007 |
| His1:CG33834 | 64.28 | 1.228 | 0.226 | 0.639 | 0.735 | 0.164 | 0.521 | 0.028 | 0.08 |
| Fen1 | 64.09 | 1.444 | 0.455 | 2.930 | 3.886 | 1.385 | 2.029 | 0.263 | 0.224 |
| **coro** | **64.09** | **1.525** | **0.514** | **1.113** | **1.439** | **0.153** | **0.730** | **0.407** | **0.84** |
| eIF2B-delta | 64.07 | 1.587 | 0.611 | 2.644 | 3.608 | 1.944 | 1.666 | 0.461 | 0.369 |
| yip2 | 63.46 | 1.793 | 0.842 | 0.723 | 0.822 | 0.012 | 0.403 | 0.097 | 0.22 |
| CTPsyn | 63.30 | 1.853 | 0.983 | 2.618 | 3.582 | 2.488 | 1.413 | 0.639 | 0.333 |
| CG8778 | 62.76 | 1.782 | 0.917 | 3.374 | 4.575 | 1.931 | 1.894 | 0.357 | 0.107 |
| Rab1 | 62.49 | 1.539 | 0.506 | 6.173 | 8.275 | 3.758 | 4.012 | 0.152 | 0.236 |
| **lat** | **62.42** | **1.731** | **0.687** | **2.298** | **3.007** | **0.676** | **1.328** | **0.544** | **0.133** |
| **CycB** | **62.30** | **1.250** | **0.234** | **1.230** | **1.512** | **0.222** | **0.984** | **0.954** | **0.301** |
| Etl1 | 62.21 | 1.580 | 0.624 | 4.215 | 5.707 | 3.128 | 2.668 | 0.257 | 0.307 |
| Prosalpha7 | 62.19 | 0.998 | 0.181 | 0.618 | 0.688 | 0.203 | 0.619 | 0.065 | 0.17 |
| Ote | 62.01 | 1.594 | 0.772 | 0.691 | 0.881 | 0.057 | 0.433 | 0.136 | 0.304 |
| **Prosbeta7** | **61.72** | **0.928** | **0.165** | **0.603** | **0.666** | **0.051** | **0.650** | **0.048** | **0.128** |
| eEF1delta | 61.63 | 1.177 | 0.190 | 0.950 | 1.228 | 0.080 | 0.807 | 0.491 | 0.757 |
| **Nipped-B** | **60.97** | **1.546** | **0.611** | **2.614** | **3.430** | **0.497** | **1.691** | **0.306** | **0.037** |

| | | | | | | | | | |
|---|---|---|---|---|---|---|---|---|---|
| GlyS | 60.46 | 1.734 | 0.756 | 1.126 | 1.453 | 0.695 | 0.649 | 0.379 | 0.704 |
| **cdc2c** | **60.21** | **1.851** | **1.006** | **3.928** | **5.383** | **2.860** | **2.123** | **0.347** | **0.127** |
| CG2469 | 60.13 | 1.492 | 0.464 | 3.613 | 4.842 | 0.804 | 2.422 | 0.178 | 0.009 |
| His2A:CG33826 | 60.06 | 1.393 | 0.346 | 1.127 | 1.324 | 0.530 | 0.809 | 0.494 | 0.867 |
| TfIIS | 60.00 | 1.461 | 0.442 | 5.867 | 7.295 | 2.008 | 4.015 | 0.057 | 0.142 |
| **aub** | **59.94** | **1.477** | **0.457** | **3.125** | **4.071** | **0.788** | **2.116** | **0.186** | **0.017** |
| Ced-12 | 59.78 | 1.653 | 0.726 | 4.478 | 5.650 | 1.105 | 2.709 | 0.1 | 0.015 |
| vig | 59.10 | 1.177 | 0.154 | 0.622 | 0.721 | 0.044 | 0.528 | 0.015 | 0.03 |
| Cul-4 | 58.97 | 1.707 | 0.771 | 3.700 | 4.545 | 2.143 | 2.168 | 0.199 | 0.294 |
| CG1091 | 58.50 | 1.492 | 0.457 | 2.928 | 3.841 | 1.350 | 1.962 | 0.21 | 0.226 |
| Caf1-180 | 58.35 | 1.622 | 0.647 | 5.274 | 7.099 | 1.812 | 3.253 | 0.142 | 0.123 |
| dec-1 | 58.28 | 1.410 | 0.441 | 2.688 | 3.124 | 0.757 | 1.907 | 0.097 | 0.045 |
| **Grip84** | **58.13** | **1.495** | **0.457** | **3.636** | **4.303** | **0.223** | **2.432** | **0.042** | **0.004** |
| Past1 | 57.70 | 1.685 | 0.782 | 4.449 | 6.143 | 5.157 | 2.641 | 0.414 | 0.434 |
| Nacalpha | 57.70 | 1.126 | 0.156 | 0.708 | 0.820 | 0.039 | 0.629 | 0.044 | 0.081 |
| **CG8636** | **57.65** | **1.451** | **0.432** | **1.278** | **1.355** | **0.086** | **0.881** | **0.548** | **0.787** |
| **pav** | **57.64** | **1.779** | **0.780** | **2.877** | **3.682** | **0.164** | **1.617** | **0.301** | **0.048** |
| Ca-P60A | 57.55 | 1.817 | 0.924 | 7.581 | 10.151 | 2.494 | 4.171 | 0.11 | 0.011 |
| Orc1 | 57.23 | 1.542 | 0.534 | 1.592 | 1.980 | 0.018 | 1.032 | 0.925 | 0.352 |
| Cul-5 | 57.22 | 1.470 | 0.441 | 2.775 | 3.317 | 0.799 | 1.887 | 0.128 | 0.041 |
| RpL36A | 56.89 | 1.172 | 0.151 | 0.700 | 0.716 | 0.007 | 0.597 | 0.029 | 0.027 |
| **Cdc16** | **56.80** | **1.847** | **0.910** | **3.244** | **4.369** | **1.374** | **1.756** | **0.364** | **0.085** |
| pic | 56.77 | 1.634 | 0.695 | 2.518 | 3.329 | 1.339 | 1.541 | 0.45 | 0.148 |
| CG9953 | 56.70 | 1.901 | 1.098 | 4.940 | 6.797 | 3.313 | 2.599 | 0.268 | 0.267 |
| dia | 56.64 | 1.562 | 0.550 | 3.897 | 4.925 | 1.009 | 2.495 | 0.113 | 0.015 |
| Rassf | 56.57 | 1.869 | 0.918 | 3.626 | 4.961 | 2.232 | 1.939 | 0.36 | 0.108 |
| rin | 56.18 | 1.329 | 0.308 | 1.119 | 1.348 | 0.005 | 0.842 | 0.51 | 0.938 |
| CG32479 | 55.89 | 1.477 | 0.487 | 3.000 | 4.058 | 1.101 | 2.031 | 0.267 | 0.033 |
| Tm1 | 55.87 | 1.653 | 0.976 | 2.661 | 3.676 | 3.477 | 1.610 | 0.612 | 0.559 |
| Jafrac1 | 55.82 | 1.388 | 0.363 | 0.533 | 0.686 | 0.074 | 0.384 | 0.031 | 0.082 |
| Hsp23 | 55.80 | 1.574 | 0.617 | 3.081 | 4.409 | 2.006 | 1.958 | 0.4 | 0.281 |
| Usp7 | 55.55 | 1.733 | 0.817 | 1.496 | 1.964 | 0.645 | 0.863 | 0.757 | 0.762 |
| Imp | 55.34 | 1.492 | 0.428 | 2.167 | 2.535 | 0.051 | 1.452 | 0.202 | 0.047 |
| Lon | 55.28 | 1.465 | 0.539 | 3.412 | 4.762 | 1.073 | 2.329 | 0.251 | 0.018 |
| CG7441 | 55.21 | 1.252 | 0.231 | 1.748 | 2.134 | 0.229 | 1.396 | 0.303 | 0.025 |
| CG5642 | 55.18 | 1.556 | 0.544 | 1.030 | 1.110 | 0.171 | 0.662 | 0.188 | 0.361 |
| Sema-2a | 54.89 | 1.497 | 0.552 | 5.422 | 7.068 | 0.848 | 3.622 | 0.083 | 0.003 |
| msn | 54.86 | 1.677 | 0.671 | 2.125 | 2.826 | 0.823 | 1.267 | 0.633 | 0.181 |
| CG11779 | 54.83 | 1.561 | 0.602 | 6.179 | 8.396 | 3.564 | 3.960 | 0.159 | 0.219 |
| l(1)G0230 | 54.81 | 1.396 | 0.425 | 5.904 | 7.571 | 1.493 | 4.229 | 0.066 | 0.094 |

| | | | | | | | | | |
|---|---|---|---|---|---|---|---|---|---|
| Nup50 | 54.65 | 1.658 | 0.656 | 2.644 | 3.566 | 1.532 | 1.595 | 0.449 | 0.136 |
| **aur** | **54.65** | **1.442** | **0.400** | **3.448** | **4.323** | **0.130** | **2.390** | **0.142** | **0.02** |
| RhoGAP1A | 54.63 | 1.664 | 0.763 | 5.252 | 7.148 | 2.482 | 3.157 | 0.177 | 0.18 |
| AGO2 | 54.47 | 1.573 | 0.563 | 4.140 | 5.550 | 1.722 | 2.632 | 0.186 | 0.169 |
| **BubR1** | **54.35** | **1.643** | **0.643** | **3.100** | **4.121** | **0.423** | **1.887** | **0.256** | **0.018** |
| CG10602 | 54.34 | 1.807 | 0.942 | 0.546 | 0.708 | 0.119 | 0.302 | 0.091 | 0.217 |
| mRpL45 | 54.29 | 1.148 | 0.138 | 0.706 | 0.831 | 0.258 | 0.615 | 0.072 | 0.16 |
| eIF-4B | 54.29 | 1.666 | 0.698 | 1.222 | 1.630 | 0.206 | 0.734 | 0.487 | 0.951 |
| pix | 54.26 | 1.378 | 0.364 | 1.323 | 1.373 | 0.082 | 0.960 | 0.814 | 0.985 |
| CG2918 | 54.18 | 1.477 | 0.453 | 2.680 | 3.723 | 0.452 | 1.814 | 0.332 | 0.012 |
| TFAM | 53.57 | 1.135 | 0.286 | 0.838 | 0.941 | 0.126 | 0.739 | 0.215 | 0.45 |
| Pgk | 53.56 | 1.939 | 1.116 | 1.044 | 1.394 | 0.344 | 0.539 | 0.297 | 0.568 |
| AGO3 | 53.40 | 1.557 | 0.560 | 2.884 | 3.784 | 1.295 | 1.853 | 0.291 | 0.069 |
| CG5608 | 53.37 | 1.721 | 0.677 | 3.901 | 5.178 | 2.039 | 2.267 | 0.238 | 0.233 |
| mRpS5 | 53.34 | 1.314 | 0.277 | 1.177 | 1.500 | 0.143 | 0.896 | 0.728 | 0.458 |
| mor | 53.23 | 1.502 | 0.504 | 2.067 | 2.565 | 0.714 | 1.376 | 0.432 | 0.14 |
| Art3 | 53.22 | 1.817 | 1.004 | 1.174 | 1.523 | 0.270 | 0.646 | 0.401 | 0.725 |
| CG15099 | 53.07 | 1.892 | 1.016 | 5.128 | 6.828 | 2.593 | 2.711 | 0.197 | 0.052 |
| **Rpn8** | **52.99** | **1.133** | **0.121** | **0.740** | **0.792** | **0.097** | **0.653** | **0.016** | **0.047** |
| Crc | 52.82 | 1.263 | 0.262 | 3.361 | 4.835 | 1.454 | 2.662 | 0.259 | 0.172 |
| CG7834 | 52.79 | 1.598 | 0.678 | 2.509 | 3.235 | 1.064 | 1.570 | 0.384 | 0.119 |
| **CG12018** | **52.76** | **1.630** | **0.712** | **6.060** | **8.094** | **1.728** | **3.718** | **0.113** | **0.009** |
| CG5384 | 52.62 | 1.484 | 0.551 | 1.014 | 0.952 | 0.146 | 0.683 | 0.227 | 0.293 |
| CG7182 | 52.60 | 1.426 | 0.428 | 2.214 | 2.946 | 0.822 | 1.552 | 0.296 | 0.008 |
| REG | 52.58 | 1.581 | 0.533 | 1.269 | 1.640 | 0.760 | 0.803 | 0.615 | 0.923 |
| Ranbp9 | 52.52 | 1.847 | 0.970 | 2.653 | 2.456 | 0.756 | 1.437 | 0.295 | 0.514 |
| Mms19 | 52.43 | 1.776 | 0.831 | 3.436 | 4.647 | 2.427 | 1.935 | 0.368 | 0.328 |
| und | 52.37 | 1.154 | 0.163 | 0.905 | 1.001 | 0.094 | 0.784 | 0.148 | 0.326 |
| Cul-3 | 52.03 | 1.665 | 0.690 | 2.543 | 3.200 | 1.262 | 1.528 | 0.396 | 0.165 |
| kuk | 51.95 | 1.550 | 0.537 | 4.264 | 5.823 | 0.929 | 2.751 | 0.172 | 0.007 |
| Clbn | 51.86 | 1.220 | 0.199 | 0.766 | 0.762 | 0.054 | 0.628 | 0.018 | 0.057 |
| CG8771 | 51.86 | 1.883 | 0.978 | 3.611 | 4.865 | 2.974 | 1.917 | 0.4 | 0.183 |
| CG8635 | 51.62 | 1.218 | 0.201 | 0.903 | 1.164 | 0.104 | 0.742 | 0.336 | 0.756 |
| **Mad1** | **51.57** | **1.826** | **0.820** | **5.130** | **6.476** | **2.424** | **2.810** | **0.13** | **0.046** |
| CG8963 | 51.45 | 1.741 | 0.739 | 2.675 | 3.574 | 0.189 | 1.536 | 0.403 | 0.047 |
| ctrip | 51.40 | 1.617 | 0.662 | 4.063 | 5.548 | 1.177 | 2.513 | 0.203 | 0.016 |
| **mts** | **51.14** | **1.490** | **0.465** | **0.643** | **0.793** | **0.139** | **0.432** | **0.054** | **0.114** |
| CG7414 | 51.13 | 1.368 | 0.345 | 1.264 | 1.323 | 0.166 | 0.924 | 0.659 | 0.88 |
| CG6767 | 51.06 | 1.566 | 0.562 | 1.778 | 1.724 | 0.448 | 1.136 | 0.603 | 0.764 |
| RpL32 | 51.01 | 1.138 | 0.172 | 0.618 | 0.675 | 0.125 | 0.543 | 0.014 | 0.049 |
| Sep2 | 50.85 | 1.365 | 0.329 | 4.817 | 6.403 | 0.153 | 3.529 | 0.16 | 0 |

| | | | | | | | | | |
|---|---|---|---|---|---|---|---|---|---|
| Rpn11 | 50.54 | 1.176 | 0.160 | 0.759 | 0.794 | 0.111 | 0.645 | 0.019 | 0.064 |
| CG5174 | 50.19 | 1.352 | 0.355 | 6.347 | 8.928 | 1.951 | 4.693 | 0.139 | 0.108 |
| wde | 50.13 | 1.708 | 0.799 | 3.913 | 4.912 | 0.210 | 2.292 | 0.116 | 0.013 |
| **dgt4** | **50.07** | **1.592** | **0.657** | **10.332** | **11.292** | **0.545** | **6.492** | **0.001** | **0** |
| Elf | 50.01 | 1.817 | 0.854 | 0.747 | 1.010 | 0.545 | 0.411 | 0.15 | 0.331 |
| CG8507 | 49.98 | 1.045 | 0.176 | 1.713 | 2.136 | 0.018 | 1.639 | 0.2 | 0.004 |
| AP-1-2beta | 49.94 | 1.625 | 0.602 | 2.503 | 3.093 | 0.490 | 1.540 | 0.286 | 0.066 |
| **Rpn10** | **49.80** | **1.264** | **0.232** | **0.979** | **1.169** | **0.278** | **0.775** | **0.333** | **0.705** |
| **dgt3** | **49.41** | **1.674** | **0.679** | **8.105** | **9.293** | **1.521** | **4.840** | **0.01** | **0.004** |
| CG5794 | 49.28 | 1.692 | 0.690 | 3.493 | 4.798 | 2.704 | 2.064 | 0.363 | 0.343 |
| CG10565 | 49.06 | 1.498 | 0.505 | 1.427 | 1.864 | 0.140 | 0.953 | 0.899 | 0.41 |
| ATPsyn-d | 49.04 | 1.434 | 0.402 | 7.467 | 9.668 | 1.873 | 5.206 | 0.062 | 0.093 |
| Spn | 49.04 | 1.318 | 0.284 | 3.491 | 4.374 | 1.775 | 2.650 | 0.133 | 0.243 |
| Aats-ala | 49.01 | 2.598 | 2.558 | 1.503 | 1.929 | 0.376 | 0.579 | 0.518 | 0.75 |
| hyx | 48.96 | 1.561 | 0.537 | 2.988 | 3.885 | 0.231 | 1.914 | 0.209 | 0.012 |
| mub | 48.90 | 1.625 | 0.663 | 2.317 | 2.786 | 0.348 | 1.426 | 0.328 | 0.115 |
| **eIF-2beta** | **48.88** | **1.596** | **0.615** | **2.314** | **3.053** | **1.672** | **1.450** | **0.538** | **0.239** |
| Rif1 | 48.86 | 1.476 | 0.510 | 3.554 | 4.692 | 1.334 | 2.407 | 0.172 | 0.028 |
| AP-2alpha | 48.84 | 1.509 | 0.481 | 2.386 | 2.997 | 0.307 | 1.581 | 0.268 | 0.032 |
| ndl | 48.62 | 1.383 | 0.387 | 2.743 | 3.606 | 1.223 | 1.984 | 0.254 | 0.219 |
| Spt6 | 48.62 | 1.498 | 0.619 | 3.440 | 4.553 | 1.774 | 2.297 | 0.231 | 0.228 |
| lig | 48.54 | 1.071 | 0.265 | 1.425 | 1.799 | 0.108 | 1.331 | 0.432 | 0.038 |
| Capr | 48.25 | 1.163 | 0.224 | 0.866 | 1.067 | 0.127 | 0.745 | 0.292 | 0.633 |
| Art1 | 48.20 | 1.844 | 1.015 | 0.513 | 0.722 | 0.273 | 0.278 | 0.103 | 0.241 |
| CG6693 | 47.95 | 1.441 | 0.388 | 0.764 | 0.864 | 0.340 | 0.530 | 0.074 | 0.189 |
| Vps35 | 47.94 | 1.906 | 0.867 | 3.112 | 4.359 | 2.240 | 1.632 | 0.499 | 0.166 |
| GstT1 | 47.81 | 1.446 | 0.464 | 2.314 | 2.913 | 0.534 | 1.600 | 0.279 | 0.046 |
| CG2943 | 47.67 | 1.432 | 0.436 | 3.984 | 5.166 | 0.429 | 2.782 | 0.161 | 0.003 |
| **Nuf2** | **47.44** | **1.500** | **0.473** | **2.887** | **3.706** | **0.909** | **1.925** | **0.214** | **0.034** |
| Cbp80 | 47.29 | 1.582 | 0.516 | 1.900 | 2.486 | 0.531 | 1.201 | 0.67 | 0.154 |
| Nup160 | 47.10 | 1.707 | 0.740 | 2.034 | 2.606 | 1.017 | 1.192 | 0.713 | 0.327 |
| CG6841 | 47.06 | 1.402 | 0.359 | 0.630 | 0.780 | 0.024 | 0.449 | 0.039 | 0.103 |
| DNApol-alpha60 | 47.02 | 1.725 | 0.751 | 1.890 | 2.617 | 1.799 | 1.096 | 0.89 | 0.477 |
| Clc | 46.90 | 1.677 | 0.727 | 0.994 | 1.172 | 0.185 | 0.593 | 0.214 | 0.427 |
| CG5792 | 46.86 | 1.660 | 0.660 | 1.835 | 2.220 | 0.608 | 1.105 | 0.784 | 0.411 |
| CG12163 | 46.81 | 1.391 | 0.416 | 2.647 | 3.417 | 0.374 | 1.902 | 0.201 | 0.012 |
| Rpd3 | 46.74 | 1.773 | 0.868 | 2.900 | 3.978 | 1.589 | 1.636 | 0.452 | 0.129 |
| l(1)G0196 | 46.70 | 1.616 | 0.767 | 3.581 | 4.742 | 2.002 | 2.216 | 0.257 | 0.248 |
| Prosbeta4 | 46.70 | 0.943 | 0.172 | 0.439 | 0.453 | 0.105 | 0.466 | 0.01 | 0.039 |
| Men | 46.67 | 1.473 | 0.488 | 3.603 | 4.774 | 1.206 | 2.446 | 0.117 | 0.02 |

| | | | | | | | | | |
|---|---|---|---|---|---|---|---|---|---|
| CG4586 | 46.65 | 1.175 | 0.168 | 0.919 | 1.158 | 0.049 | 0.782 | 0.378 | 0.901 |
| Rpn9 | 46.36 | 1.163 | 0.146 | 0.609 | 0.618 | 0.086 | 0.523 | 0.004 | 0.019 |
| **mus101** | **46.29** | **1.814** | **0.815** | **4.213** | **5.647** | **1.105** | **2.323** | **0.203** | **0.02** |
| Pdi | 46.21 | 1.296 | 0.328 | 2.460 | 3.531 | 0.695 | 1.899 | 0.854 | 0.598 |
| CG5199 | 45.81 | 1.704 | 0.827 | 1.772 | 2.207 | 0.077 | 1.040 | 0.921 | 0.475 |
| Nup93-1 | 45.56 | 1.662 | 0.713 | 2.621 | 3.195 | 1.483 | 1.576 | 0.361 | 0.204 |
| mRpL38 | 45.56 | 1.073 | 0.069 | 0.667 | 0.765 | 0.107 | 0.621 | 0.024 | 0.027 |
| su(Hw) | 45.48 | 1.532 | 0.602 | 3.838 | 5.285 | 0.627 | 2.505 | 0.201 | 0.007 |
| Glg1 | 45.19 | 1.608 | 0.665 | 8.794 | 11.750 | 4.542 | 5.468 | 0.11 | 0.191 |
| **tum** | **44.80** | **1.787** | **0.788** | **3.126** | **4.135** | **0.529** | **1.749** | **0.3** | **0.036** |
| mRpL24 | 44.75 | 1.051 | 0.090 | 0.431 | 0.429 | 0.049 | 0.410 | 0 | 0.003 |
| Ranbp21 | 44.58 | 1.637 | 0.715 | 4.588 | 5.980 | 5.052 | 2.802 | 0.357 | 0.436 |
| MEP-1 | 44.46 | 1.538 | 0.560 | 4.531 | 6.167 | 1.522 | 2.947 | 0.168 | 0.014 |
| **spn-E** | **44.43** | **1.651** | **0.640** | **5.801** | **7.981** | **2.275** | **3.513** | **0.158** | **0.016** |
| Rab11 | 44.32 | 1.425 | 0.476 | 4.644 | 6.312 | 1.478 | 3.260 | 0.086 | 0.115 |
| CG2247 | 44.31 | 1.551 | 0.550 | 3.019 | 3.905 | 1.179 | 1.946 | 0.237 | 0.051 |
| mus209 | 44.22 | 1.693 | 0.807 | 0.383 | 0.493 | 0.115 | 0.226 | 0.053 | 0.141 |
| Aats-thr | 44.20 | 1.604 | 0.686 | 1.030 | 1.346 | 0.309 | 0.642 | 0.333 | 0.663 |
| His4:CG33881 | 44.11 | 1.546 | 0.509 | 0.963 | 1.215 | 0.627 | 0.623 | 0.277 | 0.557 |
| CkIIbeta | 44.09 | 1.458 | 0.450 | 1.628 | 2.117 | 0.336 | 1.117 | 0.78 | 0.181 |
| PP2A-B' | 43.88 | 1.736 | 0.810 | 6.160 | 8.799 | 6.710 | 3.549 | 0.365 | 0.375 |
| TfIIFalpha | 43.83 | 1.626 | 0.646 | 7.941 | 11.096 | 1.773 | 4.884 | 0.189 | 0.003 |
| Mcm2 | 43.79 | 1.708 | 0.855 | 1.009 | 1.320 | 0.452 | 0.591 | 0.317 | 0.609 |
| S6k | 43.75 | 1.901 | 1.135 | 4.923 | 6.784 | 3.205 | 2.589 | 0.271 | 0.257 |
| deltaCOP | 43.40 | 1.375 | 0.344 | 1.551 | 1.940 | 0.624 | 1.128 | 0.745 | 0.268 |
| fit | 43.26 | 1.560 | 0.488 | 1.063 | 1.403 | 0.456 | 0.682 | 0.358 | 0.743 |
| **eIF-4E** | **43.19** | **1.400** | **0.352** | **2.207** | **2.798** | **0.117** | **1.577** | **0.264** | **0.014** |
| sofe | 43.19 | 1.616 | 0.594 | 3.318 | 3.859 | 0.401 | 2.053 | 0.062 | 0.02 |
| Prosalpha5 | 43.10 | 0.961 | 0.192 | 0.536 | 0.569 | 0.109 | 0.558 | 0.027 | 0.085 |
| Smn | 43.01 | 1.341 | 0.326 | 1.734 | 2.184 | 0.302 | 1.293 | 0.477 | 0.062 |
| Rbp2 | 42.95 | 1.771 | 0.713 | 3.830 | 5.189 | 1.929 | 2.163 | 0.274 | 0.219 |
| Caf1 | 42.90 | 1.512 | 0.515 | 2.519 | 3.255 | 0.677 | 1.666 | 0.297 | 0.045 |
| SA | 42.71 | 1.708 | 0.749 | 3.807 | 5.195 | 1.321 | 2.229 | 0.247 | 0.03 |
| Eno | 42.66 | 1.333 | 0.327 | 0.956 | 1.240 | 0.032 | 0.717 | 0.331 | 0.728 |
| simj | 42.64 | 1.595 | 0.566 | 6.733 | 9.196 | 1.150 | 4.222 | 0.175 | 0.002 |
| CG11120 | 42.57 | 1.560 | 0.803 | 2.472 | 3.039 | 0.463 | 1.584 | 0.294 | 0.106 |
| for | 42.55 | 1.802 | 0.887 | 4.273 | 5.870 | 0.766 | 2.371 | 0.221 | 0.013 |
| l(2)37Cc | 42.51 | 1.661 | 0.769 | 8.213 | 10.823 | 2.442 | 4.945 | 0.081 | 0.101 |
| CG12082 | 42.47 | 1.975 | 1.123 | 1.049 | 1.366 | 0.320 | 0.531 | 0.276 | 0.528 |
| synj | 42.07 | 1.528 | 0.638 | 3.191 | 4.274 | 0.260 | 2.089 | 0.221 | 0.012 |

| | | | | | | | | | |
|---|---|---|---|---|---|---|---|---|---|
| CG6455 | 42.05 | 1.438 | 0.452 | 3.839 | 4.995 | 1.059 | 2.670 | 0.13 | 0.012 |
| CG5174 | 41.81 | 1.140 | 0.198 | 4.769 | 6.636 | 1.774 | 4.183 | 0.145 | 0.14 |
| Srp72 | 41.76 | 1.588 | 0.515 | 0.674 | 0.594 | 0.812 | 0.425 | 0.175 | 0.364 |
| mRpS35 | 41.70 | 1.663 | 0.782 | 1.461 | 1.944 | 0.262 | 0.878 | 0.777 | 0.671 |
| epsilonCOP | 41.53 | 1.534 | 0.581 | 2.201 | 2.692 | 0.712 | 1.435 | 0.371 | 0.137 |
| RPA2 | 41.49 | 1.479 | 0.608 | 0.613 | 0.750 | 0.098 | 0.414 | 0.084 | 0.208 |
| tst | 41.47 | 1.710 | 0.783 | 1.527 | 1.818 | 0.225 | 0.893 | 0.753 | 0.869 |
| Ank | 41.27 | 1.767 | 0.822 | 4.177 | 5.632 | 2.028 | 2.363 | 0.239 | 0.052 |
| CG30185 | 41.25 | 1.555 | 0.600 | 1.365 | 1.232 | 0.262 | 0.878 | 0.649 | 0.539 |
| eIF4AIII | 41.24 | 1.469 | 0.490 | 1.928 | 2.516 | 0.558 | 1.313 | 0.866 | 0.52 |
| Bre1 | 41.24 | 1.842 | 0.840 | 1.346 | 1.753 | 0.433 | 0.731 | 0.493 | 0.902 |
| **Cap-D2** | **41.24** | **1.563** | **0.500** | **2.360** | **3.187** | **1.617** | **1.511** | **0.507** | **0.179** |
| Fib | 41.24 | 1.418 | 0.389 | 1.471 | 1.846 | 0.439 | 1.038 | 0.886 | 0.332 |
| piwi | 41.15 | 1.488 | 0.455 | 2.779 | 3.554 | 0.307 | 1.868 | 0.194 | 0.012 |
| CG7920 | 41.13 | 1.570 | 0.626 | 2.328 | 3.006 | 1.670 | 1.483 | 0.502 | 0.245 |
| CG8777 | 41.06 | 1.695 | 0.806 | 1.471 | 1.736 | 0.177 | 0.868 | 0.699 | 0.95 |
| Marcal1 | 40.78 | 1.745 | 0.830 | 2.805 | 3.476 | 0.701 | 1.608 | 0.293 | 0.093 |
| swm | 40.76 | 1.482 | 0.426 | 1.834 | 2.388 | 0.245 | 1.237 | 0.597 | 0.077 |
| **gammaTub23C** | **40.65** | **1.608** | **0.675** | **3.930** | **5.140** | **1.737** | **2.444** | **0.186** | **0.043** |
| RpS24 | 40.58 | 1.330 | 0.289 | 0.621 | **0.652** | 0.132 | 0.467 | 0.016 | 0.058 |
| **Cdc23** | **40.25** | **1.921** | **0.974** | **3.940** | **5.210** | **0.543** | **2.051** | **0.225** | **0.024** |
| CG14309 | 40.25 | 1.458 | 0.451 | 2.923 | 3.725 | 0.763 | 2.004 | 0.004 | 0.011 |
| eIF-3p40 | 40.18 | 1.604 | 0.561 | 1.463 | 1.672 | 0.313 | 0.912 | 0.746 | 0.89 |
| CG18190 | 40.14 | 1.787 | 0.912 | 4.429 | 6.041 | 2.412 | 2.478 | 0.249 | 0.219 |
| mRpS30 | 40.09 | 1.117 | 0.118 | 0.878 | 1.036 | 0.135 | 0.786 | 0.257 | 0.528 |
| CG3532 | 40.08 | 1.319 | 0.466 | 3.340 | 4.375 | 0.831 | 2.532 | 0.146 | 0.012 |
| MED1 | 40.05 | 1.549 | 0.562 | 3.075 | 4.026 | 0.747 | 1.985 | 0.22 | 0.023 |
| Int6 | 39.89 | 1.663 | 0.610 | 1.952 | 2.403 | 0.680 | 1.174 | 0.672 | 0.291 |
| bif | 39.87 | 1.731 | 0.839 | 5.090 | 7.040 | 1.949 | 2.941 | 0.195 | 0.022 |
| Nlp | 39.64 | 1.349 | 0.560 | 2.768 | 3.897 | 0.739 | 2.051 | 0.307 | 0.021 |
| Acon | 39.61 | 1.603 | 0.700 | 2.908 | 4.047 | 2.052 | 1.814 | 0.431 | 0.136 |
| CG10077 | 39.58 | 1.568 | 0.534 | 2.959 | 3.871 | 0.803 | 1.887 | 0.243 | 0.029 |
| Fer2LCH | 39.53 | 1.094 | 0.115 | 0.660 | 0.615 | 0.034 | 0.604 | 0.006 | 0.012 |
| Tsc1 | 39.47 | 1.783 | 0.834 | 2.847 | 3.780 | 0.965 | 1.597 | 0.396 | 0.089 |
| Dbp21E2 | 39.44 | 1.410 | 0.415 | 1.967 | 2.518 | 0.788 | 1.395 | 0.46 | 0.122 |
| EfTuM ( | 39.38 | 1.479 | 0.470 | 0.923 | 1.224 | 0.117 | 0.624 | 0.182 | 0.397 |
| Lis-1 | 39.27 | 1.436 | 0.407 | 2.903 | 4.086 | 0.790 | 2.022 | 0.305 | 0.015 |
| Snx6 | 39.10 | 1.598 | 0.695 | 3.484 | 4.736 | 2.618 | 2.180 | 0.328 | 0.123 |
| Trip1 | 39.08 | 1.691 | 0.643 | 1.142 | 1.243 | 0.160 | 0.676 | 0.233 | 0.425 |
| CG41099 | 39.07 | 1.526 | 0.582 | 3.318 | 4.592 | 1.626 | 2.173 | 0.292 | 0.05 |
| CG12512 | 38.87 | 1.808 | 0.927 | 3.039 | 4.188 | 2.032 | 1.681 | 0.462 | 0.159 |

| | | | | | | | | | |
|---|---|---|---|---|---|---|---|---|---|
| **Grip163** | **38.72** | **1.417** | **0.459** | **3.410** | **4.199** | **0.431** | **2.406** | **0.079** | **0.007** |
| CycT | 38.68 | 1.519 | 0.507 | 3.978 | 5.023 | 1.144 | 2.619 | 0.106 | 0.016 |
| Cnx99A | 38.52 | 1.844 | 0.930 | 8.276 | 11.082 | 1.537 | 4.488 | 0.093 | 0.003 |
| ball | 38.52 | 1.059 | 0.302 | 0.477 | 0.561 | 0.101 | 0.450 | 0.042 | 0.12 |
| CSN7 | 38.37 | 1.629 | 0.667 | 1.247 | 1.646 | 0.884 | 0.765 | 0.594 | 0.982 |
| Cdc6 | 38.32 | 1.566 | 0.552 | 2.771 | 3.743 | 0.148 | 1.770 | 0.296 | 0.014 |
| His2Av | 38.14 | 1.337 | 0.310 | 0.881 | 1.099 | 0.200 | 0.659 | 0.192 | 0.413 |
| wibg | 38.11 | 1.232 | 0.208 | 1.250 | 1.226 | 0.065 | 1.015 | 0.89 | 0.036 |
| mRpL1 | 38.08 | 1.060 | 0.100 | 0.517 | 0.568 | 0.071 | 0.487 | 0.003 | 0.01 |
| Bap60 | 38.00 | 1.650 | 0.658 | 2.586 | 3.443 | 1.685 | 1.567 | 0.466 | 0.175 |
| eIF6 | 37.97 | 0.861 | 0.403 | 0.212 | 0.241 | 0.038 | 0.246 | 0.051 | 0.132 |
| CG13096 | 37.87 | 1.281 | 0.243 | 1.698 | 2.080 | 0.585 | 1.326 | 0.427 | 0.111 |
| scra | 37.76 | 1.663 | 0.736 | 2.430 | 3.267 | 0.275 | 1.461 | 0.462 | 0.066 |
| Npl4 | 37.71 | 1.540 | 0.595 | 1.248 | 1.562 | 0.122 | 0.810 | 0.567 | 0.624 |
| RpS29 | 37.69 | 1.313 | 0.304 | 1.017 | 1.085 | 0.017 | 0.775 | 0.192 | 0.39 |
| mRpL30 | 37.63 | 1.036 | 0.085 | 0.458 | 0.473 | 0.015 | 0.443 | 0 | 0.003 |
| CG10777 | 37.48 | 1.663 | 0.624 | 4.216 | 5.560 | 0.240 | 2.535 | 0.141 | 0.004 |
| eIF2B-gamma | 37.47 | 1.685 | 0.729 | 2.654 | 3.666 | 2.092 | 1.575 | 0.524 | 0.397 |
| CG6512 | 37.44 | 1.364 | 0.370 | 5.358 | 6.884 | 0.621 | 3.927 | 0.603 | 0.001 |
| Arpc2 | 37.40 | 1.535 | 0.593 | 1.899 | 2.454 | 0.885 | 1.237 | 0.65 | 0.248 |
| **spas** | **37.34** | **1.492** | **0.506** | **2.715** | **3.279** | **0.382** | **1.819** | **0.135** | **0.025** |
| Uch-L5 | 37.32 | 1.467 | 0.411 | 0.844 | 0.964 | 0.225 | 0.575 | 0.091 | 0.223 |
| CG42388 | 37.11 | 1.606 | 0.606 | 3.885 | 5.197 | 1.212 | 2.419 | 0.19 | 0.019 |
| **mit(1)15** | **36.92** | **1.727** | **0.739** | **2.272** | **2.621** | **0.942** | **1.316** | **0.463** | **0.314** |
| CG4752 | 36.92 | 2.076 | 1.458 | 2.821 | 3.915 | 2.230 | 1.359 | 0.617 | 0.283 |
| mahj | 36.78 | 1.670 | 0.684 | 2.058 | 2.747 | 0.983 | 1.232 | 0.686 | 0.235 |
| mRpL39 | 36.60 | 1.200 | 0.175 | 0.842 | 1.013 | 0.148 | 0.702 | 0.16 | 0.308 |
| E(bx) | 36.45 | 1.473 | 0.436 | 2.531 | 3.223 | 0.305 | 1.718 | 0.229 | 0.017 |
| Sec16 | 36.15 | 1.632 | 0.620 | 3.457 | 4.457 | 1.102 | 2.119 | 0.189 | 0.032 |
| l(2)gl | 35.90 | 1.771 | 1.080 | 3.662 | 5.109 | 1.472 | 2.068 | 0.325 | 0.058 |
| Dbp80 | 35.88 | 1.729 | 0.868 | 3.987 | 5.398 | 3.832 | 2.306 | 0.356 | 0.182 |
| kdn | 35.86 | 1.099 | 0.127 | 1.432 | 1.490 | 0.138 | 1.303 | 0.038 | 0.046 |
| Trx-2 | 35.84 | 1.462 | 0.418 | 0.872 | 1.142 | 0.192 | 0.596 | 0.186 | 0.4 |
| nonA | 35.83 | 1.356 | 0.310 | 1.850 | 2.177 | 0.020 | 1.364 | 0.255 | 0.038 |
| GlyP | 35.77 | 1.526 | 0.531 | 0.865 | 1.108 | 0.319 | 0.567 | 0.184 | 0.403 |
| CG7208 | 35.77 | 1.862 | 0.999 | 6.196 | 8.540 | 3.022 | 3.328 | 0.185 | 0.032 |
| **PpD3** | **35.73** | **1.905** | **1.076** | **0.712** | **0.954** | **0.375** | **0.374** | **0.156** | **0.333** |
| HmgD | 35.37 | 1.223 | 0.218 | 1.933 | 2.565 | 0.109 | 1.581 | 0.333 | 0.004 |
| CG1635 | 35.36 | 1.899 | 1.210 | 8.068 | 11.329 | 4.858 | 4.249 | 0.187 | 0.04 |

| | | | | | | | | | |
|---|---|---|---|---|---|---|---|---|---|
| ms(3)72Dt | 35.19 | 1.535 | 0.682 | 2.045 | 2.492 | 0.875 | 1.332 | 0.503 | 0.257 |
| Etf-QO | 35.19 | 1.629 | 0.654 | 3.733 | 5.060 | 1.043 | 2.292 | 0.219 | 0.019 |
| cpa | 35.18 | 1.218 | 0.224 | 1.533 | 2.092 | 0.055 | 1.258 | 0.613 | 0.014 |
| **skpA** | **35.02** | **1.817** | **0.799** | **2.714** | **3.586** | **1.462** | **1.494** | **0.48** | **0.167** |
| Cdc37 | 34.87 | 1.641 | 0.680 | 0.703 | 0.895 | 0.147 | 0.428 | 0.101 | 0.242 |
| stwl | 34.69 | 1.343 | 0.315 | 1.373 | 1.518 | 0.240 | 1.022 | 0.911 | 0.556 |
| CoVb | 34.37 | 1.606 | 0.778 | 3.722 | 4.829 | 0.746 | 2.318 | 0.161 | 0.019 |
| Tap42 | 34.24 | 1.411 | 0.431 | 0.815 | 1.063 | 0.354 | 0.577 | 0.192 | 0.418 |
| CG31368 | 34.19 | 1.618 | 0.647 | 2.231 | 2.957 | 0.930 | 1.379 | 0.533 | 0.147 |
| CG9752 | 34.09 | 2.134 | 1.372 | 6.745 | 9.804 | 9.400 | 3.161 | 0.447 | 0.453 |
| Ars2 | 33.98 | 1.783 | 0.769 | 1.413 | 1.818 | 0.587 | 0.793 | 0.598 | 0.96 |
| sds22 | 33.68 | 1.479 | 0.558 | 1.789 | 2.411 | 1.099 | 1.210 | 0.728 | 0.282 |
| tsr | 33.56 | 1.453 | 0.539 | 1.036 | 1.342 | 0.210 | 0.713 | 0.402 | 0.807 |
| eIF2B-epsilon | 33.55 | 1.640 | 0.674 | 2.544 | 3.472 | 1.832 | 1.552 | 0.511 | 0.191 |
| btz | 33.55 | 1.341 | 0.426 | 2.619 | 3.546 | 1.184 | 1.953 | 0.3 | 0.051 |
| nudC | 33.51 | 1.733 | 0.788 | 0.868 | 1.105 | 0.359 | 0.500 | 0.18 | 0.384 |
| CG6498 | 33.49 | 1.675 | 0.636 | 1.848 | 2.373 | 0.324 | 1.104 | 0.803 | 0.26 |
| eIF2B-alpha | 33.42 | 1.477 | 0.462 | 2.987 | 4.061 | 3.083 | 2.022 | 0.419 | 0.218 |
| **Patronin** | **33.28** | **1.398** | **0.352** | **2.874** | **3.216** | **0.164** | **2.055** | **0.022** | **0.007** |
| CG1427 | 33.15 | 1.158 | 0.410 | 0.720 | 0.823 | 0.192 | 0.622 | 0.18 | 0.375 |
| SF2 | 33.06 | 1.241 | 0.210 | 0.837 | 0.988 | 0.013 | 0.674 | 0.106 | 0.205 |
| RhoGAP68F | 33.06 | 1.619 | 0.723 | 5.860 | 8.110 | 3.345 | 3.619 | 0.187 | 0.214 |
| CG3679 | 33.05 | 1.423 | 0.398 | 1.398 | 1.835 | 0.053 | 0.982 | 0.962 | 0.26 |
| **slmb** | **32.82** | **1.738** | **0.745** | **2.004** | **2.476** | **0.658** | **1.153** | **0.72** | **0.342** |
| Rad23 | 32.69 | 1.279 | 0.243 | 1.853 | 2.151 | 0.145 | 1.448 | 0.163 | 0.021 |
| Vha26 | 32.60 | 1.439 | 0.458 | 2.191 | 2.906 | 0.401 | 1.522 | 0.39 | 0.035 |
| CG1354 | 32.58 | 1.594 | 0.621 | 2.210 | 3.026 | 0.767 | 1.386 | 0.55 | 0.102 |
| lok | 32.55 | 1.711 | 0.787 | 3.677 | 4.861 | 1.806 | 2.149 | 0.251 | 0.067 |
| ssh | 32.33 | 1.812 | 0.916 | 8.434 | 11.669 | 3.207 | 4.653 | 0.135 | 0.012 |
| Nup75 | 32.32 | 1.827 | 0.812 | 1.544 | 1.934 | 0.696 | 0.845 | 0.695 | 0.89 |
| Mys45A | 32.17 | 1.722 | 0.780 | 1.684 | 2.232 | 0.726 | 0.978 | 0.964 | 0.516 |
| caz | 32.08 | 1.457 | 0.402 | 2.985 | 3.752 | 0.488 | 2.049 | 0.138 | 0.01 |
| Sym | 31.98 | 1.676 | 0.683 | 3.494 | 4.624 | 2.816 | 2.084 | 0.335 | 0.157 |
| RpI135 | 31.75 | 1.510 | 0.516 | 1.968 | 2.634 | 0.942 | 1.303 | 0.609 | 0.172 |
| CG4538 | 31.54 | 1.489 | 0.500 | 3.368 | 4.497 | 1.473 | 2.262 | 0.225 | 0.04 |
| RFeSP | 31.42 | 1.517 | 0.548 | 7.340 | 9.898 | 2.548 | 4.838 | 0.104 | 0.126 |
| PGRP-SB1 | 31.34 | 1.250 | 0.216 | 2.317 | 2.919 | 0.774 | 1.854 | 0.198 | 0.187 |
| vap | 31.12 | 1.738 | 0.786 | 3.111 | 4.154 | 3.322 | 1.790 | 0.481 | 0.487 |
| CG4611 | 31.06 | 1.236 | 0.204 | 1.280 | 1.705 | 0.368 | 1.036 | 0.929 | 0.153 |
| glo | 30.92 | 1.875 | 1.063 | 6.990 | 8.660 | 7.742 | 3.729 | 0.287 | 0.43 |
| SNF4Agamma | 30.90 | 1.707 | 0.701 | 3.358 | 4.581 | 0.170 | 1.967 | 0.27 | 0.012 |
| CG13993 | 30.89 | 1.433 | 0.477 | 0.949 | 1.203 | 0.177 | 0.662 | 0.273 | 0.576 |

| | | | | | | | | | |
|---|---|---|---|---|---|---|---|---|---|
| Srp54 | 30.88 | 1.406 | 0.365 | 1.359 | 1.733 | 0.545 | 0.967 | 0.929 | 0.468 |
| CG1737 | 30.76 | 1.521 | 0.493 | 2.409 | 2.959 | 0.339 | 1.584 | 0.234 | 0.039 |
| CG9062 | 30.75 | 1.561 | 0.666 | 3.091 | 3.946 | 0.357 | 1.980 | 0.182 | 0.021 |
| CG14100 | 30.66 | 1.368 | 0.328 | 2.535 | 3.335 | 1.148 | 1.853 | 0.285 | 0.235 |
| Cep97 | 30.59 | 1.958 | 1.135 | 4.493 | 6.227 | 4.071 | 2.294 | 0.366 | 0.161 |
| GstO2 | 30.49 | 1.881 | 1.195 | 1.706 | 2.392 | 1.406 | 0.907 | 0.885 | 0.689 |
| lola | 30.43 | 1.528 | 0.513 | 2.261 | 2.831 | 0.210 | 1.480 | 0.321 | 0.047 |
| muskelin | 30.41 | 1.608 | 0.621 | 1.708 | 2.088 | 0.250 | 1.062 | 0.86 | 0.392 |
| mRpL37 | 30.37 | 1.168 | 0.189 | 0.552 | 0.615 | 0.133 | 0.473 | 0.011 | 0.039 |
| CG13887 | 30.27 | 1.636 | 0.623 | 6.525 | 8.772 | 1.432 | 3.988 | 0.106 | 0.004 |
| mRpL3 | 30.26 | 1.146 | 0.129 | 0.721 | 0.835 | 0.179 | 0.629 | 0.051 | 0.103 |
| Prp3 | 30.13 | 1.283 | 0.255 | 0.660 | 0.714 | 0.031 | 0.514 | 0.017 | 0.058 |
| CG8232 | 30.08 | 1.897 | 1.017 | 3.459 | 4.807 | 2.715 | 1.824 | 0.444 | 0.356 |
| Sec13 | 30.02 | 1.389 | 0.385 | 1.144 | 1.437 | 0.422 | 0.824 | 0.579 | 0.903 |
| CG3731 | 30.01 | 1.488 | 0.511 | 3.307 | 4.344 | 0.637 | 2.222 | 0.176 | 0.011 |

## Supplementary Table 2

## Mitotic data

| Name/GO | #Peptides | Score | Mean (cycling) | Mean(mitotic) | MFI |
|---|---|---|---|---|---|
| msps (mini spindles) | 79 | 1475.34 | 1.512 | 2.971 | 1.965 |
| dhc64C (Dynein heavy chain 64C) | 111 | 1137.62 | 1.549 | 3.883 | 2.506 |
| map205 -1 (Microtubule associated protein 205) | 38 | 836.79 | 1.543 | 0.787 | 0.509 |
| map205- 2 (Microtubule associated protein 205) | 36 | 802.20 | 1.314 | 1.202 | 0.915 |
| hsp83 (Heat shock protein 83) | 33 | 728.99 | 1.684 | 1.294 | 0.768 |
| klp61F (Kinesin-like protein at 61F) | 43 | 705.65 | 1.841 | 1.204 | 0.654 |
| klp3A (Kinesin-like protein at 3A) | 53 | 690.24 | 1.619 | 3.629 | 2.241 |
| tacc (transforming acid coiled coil protein) | 40 | 539.00 | 1.648 | 2.627 | 1.594 |
| ef2 (Elongation factor 2) | 26 | 519.13 | 1.327 | 0.898 | 0.677 |
| cctgamma | 21 | 351.13 | 1.622 | 1.653 | 1.019 |
| glu (Gluon) | 31 | 327.12 | 1.599 | 3.561 | 2.226 |
| klp10A (Kinesin-like protein at 10A) | 18 | 320.10 | 1.512 | 5.603 | 3.704 |
| eIF3-S10 | 35 | 318.49 | 1.473 | 1.180 | 0.801 |
| eIF4G (Eukaryotic translation initiation factor) | 33 | 307.77 | 1.578 | 3.486 | 2.209 |
| tcp-1zeta | 20 | 297.73 | 1.543 | 1.747 | 1.131 |
| CG8258 | 20 | 275.76 | 1.528 | 1.670 | 1.092 |
| CG7033 | 21 | 267.00 | 1.510 | 1.168 | 0.773 |
| klp67A (Kinesin-like protein at 67A) | 21 | 266.94 | 1.809 | 5.183 | 2.865 |
| t-cp1 (Tcp1 like) | 20 | 260.02 | 1.586 | 0.967 | 0.609 |
| polo | 17 | 252.99 | 1.442 | 1.849 | 1.282 |
| skap (skpA associated protein) | 13 | 227.77 | 1.718 | 3.602 | 2.096 |
| CG5525 | 16 | 204.32 | 1.564 | 1.249 | 0.798 |
| sta (Stubarista) | 10 | 199.93 | 1.081 | 0.670 | 0.619 |
| mars | 20 | 199.80 | 1.431 | 3.033 | 2.119 |
| asp (Abnormal spindle) | 18 | 197.98 | 1.538 | 4.558 | 2.963 |
| tcp-1eta | 17 | 191.07 | 1.363 | 1.298 | 0.952 |
| cam (Calmodulin) | 5 | 187.29 | 1.163 | 3.892 | 3.345 |
| bel (Belle) | 23 | 182.66 | 1.641 | 3.592 | 2.188 |
| me31B (Maternal expression at 31B) | 13 | 178.58 | 1.414 | 3.242 | 2.292 |
| gl (Glued) | 17 | 177.62 | 1.520 | 2.086 | 1.372 |
| feo (Fascetto) | 17 | 177.24 | 1.497 | 3.142 | 2.098 |
| smc2 | 23 | 174.73 | 1.607 | 3.833 | 2.385 |
| cmet (CENP-meta) | 16 | 173.29 | 1.687 | 2.687 | 1.592 |
| dgt5 (dim gamma tubulin 5 - augmin subunit) | 17 | 170.42 | 1.595 | 6.889 | 4.320 |
| sub (Subito) | 18 | 156.25 | 1.892 | 4.871 | 2.574 |
| fs(2)ket (Female sterile (2) ketile) | 12 | 151.36 | 1.570 | 2.397 | 1.526 |
| mtor (Megator) | 14 | 150.62 | 1.815 | 2.387 | 1.315 |
| larp (La related protein) | 22 | 149.02 | 1.250 | 2.299 | 1.839 |
| rpt2 (Regulatory particle triple A-ATPase 2) | 13 | 146.68 | 1.309 | 1.317 | 1.006 |
| dpa (Disc proliferation abnormal) | 17 | 144.77 | 1.741 | 0.929 | 0.533 |

| | | | | | |
|---|---|---|---|---|---|
| lam (Lamin) | 21 | 144.75 | 1.496 | 1.735 | 1.159 |
| fmr1 | 15 | 135.09 | 1.349 | 1.900 | 1.408 |
| rept (Reptin) | 16 | 134.45 | 1.500 | 1.503 | 1.002 |
| pp2A-29B (Protein phosphatase 2A at 29B) | 14 | 130.20 | 1.531 | 1.018 | 0.664 |
| nat1 | 17 | 128.45 | 1.483 | 2.555 | 1.723 |
| dlic (Dynein light intermediate chain) | 14 | 128.18 | 1.449 | 3.334 | 2.300 |
| rok (Rho kinase) | 10 | 125.43 | 1.417 | 2.655 | 1.873 |
| mei-38 (Meiotic 38) | 11 | 124.93 | 1.335 | 5.851 | 4.382 |
| rfc4 (replication factor C subunit 4) | 13 | 120.28 | 1.597 | 2.918 | 1.826 |
| chb (Chromosome bows) | 13 | 119.92 | 1.585 | 1.479 | 0.932 |
| rod (Rough deal) | 12 | 115.50 | 1.704 | 2.190 | 1.285 |
| eIF-2alpha (Eukaryotic translation initiation factor 2 alpha) | 13 | 115.16 | 1.399 | 1.657 | 1.184 |
| dgt6 (Dim gamma tubulin 6 - augmin) | 15 | 110.34 | 1.604 | 7.977 | 4.974 |
| prosalpha3 (proteasome alpha 3 subunit) | 8 | 107.67 | 0.989 | 0.777 | 0.785 |
| cnn (Centrosomin) | 7 | 106.34 | 1.825 | 2.625 | 1.438 |
| su(var)2-HP2 | 3 | 105.87 | 1.388 | 5.334 | 3.843 |
| toc (Toucan) | 6 | 105.72 | 1.387 | 3.878 | 2.796 |
| DNApol-epsilon (DNA polymerase epsilon) | 10 | 105.66 | 1.778 | 3.120 | 1.754 |
| chro (Chromator) | 16 | 105.42 | 1.544 | 4.900 | 3.173 |
| ncd (non-claret disjunctional) | 12 | 101.98 | 1.689 | 1.477 | 0.874 |
| sti (Sticky) | 7 | 101.91 | 1.789 | 3.878 | 2.167 |
| dmn (Dynamitin) | 14 | 101.20 | 1.189 | 1.661 | 1.396 |
| cana ( CENP-ana) | 3 | 99.38 | 1.707 | 2.970 | 1.739 |
| 14-3-3epsilon | 11 | 97.06 | 1.498 | 1.004 | 0.670 |
| pnut (peanut) | 11 | 95.34 | 1.612 | 7.906 | 4.903 |
| arp1 (Actin-related protein 1) | 8 | 94.27 | 1.487 | 2.252 | 1.514 |
| rpA-70 (Replication Protein A 70) | 13 | 93.22 | 1.673 | 0.908 | 0.542 |
| tws (Twins) | 10 | 92.79 | 1.666 | 1.863 | 1.118 |
| cdc2 (cdk1) | 10 | 88.69 | 1.727 | 1.914 | 1.108 |
| eb1 | 11 | 88.17 | 1.534 | 2.849 | 1.857 |
| mcm3 (Minichromosomal maintenance 3) | 13 | 82.33 | 1.701 | 0.662 | 0.389 |
| rpn12 (Regulatory particle non-ATPase 12) | 6 | 78.99 | 1.242 | 0.859 | 0.691 |
| cdc27 (Cell division cycle 27 ortholog) | 6 | 78.83 | 1.715 | 3.228 | 1.882 |
| CG10932 | 9 | 77.50 | 1.779 | 1.199 | 0.673 |
| rpn13 | 9 | 77.03 | 1.313 | 0.563 | 0.428 |
| pds5 | 9 | 76.84 | 1.560 | 2.224 | 1.425 |
| gammaTub37C (γ-Tubulin at 37C) | 8 | 75.28 | 1.535 | 3.933 | 2.562 |
| nat1 | 9 | 75.28 | 1.430 | 1.430 | 0.999 |
| l(1)dd4 (lethal (1) discs degenerate 4) | 4 | 72.95 | 1.635 | 3.970 | 2.428 |
| dgt2 (dim γ-tubulin 2 - augmin) | 7 | 71.82 | 1.582 | 6.967 | 4.405 |
| rfc38 (Replication factor C 38kD subunit) | 7 | 69.65 | 1.564 | 2.727 | 1.744 |
| l(3)72Ab (lethal (3) 72Ab) | 7 | 69.57 | 1.454 | 1.135 | 0.780 |
| grip75 | 5 | 69.00 | 1.585 | 3.236 | 2.041 |
| wac (wee Augmin) | 5 | 66.99 | 1.641 | 8.027 | 4.892 |

| | | | | | |
|---|---|---|---|---|---|
| prosbeta5 (Proteasome β5 subunit) | 7 | 65.61 | 1.021 | 0.543 | 0.531 |
| 14-3-3zeta | 7 | 65.18 | 1.258 | 0.728 | 0.578 |
| coro | 7 | 64.09 | 1.525 | 1.113 | 0.729 |
| lat (latheo) | 5 | 62.42 | 1.731 | 2.298 | 1.327 |
| cycB (Cyclin B) | 7 | 62.30 | 1.250 | 1.230 | 0.984 |
| prosbeta7 (Proteasome β7 subunit) | 3 | 61.72 | 0.928 | 0.603 | 0.649 |
| nipped-B | 5 | 60.97 | 1.546 | 2.614 | 1.691 |
| cdc2c | 8 | 60.21 | 1.851 | 3.928 | 2.122 |
| aub (aubergine) | 12 | 59.94 | 1.477 | 3.125 | 2.116 |
| grip84 (gamma-tubulin ring protein 84) | 7 | 58.13 | 1.495 | 3.636 | 2.431 |
| CG8636 | 5 | 57.65 | 1.451 | 1.278 | 0.881 |
| pav (Pavarotti) | 6 | 57.64 | 1.779 | 2.877 | 1.616 |
| cdc16 (Cell division cycle 16 ortholog) | 8 | 56.80 | 1.847 | 3.244 | 1.756 |
| aur (aurora) | 9 | 54.65 | 1.442 | 3.448 | 2.390 |
| bubR1 (Bub1-related kinase) | 7 | 54.35 | 1.643 | 3.100 | 1.887 |
| rpn8 (Regulatory particle non-ATPase 8) | 3 | 52.99 | 1.133 | 0.740 | 0.652 |
| CG12018 | 8 | 52.76 | 1.630 | 6.060 | 3.718 |
| mad1 | 3 | 51.57 | 1.826 | 5.130 | 2.809 |
| mts (microtubule star) | 3 | 51.14 | 1.490 | 0.643 | 0.431 |
| dgt4 (dim γ-tubulin 4 - augmin) | 4 | 50.07 | 1.592 | 10.332 | 6.492 |
| rpn10 (Regulatory particle non-ATPase 10) | 5 | 49.80 | 1.264 | 0.979 | 0.774 |
| dgt3 (dim γ-tubulin 3 - augmin) | 6 | 49.41 | 1.674 | 8.105 | 4.840 |
| eIF-2beta (Eukaryotic initiation factor 2β) | 7 | 48.88 | 1.596 | 2.314 | 1.449 |
| nuf2 | 5 | 47.44 | 1.500 | 2.887 | 1.924 |
| mus101 (mutagen-sensitive 101) | 5 | 46.29 | 1.814 | 4.213 | 2.322 |
| tum (tumbleweed) | 5 | 44.80 | 1.787 | 3.126 | 1.749 |
| spn-E (spindle E) | 6 | 44.43 | 1.651 | 5.801 | 3.513 |
| eIF-4E (Eukaryotic initiation factor 4E) | 4 | 43.19 | 1.400 | 2.207 | 1.577 |
| cap-D2 (CAP-D2 condensin subunit) | 5 | 41.24 | 1.563 | 2.360 | 1.510 |
| gammaTub23C (γ-Tubulin at 23C) | 4 | 40.65 | 1.608 | 3.930 | 2.443 |
| cdc23 (Cell division cycle 23 ortholog) | 8 | 40.25 | 1.921 | 3.940 | 2.051 |
| grip163 | 6 | 38.72 | 1.417 | 3.410 | 2.405 |
| spas (spastin) | 3 | 37.34 | 1.492 | 2.715 | 1.819 |
| mit(1)15 (mitotic 15) | 5 | 36.92 | 1.727 | 2.272 | 1.315 |
| ppD3 (Protein phosphatase D3) | 5 | 35.73 | 1.905 | 0.712 | 0.373 |
| skpA | 6 | 35.02 | 1.817 | 2.714 | 1.493 |
| Patronin | 6 | 33.28 | 1.398 | 2.874 | 2.055 |
| slmb (supernumerary limbs) | 5 | 32.82 | 1.738 | 2.004 | 1.153 |

Supplementary table 2 – all mitotic proteins in the data set. Those highlighted are significantly increased in mitosis.

## Supplementary Table 3

## Ribosomal data

| Name | Peptides | Score | Mean cycling | Mean mitotic | MFI |
|---|---|---|---|---|---|
| RpL4 (Ribosomal protein L4) | 21 | 508.83 | 1.107 | 0.636 | 0.575 |
| RpL22 (Ribosomal protein L22) | 17 | 452.71 | 1.138 | 0.976 | 0.858 |
| RpL23A (Ribosomal protein L23A) | 16 | 409.98 | 1.014 | 0.567 | 0.559 |
| RpL5 (Ribosomal protein L5) | 16 | 367.41 | 1.057 | 0.567 | 0.536 |
| RpS3 (Ribosomal protein S3) | 16 | 336.12 | 1.396 | 1.016 | 0.728 |
| RpL26 (Ribosomal proteinL26) | 6 | 213.57 | 1.091 | 0.633 | 0.580 |
| RpS27A (Ribosomal protein S27A) | 10 | 314.88 | 1.294 | 1.466 | 1.133 |
| RpL7A (Ribosomal protein L7a) | 13 | 293.79 | 1.039 | 0.563 | 0.542 |
| RpS6 (Ribosomal protein S6) | 12 | 283.17 | 1.195 | 0.714 | 0.598 |
| RpL3 (Ribosomal protein L3) | 15 | 282.50 | 1.138 | 0.564 | 0.495 |
| RpL7 (Ribosomal protein L7) | 12 | 275.40 | 1.089 | 0.595 | 0.547 |
| RpS19a (Ribosomal protein S19a) | 11 | 256.72 | 1.140 | 0.756 | 0.664 |
| RpS4 (Ribosomal protein S4) | 12 | 255.52 | 1.172 | 0.609 | 0.519 |
| RpS3A (Ribosomal protein S3A) | 14 | 252.82 | 1.272 | 0.881 | 0.693 |
| RpL14 (Ribosomal protein L14) | 10 | 249.18 | 1.085 | 0.597 | 0.550 |
| RpS2 (Ribosomal protein S2) | 12 | 247.60 | 1.151 | 0.669 | 0.581 |
| RpL28 (Ribosomal protein L28) | 11 | 236.50 | 1.070 | 0.518 | 0.484 |
| RpL13A (Ribosomal protein 13A) | 9 | 235.09 | 1.156 | 0.578 | 0.500 |
| RpS9 (Ribosomal protein S9) | 14 | 229.96 | 1.239 | 0.710 | 0.573 |
| RpL13 (Ribosomal protein L13) | 11 | 220.11 | 1.083 | 0.516 | 0.476 |
| RpL6 (Ribosomal protein L6) | 11 | 219.03 | 1.072 | 0.585 | 0.546 |
| RpLP0 (Ribosomal protein LP0) | 8 | 216.68 | 1.051 | 0.524 | 0.498 |
| RpL26 (Ribosomal proteinL26) | 6 | 213.57 | 1.091 | 0.633 | 0.580 |
| RpL8 (Ribosomal protein L8) | 9 | 212.29 | 1.129 | 0.603 | 0.534 |
| RpS7 (Ribosomal protein S7) | 10 | 200.34 | 1.250 | 0.734 | 0.588 |
| sta (Stubarista) | 10 | 199.93 | 1.081 | 0.670 | 0.620 |
| RpL10 (Ribosomal protein L10) | 11 | 197.39 | 1.309 | 0.715 | 0.546 |
| RpS18 (Ribosomal protein S18) | 12 | 193.85 | 1.263 | 0.773 | 0.612 |
| RpS13 (Ribosomal protein S13) | 7 | 179.58 | 1.152 | 0.634 | 0.550 |
| RpL35A (Ribosomal protein L35A) | 10 | 175.51 | 1.048 | 0.523 | 0.499 |
| RpL24 (Ribosomal protein L24) | 9 | 170.27 | 1.085 | 0.526 | 0.485 |

| | | | | | |
|---|---|---|---|---|---|
| RpL18A (Ribosomal protein L18A) | 9 | 169.39 | 1.094 | 0.586 | 0.535 |
| RpL17 (Ribosomal protein L17) | 8 | 167.85 | 1.113 | 0.550 | 0.494 |
| RpS16 (Ribosomal protien S16) | 11 | 167.60 | 1.215 | 0.740 | 0.609 |
| RpS5a (Ribosomal protein S5a) | 7 | 164.88 | 1.176 | 0.771 | 0.656 |
| RpS12 (Ribosomal protein S12) | 6 | 161.47 | 1.601 | 0.784 | 0.490 |
| RpS11 (Ribosomal protein S11) | 8 | 161.41 | 1.126 | 0.641 | 0.570 |
| RpL9 (Ribosomal protein L9) | 8 | 158.46 | 1.160 | 0.632 | 0.545 |
| RpS8 (Ribosomal protein S8) | 11 | 149.92 | 1.193 | 0.729 | 0.611 |
| RpS15Aa (Ribosomal protein S15Aa) | 6 | 136.89 | 1.156 | 0.678 | 0.587 |
| RpL19 (Ribosomal protein L19) | 7 | 134.33 | 1.111 | 0.542 | 0.488 |
| RpL18 (Ribosomal protein L18) | 4 | 130.52 | 1.147 | 0.529 | 0.461 |
| RpL31 (Ribosomal protein L31) | 5 | 129.19 | 1.129 | 0.525 | 0.465 |
| RpS23 (Ribosomal protein S23) | 6 | 124.93 | 1.250 | 0.830 | 0.664 |
| RpL11 (Ribosomal protein L11) | 4 | 116.26 | 1.188 | 0.672 | 0.565 |
| RpS10b (Ribosomal protein S10b) | 11 | 114.99 | 1.357 | 1.000 | 0.737 |
| RpL30 (Ribosomal protein L30) | 7 | 114.51 | 1.113 | 0.528 | 0.474 |
| RpL27A (Ribosomal protein L27A) | 5 | 112.66 | 1.033 | 0.516 | 0.500 |
| RpL35 (Ribosomal protein L35) | 3 | 111.60 | 1.150 | 0.491 | 0.427 |
| RpL12 (Ribosomal protein L12) | 6 | 110.53 | 1.202 | 0.618 | 0.514 |
| RpS25 (Ribosomal protein S25) | 4 | 108.33 | 1.191 | 0.747 | 0.627 |
| RpS17 (Ribosomal protein S17) | 7 | 105.98 | 1.173 | 0.662 | 0.564 |
| RpS21 (Ribosomal protein S21) | 5 | 105.10 | 1.219 | 0.797 | 0.654 |
| RpS14b (Ribosomal protein S14b) | 6 | 101.21 | 1.304 | 0.998 | 0.766 |
| RpL15 (Ribosomal protein L15) | 6 | 97.99 | 1.232 | 0.839 | 0.681 |
| RpL23 (Ribosomal protein L23) | 5 | 93.39 | 1.140 | 0.762 | 0.668 |
| RpL21 (Ribosomal protein L21) | 6 | 87.21 | 1.004 | 0.507 | 0.504 |
| RpL34b (Ribosomal protein L34b) | 5 | 87.07 | 1.111 | 0.421 | 0.379 |
| RpL36 (Ribosomal protein L36) | 5 | 83.89 | 1.032 | 0.463 | 0.449 |
| RpS20(Ribosomal protein S20) | 4 | 82.58 | 1.333 | 1.231 | 0.924 |
| RpL27 (Ribosomal protein L27) | 6 | 80.63 | 1.041 | 0.568 | 0.545 |
| RpS28b (Ribosomal protein S28b) | 3 | 72.90 | 1.213 | 0.827 | 0.682 |
| RpL37a (Ribosomal protein L37a) | 4 | 70.03 | 1.039 | 0.484 | 0.466 |
| RpL37a (Ribosomal protein L37a) | 6 | 68.15 | 1.079 | 0.457 | 0.423 |
| CG10602 | 3 | 54.34 | 1.807 | 0.546 | 0.302 |

| | | | | | |
|---|---|---|---|---|---|
| mRpL45 (mitochondrial ribosomal protein L45) | 7 | 54.29 | 1.148 | 0.706 | 0.615 |
| mRpS5 (mitochondrial ribosomal protein S5) | 4 | 53.34 | 1.314 | 1.177 | 0.896 |
| RpL32 (Ribosomal protein L32) | 3 | 51.01 | 1.138 | 0.618 | 0.543 |
| mRpL38 (mitochondrial ribosomal protein L38) | 3 | 45.56 | 1.073 | 0.667 | 0.621 |
| mRpL24 (mitochondrial ribosomal protein L24) | 3 | 44.75 | 1.051 | 0.431 | 0.410 |
| S6k (RPS6-p70-protein kinase) | 3 | 43.75 | 1.901 | 4.923 | 2.589 |
| mRpS35 (mitochondrial ribosomal protein S35) | 3 | 41.70 | 1.663 | 1.461 | 0.878 |
| RpS24 (Ribosomal protein S24) | 3 | 40.58 | 1.330 | 0.621 | 0.467 |
| mRpS30 (mitochondrial ribosomal protein S30) | 5 | 40.09 | 1.117 | 0.878 | 0.786 |
| mRpL1 (mitochondrial ribosomal protein L1) | 3 | 38.08 | 1.060 | 0.517 | 0.487 |
| RpS29 (Ribosomal protein S29) | 3 | 37.69 | 1.313 | 1.017 | 0.775 |
| mRpL30 (mitochondrial ribosomal protein L30) | 6 | 37.63 | 1.036 | 0.458 | 0.443 |
| mRpL39 (mitochondrial ribosomal protein L39) | 4 | 36.60 | 1.200 | 0.842 | 0.702 |
| mRpL37 (mitochondrial ribosomal protein L37) | 3 | 30.37 | 1.168 | 0.552 | 0.473 |
| mRpL3 (mitochondrial ribosomal protein L3) | 4 | 30.26 | 1.146 | 0.721 | 0.629 |

Supplementary Table 4

Hatch rates for RFC2 RNAi lines

| Valium 20 RfC2 | | | |
|---|---|---|---|
| | Control | Driven (25) | Driven (18) |
| | 98 | 0 | 0 |
| | 97 | 0 | 1 |
| | 99 | 1 | 1 |
| | | | |
| Average | 98 | 0.33 | 0.67 |
| Valium 22 RfC2 | | | |
| | Control | Driven (25) | Driven (18) |
| | 96 | 1 | 1 |
| | 99 | 0 | 1 |
| | 97 | 0 | 0 |
| | | | |
| Average | 97.33 | 0.33 | 0.67 |

Supplementary Table 5

Hatch rates for DCC1 RNAi

| Valium 20 Dcc1 | | |
|---|---|---|
| | Control | Driven (18) |
| | 99 | 0 |
| | 96 | 1 |
| | 95 | 1 |
| | | |
| Average | 96.67 | 0.67 |

References

Adachi, Y., Pavlakis, G.N. & Copeland, T.D., 1994. Identification and characterization of SET, a nuclear phosphoprotein encoded by the translocation break point in acute undifferentiated leukemia. *The Journal of biological chemistry*, 269(3), pp.2258–2262.

Aebersold, R. & Mann, M., 2003. Mass spectrometry-based proteomics. *Nature*, 422(6928), pp.198–207.

Akhmanova, A. & Steinmetz, M.O., 2008. Tracking the ends: a dynamic protein network controls the fate of microtubule tips. *Nature reviews. Molecular cell biology*, 9(4), pp.309–322.

Al-Bassam, J. & Chang, F., 2011. Regulation of microtubule dynamics by TOG-domain proteins XMAP215/Dis1 and CLASP. *Trends in cell biology*, 21(10), pp.604–614.

Amos, L. & Klug,  a, 1974. Arrangement of subunits in flagellar microtubules. *Journal of cell science*, 14(3), pp.523–549.

Archambault, V. et al., 2008. Sequestration of Polo kinase to microtubules by phosphopriming-independent binding to Map205 is relieved by phosphorylation at a CDK site in mitosis. *Genes & development*, 22(19), pp.2707–2720.

Aroya, S. Ben & Kupiec, M., 2005. The Elg1 replication factor C-like complex: a novel guardian of genome stability. *DNA repair*, 4(4), pp.409–417.

Ashburner M, Hawley RS, Golic KG. *Drosophila*: a Laboratory Handbook. 2nd ed. Cold Spring Harbour, N.Y.: Cold Spring Harbour Laboratory Press; 2005.

Axton, J.M. et al., 1990. One of the protein phosphatase 1 isoenzymes in *Drosophila* is essential for mitosis. *Cell*, 63(1), pp.33–46.

Bellaoui, M. et al., 2003. Elg1 forms an alternative RFC complex important for DNA replication and genome integrity. *The EMBO journal*, 22(16), pp.4304–4313.

Beller, M. & Oliver, B., 2006. One hundred years of high-throughput *Drosophila*

research. *Chromosome research : an international journal on the molecular, supramolecular and evolutionary aspects of chromosome biology*, 14(4), pp.349–362.

Bermudez, V.P. et al., 2003. The alternative Ctf18-Dcc1-Ctf8-replication factor C complex required for sister chromatid cohesion loads proliferating cell nuclear antigen onto DNA. *Proceedings of the National Academy of Sciences of the United States of America*, 100(18), pp.10237–10242.

Bier, E., 2005. *Drosophila*, the golden bug, emerges as a tool for human genetics. *Nature reviews. Genetics*, 6(1), pp.9–23.

Blagden, S.P. et al., 2009. *Drosophila* Larp associates with poly(A)-binding protein and is required for male fertility and syncytial embryo development. *Developmental biology*, 334(1), pp.186–197.

Bobinnec, Y. et al., 1998. Centriole disassembly in vivo and its effect on centrosome structure and function in vertebrate cells. *The Journal of cell biology*, 143(6), pp.1575–1589.

Boddy, M.N. & Russell, P., 2001. DNA replication checkpoint. *Current biology : CB*, 11(23), pp.R953–6.

Bonaccorsi, S., Giansanti, M.G. & Gatti, M., 1998. Spindle self-organization and cytokinesis during male meiosis in asterless mutants of *Drosophila* melanogaster. *The Journal of cell biology*, 142(3), pp.751–761.

Borisy, G.G. et al., 1975. Purification of tubulin and associated high molecular weight proteins from porcine brain and characterization of microtubule assembly in vitro. *Annals of the New York Academy of Sciences*, 253, pp.107–132.

Bowman, G.D., O'Donnell, M. & Kuriyan, J., 2004. Structural analysis of a eukaryotic sliding DNA clamp-clamp loader complex. *Nature*, 429(6993), pp.724–730.

Brouhard, G.J. et al., 2008. XMAP215 is a processive microtubule polymerase. *Cell*, 132(1), pp.79–88.

Brust-Mascher, I. et al., 2009. Kinesin-5-dependent poleward flux and spindle length

control in *Drosophila* embryo mitosis. *Molecular biology of the cell*, 20(6), pp.1749–1762.

Campbell S (2014). Investigating the role of the Chromosomal Passenger Complex and putative interactors in *Drosophila* spindle and central spindle formation. MbyRes thesis.

Carazo-Salas, R.E. et al., 1999. Generation of GTP-bound Ran by RCC1 is required for chromatin-induced mitotic spindle formation. *Nature*, 400(6740), pp.178–181.

do Carmo Avides, M. & Glover, D.M., 1999. Abnormal spindle protein, Asp, and the integrity of mitotic centrosomal microtubule organizing centers. *Science (New York, N.Y.)*, 283(5408), pp.1733–1735.

do Carmo Avides, M., Tavares, A. & Glover, D.M., 2001. Polo kinase and Asp are needed to promote the mitotic organizing activity of centrosomes. *Nature cell biology*, 3(4), pp.421–424.

Cassimeris, L., 1999. Accessory protein regulation of microtubule dynamics throughout the cell cycle. *Current opinion in cell biology*, 11(1), pp.134–141.

Cermelli, S. et al., 2006. The lipid-droplet proteome reveals that droplets are a protein-storage depot. *Current biology : CB*, 16(18), pp.1783–1795.

Chen, F. et al., 2007. Multiple Protein Phosphatases Are Required for Mitosis in Drosophila. *Current Biology*, 17(4), pp.293–303.

Ciosk, R. et al., 1998. An ESP1/PDS1 complex regulates loss of sister chromatid cohesion at the metaphase to anaphase transition in yeast. *Cell*, 93(6), pp.1067–1076.

Cohen-Fix, O. et al., 1996. Anaphase initiation in Saccharomyces cerevisiae is controlled by the APC-dependent degradation of the anaphase inhibitor Pds1p. *Genes & development*, 10(24), pp.3081–3093.

Collins, C.A. & Vallee, R.B., 1989. Preparation of microtubules from rat liver and testis: cytoplasmic dynein is a major microtubule associated protein. *Cell motility and the cytoskeleton*, 14(4), pp.491–500.

Crabbe, L. et al., 2010. Analysis of replication profiles reveals key role of RFC-Ctf18 in yeast replication stress response. *Nature structural & molecular biology*, 17(11), pp.1391–1397.

Cullen, C.F. et al., 1999. mini spindles: A gene encoding a conserved microtubule-associated protein required for the integrity of the mitotic spindle in *Drosophila*. *The Journal of cell biology*, 146(5), pp.1005–1018.

Cullmann, G. et al., 1995. Characterization of the five replication factor C genes of Saccharomyces cerevisiae. *Molecular and cellular biology*, 15(9), pp.4661–4671.

Desai, A. & Mitchison, T.J., 1997. Microtubule polymerization dynamics. *Annual review of cell and developmental biology*, 13, pp.83–117. Available at: http://www.ncbi.nlm.nih.gov/pubmed/9442869.

Duncan, T. & Wakefield, J.G., 2011. 50 ways to build a spindle: the complexity of microtubule generation during mitosis. *Chromosome research : an international journal on the molecular, supramolecular and evolutionary aspects of chromosome biology*, 19(3), pp.321–333.

Ellison, V. & Stillman, B., 2003. Biochemical characterization of DNA damage checkpoint complexes: clamp loader and clamp complexes with specificity for 5' recessed DNA. *PLoS biology*, 1(2), p.E33.

Fairman, M. et al., 1988. Identification of cellular components required for SV40 DNA replication in vitro. *Biochimica et biophysica acta*, 951(2-3), pp.382–387.

Flybase. (1992). Flybase curation.

Foe, V.E. & Alberts, B.M., 1983. Studies of nuclear and cytoplasmic behaviour during the five mitotic cycles that precede gastrulation in *Drosophila* embryogenesis. *Journal of cell science*, 61, pp.31–70.

Font-Burgada, J. et al., 2008. *Drosophila* HP1c isoform interacts with the zinc-finger proteins WOC and Relative-of-WOC to regulate gene expression. *Genes & development*, 22(21), pp.3007–3023.

Gard, D.L. & Kirschner, M.W., 1987. Microtubule assembly in cytoplasmic extracts of *Xenopus* oocytes and eggs. *The Journal of cell biology*, 105(5), pp.2191–2201.

Gause, M. et al., 2008. Functional links between *Drosophila* Nipped-B and cohesin in somatic and meiotic cells. *Chromosoma*, 117(1), pp.51–66.

Gellon, L. et al., 2011. New functions of Ctf18-RFC in preserving genome stability outside its role in sister chromatid cohesion. *PLoS genetics*, 7(2), p.e1001298.

Gergely, F., Kidd, D., et al., 2000. D-TACC: a novel centrosomal protein required for normal spindle function in the early *Drosophila* embryo. *The EMBO journal*, 19(2), pp.241–252.

Gergely, F., Karlsson, C., et al., 2000. The TACC domain identifies a family of centrosomal proteins that can interact with microtubules. *Proceedings of the National Academy of Sciences of the United States of America*, 97(26), pp.14352–14357.

Glotzer, M., 2009. The 3Ms of central spindle assembly: microtubules, motors and MAPs. *Nature reviews. Molecular cell biology*, 10(1), pp.9–20.

Goldstein, L. S. B. and S. Gunawardena (2000). Table S2. Identified cytalskeletal protein coding genes in *Drosophila*. 150.

Gonzalez, C. et al., 1990. Mutations at the asp locus of *Drosophila* lead to multiple free centrosomes in syncytial embryos, but restrict centrosome duplication in larval neuroblasts. *Journal of cell science*, 96 ( Pt 4), pp.605–616.

Goodwin, S.S. & Vale, R.D., 2010. Patronin regulates the microtubule network by protecting microtubule minus ends. *Cell*, 143(2), pp.263–274.

Goshima, G. et al., 2008. Augmin: a protein complex required for centrosome-independent microtubule generation within the spindle. *The Journal of cell biology*, 181(3), pp.421–429.

Goshima, G. et al., 2007. Genes required for mitotic spindle assembly in *Drosophila* S2 cells. *Science (New York, N.Y.)*, 316(5823), pp.417–421.

Goshima, G. & Scholey, J.M., 2010. Control of mitotic spindle length. *Annual review of cell and developmental biology*, 26, pp.21–57.

Greenspan, R.J. (2004) Fly Pushing: The theory and practice of *Drosophila* genetics. 2nd ed. New York: Cold Spring Harbor.

Gregson, H.C. et al., 2001. A potential role for human cohesin in mitotic spindle aster assembly. *The Journal of biological chemistry*, 276(50), pp.47575–47582.

Griffiths, D.J. et al., 1995. Fission yeast rad17: a homologue of budding yeast RAD24 that shares regions of sequence similarity with DNA polymerase accessory proteins. *The EMBO journal*, 14(23), pp.5812–5823.

Gstaiger, M. & Aebersold, R., 2009. Applying mass spectrometry-based proteomics to genetics, genomics and network biology. *Nature reviews. Genetics*, 10(9), pp.617–627.

Hafen, E., Kuroiwa, A. & Gehring, W.J., 1984. Spatial distribution of transcripts from the segmentation gene fushi tarazu during *Drosophila* embryonic development. *Cell*, 37(3), pp.833–841.

Han, X., Aslanian, A. & Yates, J.R. 3rd, 2008. Mass spectrometry for proteomics. *Current opinion in chemical biology*, 12(5), pp.483–490.

Hanna, J.S. et al., 2001. Saccharomyces cerevisiae CTF18 and CTF4 are required for sister chromatid cohesion. *Molecular and cellular biology*, 21(9), pp.3144–3158.

Harrison, S.D., Solomon, N. & Rubin, G.M., 1995. A genetic analysis of the 63E-64A genomic region of *Drosophila melanogaster*: identification of mutations in a replication factor C subunit. *Genetics*, 139(4), pp.1701–1709.

Hayward, D. & Wakefield, J.G., 2014. Chromatin-mediated microtubule nucleation in *Drosophila* syncytial embryos. *Communicative & integrative biology*, 7, p.e28512.

Heald, R. et al., 1996. Self-organization of microtubules into bipolar spindles around artificial chromosomes in Xenopus egg extracts. *Nature*, 382(6590), pp.420–

425.

Hirano, T., 2012. Condensins: universal organizers of chromosomes with diverse functions. *Genes & development*, 26(15), pp.1659–1678.

Hughes, J.R. et al., 2008. A microtubule interactome: Complexes with roles in cell cycle and mitosis. *PLoS Biology*, 6(4), pp.785–795.

Hush, J.M. et al., 1994. Quantification of microtubule dynamics in living plant cells using fluorescence redistribution after photobleaching. *Journal of cell science*, 107 ( Pt 4, pp.775–784.

Hutter, P. & Karch, F., 1994. Molecular analysis of a candidate gene for the reproductive isolation between sibling species of *Drosophila*. *Experientia*, 50(8), pp.749–762.

Hyman, A.A. & Mitchison, T.J., 1990. Modulation of microtubule stability by kinetochores in vitro. *The Journal of cell biology*, 110(5), pp.1607–1616.

Inoue, S. & Salmon, E.D., 1995. Force generation by microtubule assembly/disassembly in mitosis and related movements. *Molecular biology of the cell*, 6(12), pp.1619–1640.

Ishiguro, K. & Watanabe, Y., 2007. Chromosome cohesion in mitosis and meiosis. *Journal of cell science*, 120(Pt 3), pp.367–369.

Jaffe, A.B. & Jongens, T.A., 2001. Structure-specific abnormalities associated with mutations in a DNA replication accessory factor in *Drosophila*. *Developmental biology*, 230(2), pp.161–176.

Janssens, V. & Goris, J., 2001. Protein phosphatase 2A: a highly regulated family of serine/threonine phosphatases implicated in cell growth and signalling. *The Biochemical journal*, 353(Pt 3), pp.417–439.

Johnstone, O. & Lasko, P., 2001. Translational regulation and RNA localization in *Drosophila* oocytes and embryos. *Annual review of genetics*, 35, pp.365–406.

Kachaner, D. et al., 2014. Interdomain allosteric regulation of Polo kinase by Aurora

B and Map205 is required for cytokinesis. *The Journal of cell biology*, 207(2), pp.201–211.

Kai, M., Tanaka, H. & Wang, T.S., 2001. Fission yeast Rad17 associates with chromatin in response to aberrant genomic structures. *Molecular and cellular biology*, 21(10), pp.3289–3301.

Kalab, P., Pu, R.T. & Dasso, M., 1999. The ran GTPase regulates mitotic spindle assembly. *Current biology : CB*, 9(9), pp.481–484.

Kamasaki, T. et al., 2013. Augmin-dependent microtubule nucleation at microtubule walls in the spindle. *The Journal of cell biology*, 202(1), pp.25–33.

Kang Ju-Seop (2012). Principles and Applications of LC-MS/MS for the Quatitiative Bioanalysis of Analytes in Various Biological Samples, Tandem Mass Spectrometry - Applications and Principles, Dr Jeevan Prasain (Ed.), ISBN 978-953-51-0141-3, InTech, DOI: 10.5772/320825.

Karr, T.L. & Alberts, B.M., 1986. Organization of the cytoskeleton in early *Drosophila* embryos. *The Journal of cell biology*, 102(4), pp.1494–1509.

Karsenti, E., 1993. Microtubule dynamics: severing microtubules in mitosis. *Current biology : CB*, 3(4), pp.208–210.

Karsenti, E., 1991. Mitotic spindle morphogenesis in animal cells. *Seminars in cell biology*, 2(4), pp.251–260.

Kellogg, D.R. et al., 1995. Members of the NAP/SET family of proteins interact specifically with B-type cyclins. *The Journal of cell biology*, 130(3), pp.661–673.

Kellogg, D.R., Field, C.M. & Alberts, B.M., 1989. Identification of microtubule-associated proteins in the centrosome, spindle, and kinetochore of the early *Drosophila* embryo. *The Journal of cell biology*, 109(6 Pt 1), pp.2977–2991.

Kellogg, D.R., Mitchison, T.J. & Alberts, B.M., 1988. Behaviour of microtubules and actin filaments in living *Drosophila* embryos. *Development (Cambridge, England)*, 103(4), pp.675–686.

Khodjakov, A. et al., 2003. Minus-end capture of preformed kinetochore fibers contributes to spindle morphogenesis. *The Journal of cell biology*, 160(5), pp.671–683.

Kim, J. & MacNeill, S.A., 2003. Genome stability: a new member of the RFC family. *Current biology : CB*, 13(22), pp.R873–5.

Kolodner, R.D., Putnam, C.D. & Myung, K., 2002. Maintenance of genome stability in *Saccharomyces cerevisiae*. *Science (New York, N.Y.)*, 297(5581), pp.552–557.

Kondo, S. & Perrimon, N., 2011. A genome-wide RNAi screen identifies core components of the G(2)-M DNA damage checkpoint. *Science signaling*, 4(154), p.rs1.

Krauchunas, A.R., Horner, V.L. & Wolfner, M.F., 2012. Protein phosphorylation changes reveal new candidates in the regulation of egg activation and early embryogenesis in *D. melanogaster*. *Developmental biology*, 370(1), pp.125–134.

Krause, S.A. et al., 2001. Loss of cell cycle checkpoint control in *Drosophila* Rfc4 mutants. *Molecular and cellular biology*, 21(15), pp.5156–5168.

Lau, A.C. & Csankovszki, G., 2014. Condensin-mediated chromosome organization and gene regulation. *Frontiers in genetics*, 5, p.473.

Lee, M.J. et al., 2001. Msps/XMAP215 interacts with the centrosomal protein D-TACC to regulate microtubule behaviour. *Nature cell biology*, 3(7), pp.643–649.

Li, W. et al., 2012. Reconstitution of dynamic microtubules with drosophila XMAP215, EB1, and sentin. *Journal of Cell Biology*, 199(5), pp.849–862.

von Lindern, M. et al., 1992. Characterization of the translocation breakpoint sequences of two DEK-CAN fusion genes present in t(6;9) acute myeloid leukemia and a SET-CAN fusion gene found in a case of acute undifferentiated leukemia. *Genes, chromosomes & cancer*, 5(3), pp.227–234.

Lindsey-Boltz, L.A. et al., 2001. Purification and characterization of human DNA damage checkpoint Rad complexes. *Proceedings of the National Academy of*

*Sciences of the United States of America*, 98(20), pp.11236–11241.

Maiato, H., Rieder, C.L. & Khodjakov, A., 2004. Kinetochore-driven formation of kinetochore fibers contributes to spindle assembly during animal mitosis. *The Journal of cell biology*, 167(5), pp.831–840.

Majka, J. & Burgers, P.M.J., 2004. The PCNA-RFC families of DNA clamps and clamp loaders. *Progress in nucleic acid research and molecular biology*, 78, pp.227–260.

Martinez-Campos, M. et al., 2004. The *Drosophila* pericentrin-like protein is essential for cilia/flagella function, but appears to be dispensable for mitosis. *The Journal of cell biology*, 165(5), pp.673–683.

Mayer, M.L. et al., 2001. Identification of RFC(Ctf18p, Ctf8p, Dcc1p): an alternative RFC complex required for sister chromatid cohesion in S. cerevisiae. *Molecular cell*, 7(5), pp.959–970.

McGill, M. & Brinkley, B.R., 1975. Human chromosomes and centrioles as nucleating sites for the in vitro assembly of microtubules from bovine brain tubulin. *The Journal of cell biology*, 67(1), pp.189–199.

Megraw, T.L., Kao, L.R. & Kaufman, T.C., 2001. Zygotic development without functional mitotic centrosomes. *Current biology : CB*, 11(2), pp.116–120.

Merkle, C.J. et al., 2003. Cloning and characterization of hCTF18, hCTF8, and hDCC1. Human homologs of a Saccharomyces cerevisiae complex involved in sister chromatid cohesion establishment. *The Journal of biological chemistry*, 278(32), pp.30051–30056.

Michaelis, C., Ciosk, R. & Nasmyth, K., 1997. Cohesins: chromosomal proteins that prevent premature separation of sister chromatids. *Cell*, 91(1), pp.35–45.

Mitchison, T. & Kirschner, M., 1984. Dynamic instability of microtubule growth. *Nature*, 312(5991), pp.237–242.

Moore, W., Zhang, C. & Clarke, P.R., 2002. Targeting of RCC1 to chromosomes is required for proper mitotic spindle assembly in human cells. *Current biology :*

*CB*, 12(16), pp.1442–1447.

Morales-Mulia, S. & Scholey, J.M., 2005. Spindle pole organization in *Drosophila* S2 cells by dynein, abnormal spindle protein (Asp), and KLP10A. *Molecular biology of the cell*, 16(7), pp.3176–3186.

Moritz, M. et al., 1995. Microtubule nucleation by gamma-tubulin-containing rings in the centrosome. *Nature*, 378(6557), pp.638–640.

Murakami, T. et al., 2010. Stable interaction between the human proliferating cell nuclear antigen loader complex Ctf18-replication factor C (RFC) and DNA polymerase {epsilon} is mediated by the cohesion-specific subunits, Ctf18, Dcc1, and Ctf8. *The Journal of biological chemistry*, 285(45), pp.34608–34615.

Naiki, T. et al., 2000. Rfc5, in cooperation with rad24, controls DNA damage checkpoints throughout the cell cycle in *Saccharomyces cerevisiae*. *Molecular and cellular biology*, 20(16), pp.5888–5896.

Nelson, D.R., 2000. Mitochondrial carrier genes.

Nicklas, R.B., 1997. How cells get the right chromosomes. *Science (New York, N.Y.)*, 275(5300), pp.632–637.

O'Connell, M.J., Walworth, N.C. & Carr, A.M., 2000. The G2-phase DNA-damage checkpoint. *Trends in cell biology*, 10(7), pp.296–303.

Odunuga, O.O., Longshaw, V.M. & Blatch, G.L., 2004. Hop: more than an Hsp70/Hsp90 adaptor protein. *BioEssays : news and reviews in molecular, cellular and developmental biology*, 26(10), pp.1058–1068.

Ohkura, H., Garcia, M.A. & Toda, T., 2001. Dis1/TOG universal microtubule adaptors - one MAP for all? *Journal of cell science*, 114(Pt 21), pp.3805–3812.

Ohta, S. et al., 2002. A proteomics approach to identify proliferating cell nuclear antigen (PCNA)-binding proteins in human cell lysates. Identification of the human CHL12/RFCs2-5 complex as a novel PCNA-binding protein. *The Journal of biological chemistry*, 277(43), pp.40362–40367.

Ono, T. et al., 2004. Spatial and temporal regulation of Condensins I and II in mitotic chromosome assembly in human cells. *Molecular biology of the cell*, 15(7), pp.3296–3308.

Parnas, O. et al., 2009. The ELG1 clamp loader plays a role in sister chromatid cohesion. *PloS one*, 4(5), p.e5497.

Pek, J.W. & Kai, T., 2011. A role for vasa in regulating mitotic chromosome condensation in *Drosophila*. *Current biology : CB*, 21(1), pp.39–44.

Pereira, A. et al., 1992. Genetic analysis of a *Drosophila* microtubule-associated protein. *The Journal of cell biology*, 116(2), pp.377–383.

Peset, I. & Vernos, I., 2008. The TACC proteins: TACC-ling microtubule dynamics and centrosome function. *Trends in cell biology*, 18(8), pp.379–388.

Prokopenko, S.N. et al., 2000. Mutations affecting the development of the peripheral nervous system in *Drosophila*: a molecular screen for novel proteins. *Genetics*, 156(4), pp.1691–1715.

Ripoll, P. et al., 1985. A cell division mutant of *Drosophila* with a functionally abnormal spindle. *Cell*, 41(3), pp.907–912.

Rogers, G.C. et al., 2004. Two mitotic kinesins cooperate to drive sister chromatid separation during anaphase. *Nature*, 427(6972), pp.364–370.

Rogers, S.L. et al., 2002. *Drosophila* EB1 is important for proper assembly, dynamics, and positioning of the mitotic spindle. *The Journal of cell biology*, 158(5), pp.873–884.

Rollins, R.A. et al., 2004. *Drosophila* nipped-B protein supports sister chromatid cohesion and opposes the stromalin/Scc3 cohesion factor to facilitate long-range activation of the cut gene. *Molecular and cellular biology*, 24(8), pp.3100–3111.

Rujano, M.A. et al., 2013. The microcephaly protein Asp regulates neuroepithelium morphogenesis by controlling the spatial distribution of myosin II. *Nature cell biology*, 15(11), pp.1294–1306.

Sakurai, H. et al., 2011. Anaphase DNA bridges induced by lack of RecQ5 in *Drosophila* syncytial embryos. *FEBS letters*, 585(12), pp.1923–1928.

Salmon, E.D. et al., 1984. Spindle microtubule dynamics in sea urchin embryos: analysis using a fluorescein-labeled tubulin and measurements of fluorescence redistribution after laser photobleaching. *The Journal of cell biology*, 99(6), pp.2165–2174.

Sardiello, M. et al., 2003. MitoDrome: a database of *Drosophila melanogaster* nuclear genes encoding proteins targeted to the mitochondrion. *Nucleic acids research*, 31(1), pp.322–324.

Saxton, W.M. et al., 1984. Tubulin dynamics in cultured mammalian cells. *The Journal of cell biology*, 99(6), pp.2175–2186.

Schisa, J.A., Pitt, J.N. & Priess, J.R., 2001. Analysis of RNA associated with P granules in germ cells of C. elegans adults. *Development (Cambridge, England)*, 128(8), pp.1287–1298.

Schneider, D., 2000. Using *Drosophila* as a model insect. *Nature reviews. Genetics*, 1(3), pp.218–226.

Scholey, J.M., Brust-Mascher, I. & Mogilner, A., 2003. Cell division. *Nature*, 422(6933), pp.746–752.

Shimamura, M. et al., 2004. Gamma-tubulin in basal land plants: characterization, localization, and implication in the evolution of acentriolar microtubule organizing centers. *The Plant cell*, 16(1), pp.45–59.

Shiomi, Y. et al., 2002. Clamp and clamp loader structures of the human checkpoint protein complexes, Rad9-1-1 and Rad17-RFC. *Genes to cells : devoted to molecular & cellular mechanisms*, 7(8), pp.861–868.

Shirasu-Hiza, M., Coughlin, P. & Mitchison, T., 2003. Identification of XMAP215 as a microtubule-destabilizing factor in *Xenopus* egg extract by biochemical purification. *The Journal of cell biology*, 161(2), pp.349–358.

Skibbens, R. V, 2005. Unzipped and loaded: the role of DNA helicases and RFC

clamp-loading complexes in sister chromatid cohesion. *The Journal of cell biology*, 169(6), pp.841–846.

Slep, K.C., 2010. Structural and mechanistic insights into microtubule end-binding proteins. *Current opinion in cell biology*, 22(1), pp.88–95.

Snaith, H.A. et al., 1996. Deficiency of protein phosphatase 2A uncouples the nuclear and centrosome cycles and prevents attachment of microtubules to the kinetochore in *Drosophila* microtubule star (mts) embryos. *Journal of cell science*, 109 ( Pt 1, pp.3001–3012.

Snee, M.J. & Macdonald, P.M., 2009. Bicaudal C and trailer hitch have similar roles in gurken mRNA localization and cytoskeletal organization. *Developmental biology*, 328(2), pp.434–444.

Snyder, J.A. & McIntosh, J.R., 1975. Initiation and growth of microtubules from mitotic centers in lysed mammalian cells. *The Journal of cell biology*, 67(3), pp.744–760.

Sparkman, 2000. Review of the 48th ASMS conference on mass spectrometry and allied topics held in Long Beach, California June 11-15, 2000. *Journal of the American Society for Mass Spectrometry*, 11(10), p.921.

stattrek.com/estimation/confidence-interval.aspx

Su, L.K. et al., 1995. APC binds to the novel protein EB1. *Cancer research*, 55(14), pp.2972–2977.

Sullivan, W. & Theurkauf, W.E., 1995. The cytoskeleton and morphogenesis of the early Drosophila embryo. *Current opinion in cell biology*, 7(1), pp.18–22.

Takada, S., Collins, E.R. & Kurahashi, K., 2015. The FHA domain determines *Drosophila* Chk2/Mnk localization to key mitotic structures and is essential for early embryonic DNA damage responses. *Molecular biology of the cell*, 26(10), pp.1811–1828.

Takada, S., Kelkar, A. & Theurkauf, W.E., 2003. *Drosophila* checkpoint kinase 2 couples centrosome function and spindle assembly to genomic integrity. *Cell*,

113(1), pp.87–99.

Tan, S. et al., 2008. Mars promotes dTACC dephosphorylation on mitotic spindles to ensure spindle stability. *The Journal of cell biology*, 182(1), pp.27–33.

Tanaka, T. et al., 1999. Identification of cohesin association sites at centromeres and along chromosome arms. *Cell*, 98(6), pp.847–858.

Tavares, A.A., Glover, D.M. & Sunkel, C.E., 1996. The conserved mitotic kinase polo is regulated by phosphorylation and has preferred microtubule-associated substrates in *Drosophila* embryo extracts. *The EMBO journal*, 15(18), pp.4873–4883.

Terhzaz, S. et al., 2010. Mislocalization of mitochondria and compromised renal function and oxidative stress resistance in *Drosophila* SesB mutants. *Physiological genomics*, 41(1), pp.33–41.

Thompson, A. et al., 2003. Tandem mass tags: a novel quantification strategy for comparative analysis of complex protein mixtures by MS/MS. *Analytical chemistry*, 75(8), pp.1895–1904.

Tirnauer, J.S. & Bierer, B.E., 2000. EB1 proteins regulate microtubule dynamics, cell polarity, and chromosome stability. *The Journal of cell biology*, 149(4), pp.761–766.

Tomida, J. et al., 2008. DNA damage-induced ubiquitylation of RFC2 subunit of replication factor C complex. *The Journal of biological chemistry*, 283(14), pp.9071–9079.

Toth, A. et al., 1999. Yeast cohesin complex requires a conserved protein, Eco1p(Ctf7), to establish cohesion between sister chromatids during DNA replication. *Genes & development*, 13(3), pp.320–333.

Tsuchiya, A. et al., 2007. Transcriptional regulation of the *Drosophila* rfc1 gene by the DRE-DREF pathway. *The FEBS journal*, 274(7), pp.1818–1832.

Tulu, U.S. et al., 2006. Molecular requirements for kinetochore-associated microtubule formation in mammalian cells. *Current biology : CB*, 16(5), pp.536–

541.

Uehara, R. et al., 2009. The augmin complex plays a critical role in spindle microtubule generation for mitotic progression and cytokinesis in human cells. *Proceedings of the National Academy of Sciences of the United States of America*, 106(17), pp.6998–7003.

Uhlmann, F. et al., 2000. Cleavage of cohesin by the CD clan protease separin triggers anaphase in yeast. *Cell*, 103(3), pp.375–386.

Uhlmann, F., Lottspeich, F. & Nasmyth, K., 1999. Sister-chromatid separation at anaphase onset is promoted by cleavage of the cohesin subunit Scc1. *Nature*, 400(6739), pp.37–42.

Varmark, H., 2004. Functional role of centrosomes in spindle assembly and organization. *Journal of cellular biochemistry*, 91(5), pp.904–914.

Vasquez, R.J., Gard, D.L. & Cassimeris, L., 1994. XMAP from Xenopus eggs promotes rapid plus end assembly of microtubules and rapid microtubule polymer turnover. *The Journal of cell biology*, 127(4), pp.985–993.

Veraksa, A., 2010. When peptides fly: advances in *Drosophila* proteomics. *Journal of proteomics*, 73(11), pp.2158–2170.

Viquez, N.M. et al., 2006. The B' protein phosphatase 2A regulatory subunit well-rounded regulates synaptic growth and cytoskeletal stability at the *Drosophila* neuromuscular junction. *The Journal of neuroscience : the official journal of the Society for Neuroscience*, 26(36), pp.9293–9303.

Waga, S. & Stillman, B., 1994. Anatomy of a DNA replication fork revealed by reconstitution of SV40 DNA replication in vitro. *Nature*, 369(6477), pp.207–212.

Wakefield, J.G., Bonaccorsi, S. & Gatti, M., 2001. The *Drosophila* protein asp is involved in microtubule organization during spindle formation and cytokinesis. *The Journal of cell biology*, 153(4), pp.637–648.

Walther, T.C. & Mann, M., 2010. Mass spectrometry-based proteomics in cell biology. *The Journal of cell biology*, 190(4), pp.491–500.

Wang, Z. et al., 2000. Pol kappa: A DNA polymerase required for sister chromatid cohesion. *Science (New York, N.Y.)*, 289(5480), pp.774–779.

Wittmann, T., Hyman, A. & Desai, A., 2001. The spindle: a dynamic assembly of microtubules and motors. *Nature cell biology*, 3(1), pp.E28–34.

Yang, C.-P. & Fan, S.-S., 2008. *Drosophila* mars is required for organizing kinetochore microtubules during mitosis. *Experimental cell research*, 314(17), pp.3209–3220.

Yao, N.Y. & O'Donnell, M., 2012. The RFC clamp loader: structure and function. *Sub-cellular biochemistry*, 62, pp.259–279.

Zhai, Y. et al., 1996. Microtubule dynamics at the G2/M transition: abrupt breakdown of cytoplasmic microtubules at nuclear envelope breakdown and implications for spindle morphogenesis. *The Journal of cell biology*, 135(1), pp.201–214.

Zhang, G. et al., 2009. Mars, a *Drosophila* protein related to vertebrate HURP, is required for the attachment of centrosomes to the mitotic spindle during syncytial nuclear divisions. *Journal of cell science*, 122(Pt 4), pp.535–545.

Zhang, J. & Megraw, T.L., 2007. Proper recruitment of gamma-tubulin and D-TACC/Msps to embryonic *Drosophila* centrosomes requires Centrosomin Motif 1. *Molecular biology of the cell*, 18(10), pp.4037–4049.

Zheng, Y. et al., 1995. Nucleation of microtubule assembly by a gamma-tubulin-containing ring complex. *Nature*, 378(6557), pp.578–583.

Zhou, B.B. & Elledge, S.J., 2000. The DNA damage response: putting checkpoints in perspective. *Nature*, 408(6811), pp.433–439.

Zimmerman, W.C. et al., 2004. Mitosis-specific anchoring of gamma tubulin complexes by pericentrin controls spindle organization and mitotic entry. *Molecular biology of the cell*, 15(8), pp.3642–3657.